J. Fluid Mech. (2019), *vol.* 864, *pp.* 1125–1176.
doi:10.1017/jfm.2019.5

Theory for the rheology of dense non-Brownian suspensions: divergence of viscosities and μ–J rheology

Koshiro Suzuki[1,†] **and Hisao Hayakawa**[2]

[1]Simulation & Analysis R&D Center, Canon Inc., 30-2 Shimomaruko 3-chome, Ohta-ku, Tokyo 146-8501, Japan

[2]Yukawa Institute for Theoretical Physics, Kyoto University, Kitashirakawaoiwake-cho, Sakyo-ku, Kyoto 606-8502, Japan

(Received 15 December 2017; revised 12 October 2018; accepted 30 December 2018; first published online 14 February 2019)

A systematic microscopic theory for the rheology of dense non-Brownian suspensions characterized by the volume fraction φ is developed. The theory successfully derives the critical behaviour in the vicinity of the jamming point (volume fraction φ_J), for both the pressure P and the shear stress σ_{xy}, i.e. $P \sim \sigma_{xy} \sim \dot{\gamma}\eta_0\delta\varphi^{-2}$, where $\dot{\gamma}$ is the shear rate, η_0 is the shear viscosity of the solvent and $\delta\varphi = \varphi_J - \varphi > 0$ is the distance from the jamming point. It also successfully describes the behaviour of the stress ratio $\mu = \sigma_{xy}/P$ with respect to the viscous number $J = \dot{\gamma}\eta_0/P$.

Key words: rheology, suspensions

1. Introduction

The physics of the rheology of suspensions begins with the seminal work by Einstein (Einstein 1905; Mewis & Wagner 2012). He has shown that the effective shear viscosity $\eta_s(\varphi)$ defined by the ratio of the shear stress $\sigma_{xy}(\varphi)$ to the shear rate $\dot{\gamma}$ as $\eta_s(\varphi) = \sigma_{xy}(\varphi)/\dot{\gamma}$ is enhanced as $\eta_s(\varphi)/\eta_0 = 1 + 5\varphi/2 + O(\varphi^2)$ in dilute suspensions, where φ is the volume fraction of the suspended particles and η_0 is the viscosity of the solvent. On the other hand, it has been empirically shown that $\eta_s(\varphi)$ behaves as $\eta_s(\varphi)/\eta_0 \sim (\varphi_m - \varphi)^{-2}$ near a critical volume fraction φ_m in dense suspensions (Chong, Christiansen & Baer 1971; Krieger 1972; Quemada 1977; Zarraga, Hill & Leighton 2000).

Recently, the divergence of the shear stress σ_{xy} has been well studied in the context of the jamming transition, which is an athermal phase transition of dense disordered materials such as suspensions (Pusey 1991), emulsions, foams (Durian & Weitz 1994) and granular materials (O'Hern *et al.* 2002, 2003; Coulais, Seguin & Dauchot 2014; Otsuki & Hayakawa 2014). It is well established that the shear viscosity of non-Brownian suspensions which are insensitive to thermal fluctuations near the jamming point behaves as $\eta_s(\varphi)/\eta_0 \sim (\varphi_J - \varphi)^{-\lambda}$ with $\lambda \approx 2$ and φ_J the jamming volume fraction (Bonnoit *et al.* 2010; Boyer, Guazzelli & Pouliquen 2011),

† Email address for correspondence: suzuki.koshiro@mail.canon

although numerical simulations for soft spheres exhibit $\lambda \approx 2.2$ (Andreotti, Barrat & Heussinger 2012) or $\lambda \approx 1.67 - 2.55$ (Kawasaki *et al.* 2015), and a theoretical approach by DeGiuli *et al.* asserts $\lambda \approx 2.83$ (DeGiuli *et al.* 2015).

On the other hand, the pressure of suspensions, P, has been less investigated. Experimentally, it has been shown that the pressure viscosity defined by $\eta_n(\varphi) = P(\varphi)/\dot{\gamma}$ exhibits $\eta_n(\varphi)/\eta_0 \sim (\varphi_J - \varphi)^{-2}$ (Deboeuf *et al.* 2009; Boyer *et al.* 2011; Cwalina & Wagner 2014; Dagois-Bohy *et al.* 2015). This is non-trivial, since it differs from the pressure at equilibrium given by $P^{(eq)}(\varphi) = nT[1 + 4\varphi g_0(\varphi)]$, where $n = 6\varphi/(\pi d^3)$ is the average number density, d is the diameter of the particle, T is the temperature and $g_0(\varphi)$ is the radial distribution function at contact (Hansen & McDonald 2006). Together with the relation $g_0(\varphi) \sim (\varphi_J - \varphi)^{-1}$ (Donev, Torquato & Stillinger 2005), this leads to $P^{(eq)}(\varphi) \sim nT(\varphi_J - \varphi)^{-1}$, which is inconsistent with the experimental observations for non-Brownian suspensions. To be consistent with the experimental expression $P(\varphi) \sim \eta_0\dot{\gamma}(\varphi_J - \varphi)^{-2}$, we need to explain two non-trivial relations, i.e. $P \propto \dot{\gamma}\eta_0$ and $P \propto (\varphi_J - \varphi)^{-2}$. The former one, $P \propto \dot{\gamma}\eta_0$, has been argued by phenomenological considerations (Jenkins & McTigue 1990; Nott & Brady 1994) or by microstructural and structure-property analyses (Brady & Morris 1997). The latter one, $P \propto (\varphi_J - \varphi)^{-2}$, is more non-trivial. Several phenomenological models are proposed to explain this property (Zarraga *et al.* 2000; Mills & Snabre 2009), but practically it is merely given as an empirical law without a theoretical basis (Morris & Boulay 1999).

Another rheological property of our interest is the stress ratio, $\mu = \sigma_{xy}/P$. It is known that μ converges to a constant in approaching the jamming point, while it varies on departure from the point, by experiments and simulations (GDR Midi 2004; Boyer *et al.* 2011; Kuwano & Hatano 2011; Irani, Chaudhuri & Heussinger 2014; Dagois-Bohy *et al.* 2015; Kawasaki *et al.* 2015). In fact, a constitutive equation for $\mu(J) = \sigma_{xy}/P$ together with $\varphi = \varphi(J)$, where $J = \dot{\gamma}\eta_0/P$ is the viscous number, is proposed and confirmed by experiments conducted with a pressure-imposed cell (μ–J rheology) (Boyer *et al.* 2011; Dagois-Bohy *et al.* 2015). The reported result exhibits $\mu(J) = \mu_0 + CJ^{1/2}$, where C is a constant and μ_0 is its value in the jamming limit, $J \to 0$. However, there exists no theory to explain this law so far.

Derivation of the rheological properties of suspensions from a microscopic theory is difficult even for the shear viscosity. It has been shown by Brady and his coworkers that the effective self-diffusion constant satisfies $D(\varphi) \propto D_0(\varphi_m - \varphi)$, where $D_0 = T_s/(3\pi\,\mathrm{d}\eta_0)$ with T_s the solvent temperature, which is crucial to obtain $\eta_s(\varphi)/\eta_0 \sim (\varphi_m - \varphi)^{-2}$ for Brownian suspensions (Brady 1993; Brady & Morris 1997; Foss & Brady 2000). However, this theory is not applicable to non-Brownian suspensions, because $D(\varphi)$ is an increasing function of φ in non-Brownian suspensions (Leighton & Acrivos 1987*a*,*b*; Breedveld *et al.* 1998, 2002; Heussinger, Berthier & Barrat 2010; Olsson 2010). Hence, an alternative framework is necessary for dense non-Brownian suspensions. In this paper, we attempt to derive the divergent behaviour of the shear and pressure viscosities, $\eta_s/\eta_0 \sim \eta_n/\eta_0 \sim (\varphi_J - \varphi)^{-2}$, and the μ–J rheology, $\mu(J) = \mu_0 + CJ^{1/2}$, by means of a microscopic theory for an idealistic model of non-Brownian suspensions.

2. Basic equations and exact equations for the stress

2.1. *Microscopic basic equations*

We consider an assembly of N frictionless monodisperse spherical particles of diameter d contained in a box of volume V and immersed in a liquid of viscosity η_0.

A simple steady shear with shear rate $\dot{\gamma}$ is applied to the system. The coordinate is chosen such that the flow is in the x-direction and the velocity gradient is in the y-direction. We consider the overdamped equation of motion

$$\sum_{j=1}^{N} \zeta_{ij}^{(N)}(\dot{\boldsymbol{r}}_j - \dot{\gamma} y_j \boldsymbol{e}_x) = \boldsymbol{F}_i^{(p)} \quad (i = 1, \ldots, N), \tag{2.1}$$

where $\boldsymbol{r}_i$ and $\dot{\boldsymbol{r}}_i$ are the position and velocity of particle i, respectively, $\boldsymbol{e}_x$ is the unit vector in the x-direction, $\boldsymbol{F}_i^{(p)}$ is the interparticle force exerted on particle i from other particles and $\{\zeta_{ij}^{(N)}\}_{i,j=1}^{N}$ is the resistance matrix of the suspension, which depends on the configuration of the particles, $\{\boldsymbol{r}_i\}_{i=1}^{N}$. Note that $\{\zeta_{ij}^{(N)}\}_{i,j=1}^{N}$ is a $3N \times 3N$ matrix, where each component $\zeta_{ij}^{(N)}$ is a 3×3 matrix. In particle suspensions, the inertia of the particles is absorbed by the background fluid and hence insignificant. Thus we neglect it in (2.1). We also neglect the rotation of the particles and the thermal fluctuating force exerted on the particles from the solvent in (2.1).

The time evolution of an arbitrary observable $A(\boldsymbol{\Gamma})$ is determined by the Liouville equation

$$\dot{A}(\boldsymbol{\Gamma}(t)) = \dot{\boldsymbol{\Gamma}} \cdot \frac{\partial}{\partial \boldsymbol{\Gamma}} A(\boldsymbol{\Gamma}(t)) := \mathrm{i}\mathcal{L} A(\boldsymbol{\Gamma}(t)), \tag{2.2}$$

where $\mathrm{i}\mathcal{L}$ is the Liouvillian. In simple shear flows, $\boldsymbol{\Gamma}$ is given by $\boldsymbol{\Gamma} = \{\boldsymbol{r}_i, \boldsymbol{v}_i\}_{i=1}^{N}$, where

$$\boldsymbol{v}_i := \dot{\boldsymbol{r}}_i - \dot{\gamma} y_i \boldsymbol{e}_x = \sum_{j=1}^{N} \zeta_{ij}^{(N)-1} \boldsymbol{F}_j^{(p)} \tag{2.3}$$

is the peculiar velocity, which is the velocity in the sheared frame. For (2.1), $\mathrm{i}\mathcal{L}$ is given by

$$\mathrm{i}\mathcal{L} := \sum_{i=1}^{N} \left(\boldsymbol{v}_i \cdot \frac{\partial}{\partial \boldsymbol{r}_i} + \dot{\boldsymbol{v}}_i \cdot \frac{\partial}{\partial \boldsymbol{v}_i} \right) = \sum_{i=1}^{N} \left(\sum_{j=1}^{N} \zeta_{ij}^{(N)-1} \boldsymbol{F}_j^{(p)} \cdot \frac{\partial}{\partial \boldsymbol{r}_i} + \dot{\boldsymbol{v}}_i \cdot \frac{\partial}{\partial \boldsymbol{v}_i} \right), \tag{2.4}$$

where $\dot{\boldsymbol{v}}_i$ is evaluated as

$$\dot{\boldsymbol{v}}_i = \ddot{\boldsymbol{r}}_i - \dot{\gamma} \dot{y}_i \boldsymbol{e}_x = \ddot{\boldsymbol{r}}_i - \dot{\gamma} \sum_{j=1}^{N} \zeta_{ij}^{(N)-1} F_{j,y}^{(p)} \boldsymbol{e}_x. \tag{2.5}$$

Note that (2.3) is utilized in the second equality of (2.5). In the formulation of overdamped Liouville equation, we neglect $\ddot{\boldsymbol{r}}_i$ in (2.5), because $\boldsymbol{v}_i$ rather than $\ddot{\boldsymbol{r}}_i$ resides in the equation of motion, equation (2.3). This leads us to the expression

$$\mathrm{i}\mathcal{L} = \sum_{i=1}^{N} \left(\sum_{j=1}^{N} \zeta_{ij}^{(N)-1} \boldsymbol{F}_j^{(p)} \cdot \frac{\partial}{\partial \boldsymbol{r}_i} - \dot{\gamma} F_{i,y}^{(p)} \frac{\partial}{\partial F_{i,x}^{(p)}} \right). \tag{2.6}$$

Note, however, that neglecting $\ddot{\boldsymbol{r}}_i$ in (2.5) does not mean the absence of $\dot{\boldsymbol{v}}_i$ as can be seen in (2.5). In fact, because of the existence of $\boldsymbol{v}_i$, trajectories of the particles can be curved.

The Liouville equation of the microscopic stress tensor $\tilde{\sigma}_{\alpha\beta}(\boldsymbol{\Gamma})$ $(\alpha, \beta = x, y, z)$ reads

$$\frac{\mathrm{d}}{\mathrm{d}t} \tilde{\sigma}_{\alpha\beta}(\boldsymbol{\Gamma}) = \sum_{i=1}^{N} \left(\sum_{j=1}^{N} \zeta_{ij}^{(N)-1} \boldsymbol{F}_j^{(p)} \cdot \frac{\partial \tilde{\sigma}_{\alpha\beta}(\boldsymbol{\Gamma})}{\partial \boldsymbol{r}_i} - \dot{\gamma} F_{i,y}^{(p)} \frac{\partial \tilde{\sigma}_{\alpha\beta}(\boldsymbol{\Gamma})}{\partial F_{i,x}^{(p)}} \right), \tag{2.7}$$

where $\tilde{\sigma}_{\alpha\beta}(\boldsymbol{\Gamma})$ is given by

$$\tilde{\sigma}_{\alpha\beta}(\boldsymbol{\Gamma}) := -\frac{1}{2V}\sum_{i=1}^{N}(r_{i,\beta}F_{i,\alpha}^{(p)} + r_{i,\alpha}F_{i,\beta}^{(p)}). \tag{2.8}$$

In simple shear flows, the only non-zero components of $\tilde{\sigma}_{\alpha\beta}(\boldsymbol{\Gamma})$ are $\tilde{\sigma}_{xy}(\boldsymbol{\Gamma})$ and the diagonal ones, from which the microscopic pressure is given by $\tilde{P}(\boldsymbol{\Gamma}) = -(\tilde{\sigma}_{xx}(\boldsymbol{\Gamma}) + \tilde{\sigma}_{yy}(\boldsymbol{\Gamma}) + \tilde{\sigma}_{zz}(\boldsymbol{\Gamma}))/3$. Note that we mainly consider the Cauchy stress, which contributes to the divergence at $\varphi \approx \varphi_J$, but it is possible to define the kinetic stress by the peculiar velocity.

2.2. *Exact equations for the stress*

Macroscopic equation of continuity of the stress tensor is obtained by multiplying (2.7) by the non-equilibrium distribution function $f(\boldsymbol{\Gamma}, t)$ and integrating over $\boldsymbol{\Gamma}$,

$$\frac{\mathrm{d}}{\mathrm{d}t}\sigma_{\alpha\beta} + \frac{1}{2}\dot{\gamma}(\delta_{\alpha x}\sigma_{y\beta} + \delta_{\beta x}\sigma_{y\alpha}) = -\frac{1}{2V}\sum_{i}\left\langle \sum_{j}\zeta_{ij}^{(N)-1}F_{j,\beta}^{(p)}F_{i,\alpha}^{(p)}\right\rangle + (\alpha \leftrightarrow \beta)$$
$$-\frac{1}{2V}{\sum_{i,j}}'\left\langle \sum_{k}\zeta_{ik}^{(N)-1}F_{k,\lambda}^{(p)}r_{j,\beta}\frac{\partial F_{j,\alpha}^{(p)}}{\partial r_{i,\lambda}}\right\rangle + (\alpha \leftrightarrow \beta), \tag{2.9}$$

where

$$\langle \cdots \rangle := \int \mathrm{d}\boldsymbol{\Gamma} f(\boldsymbol{\Gamma}, t)\cdots \tag{2.10}$$

is the macroscopic average, $\sum_{i,j}'$ denotes the summation over i and j with $i \neq j$ and the macroscopic stress tensor denotes

$$\sigma_{\alpha\beta} := \int \mathrm{d}\boldsymbol{\Gamma} f(\boldsymbol{\Gamma}, t)\tilde{\sigma}_{\alpha\beta}(\boldsymbol{\Gamma}). \tag{2.11}$$

It might be noteworthy that the equation of continuity of the stress tensor, equation (2.9), is consistent with that for the Enskog theory of moderately dense inertial suspensions (Hayakawa, Takada & Garzó 2017). In fact, the two terms on the right-hand side of (2.9), which are proportional to $\zeta_{ij}^{(N)-1}$ and originate from particle contacts, correspond to the collision integral terms in the Enskog theory.

3. Approximate expression of the interparticle force for dense frictionless hard spheres

To proceed, let us derive the specific form of the interparticle force $\boldsymbol{F}_i^{(p)}(\{\boldsymbol{r}_j\}_{j=1}^N)$ for dense frictionless hard spheres. For dense spheres where all of them are at or close to contact, we can expect that the far-field part of $\overleftrightarrow{\zeta}^{(N)}(\{\boldsymbol{r}_i\}_{i=1}^N)$ does not contribute and only the lubrication part, which is well approximated by the sum of the two-body terms $\overleftrightarrow{\zeta}_{lub}^{(2)}(\boldsymbol{r}_{ij})$, is significant (Kim & Karrila 2005; Seto *et al.* 2013; Mari *et al.* 2014). Thus, we approximate the resistance matrix $\overleftrightarrow{\zeta}^{(N)}$ as

$$\overleftrightarrow{\zeta}^{(N)}(\{\boldsymbol{r}_i\}_{i=1}^N) \approx \zeta_0 \boldsymbol{I} + \overleftrightarrow{\zeta}_{lub}^{(2)}(\boldsymbol{r}_{ij}), \tag{3.1}$$

where the first term on the right-hand side with $\zeta_0 := 3\pi\eta_0 d$ and $\boldsymbol{I}$ the unit matrix is the Stokesean one-body drag force. This leads to the approximate equation of motion

$$\zeta_0(\dot{\boldsymbol{r}}_i - \dot{\gamma} y_i \boldsymbol{e}_x) + \sum_{j\neq i} \zeta^{(2)}_{lub,ij}(\dot{\boldsymbol{r}}_j - \dot{\gamma} y_j \boldsymbol{e}_x) \approx \boldsymbol{F}^{(p)}_i. \tag{3.2}$$

Then, accordingly, the interparticle force should be well approximated by a sum of two-body forces,

$$\boldsymbol{F}^{(p)}_i \approx \sum_{j\neq i} \boldsymbol{F}^{(p)}_{ij}, \tag{3.3}$$

where $\boldsymbol{F}^{(p)}_{ij}$ is the two-body force exerted on particle i from j. The dynamics of the interacting two spheres is schematically described in figure 2. When the approaching two spheres come into contact (*a*), they slide in the tangential direction until they are aligned in the velocity-gradient direction (*b*), and then depart (*c*). In general, there are not only two but multiple of particles in contact, but every pair slides mutually in the tangential direction until their departure, so it is reasonable to consider the dynamics as a superposition of the two-body counterpart. Indeed, the simulation in terms of Stokesean dynamics is performed in terms of the superposition of the two-body interactions (Seto *et al.* 2013; Mari *et al.* 2014). Hence, it is sufficient to consider the two-body dynamics to determine $\boldsymbol{F}^{(p)}_{ij}$.

Let us consider two spheres i and j in contact. The equation of motion of the two spheres is given by

$$\zeta_0 \begin{bmatrix} \dot{\boldsymbol{r}}_i - \dot{\gamma} y_i \boldsymbol{e}_x \\ \dot{\boldsymbol{r}}_j - \dot{\gamma} y_j \boldsymbol{e}_x \end{bmatrix} + \overleftrightarrow{\zeta}^{(2)}_{lub}(\boldsymbol{r}_{ij}) \begin{bmatrix} \dot{\boldsymbol{r}}_i - \dot{\gamma} y_i \boldsymbol{e}_x \\ \dot{\boldsymbol{r}}_j - \dot{\gamma} y_j \boldsymbol{e}_x \end{bmatrix} = \begin{bmatrix} \boldsymbol{F}^{(p)}_{ij} \\ -\boldsymbol{F}^{(p)}_{ij} \end{bmatrix}, \tag{3.4}$$

where we have utilized $\boldsymbol{F}^{(p)}_{ji} = -\boldsymbol{F}^{(p)}_{ij}$. The matrix $\overleftrightarrow{\zeta}^{(2)}_{lub}$ is explicitly given by (Jeffrey & Onishi 1984)

$$\overleftrightarrow{\zeta}^{(2)}_{lub}(\boldsymbol{r}_{ij}) = \zeta_0 \begin{bmatrix} \Pi(\boldsymbol{r}_{ij}) & -\Pi(\boldsymbol{r}_{ij}) \\ -\Pi(\boldsymbol{r}_{ij}) & \Pi(\boldsymbol{r}_{ij}) \end{bmatrix}, \tag{3.5}$$

$$\Pi(\boldsymbol{r}_{ij}) := \frac{1}{8}\frac{1}{\delta r_{ij} + \epsilon} P_{ij} + \frac{1}{12} \ln \frac{1}{\delta r_{ij} + \epsilon} P'_{ij}, \tag{3.6}$$

where $\zeta_0 := 3\pi\eta_0 d$, $\delta r_{ij} := r_{ij} - d$ and $P_{ij} := \hat{\boldsymbol{r}}_{ij}\hat{\boldsymbol{r}}_{ij}$, $P'_{ij} := \boldsymbol{I} - \hat{\boldsymbol{r}}_{ij}\hat{\boldsymbol{r}}_{ij}$ are projection operators. At contact, i.e. $\delta r_{ij} = 0$, $\overleftrightarrow{\zeta}^{(2)}_{lub}$ exhibits singularities of the form ϵ^{-1} and $\ln \epsilon^{-1}$, where ϵ is a cut off which is physically interpreted as e.g. surface roughness. In this work we keep ϵ finite and do not consider these singularities. Then, equation (3.4) is given by

$$\zeta_0 \begin{bmatrix} (\dot{\boldsymbol{r}}_i - \dot{\gamma} y_i \boldsymbol{e}_x) + \dfrac{1}{8\epsilon} P_{ij} \cdot (\dot{\boldsymbol{r}}_{ij} - \dot{\gamma} y_{ij} \boldsymbol{e}_x) + \dfrac{1}{12} \ln \epsilon^{-1} P'_{ij} \cdot (\dot{\boldsymbol{r}}_{ij} - \dot{\gamma} y_{ij} \boldsymbol{e}_x) \\ (\dot{\boldsymbol{r}}_j - \dot{\gamma} y_j \boldsymbol{e}_x) - \dfrac{1}{8\epsilon} P_{ij} \cdot (\dot{\boldsymbol{r}}_{ij} - \dot{\gamma} y_{ij} \boldsymbol{e}_x) - \dfrac{1}{12} \ln \epsilon^{-1} P'_{ij} \cdot (\dot{\boldsymbol{r}}_{ij} - \dot{\gamma} y_{ij} \boldsymbol{e}_x) \end{bmatrix} = \begin{bmatrix} \boldsymbol{F}^{(p)}_{ij} \\ -\boldsymbol{F}^{(p)}_{ij} \end{bmatrix}. \tag{3.7}$$

By subtracting the two equations, equation (3.7) reduces to

$$\boldsymbol{F}_{ij}^{(p)} = \zeta_0 \left[\frac{1}{2}(\dot{\boldsymbol{r}}_{ij} - \dot{\gamma} y_{ij} \boldsymbol{e}_x) + \frac{1}{8\epsilon} P_{ij} \cdot (\dot{\boldsymbol{r}}_{ij} - \dot{\gamma} y_{ij} \boldsymbol{e}_x) + \frac{1}{12} \ln \epsilon^{-1} P'_{ij} \cdot (\dot{\boldsymbol{r}}_{ij} - \dot{\gamma} y_{ij} \boldsymbol{e}_x) \right], \quad (3.8)$$

where the right-hand side consists of the Stokesean drag force (first term), the normal lubrication force (second term) and the tangential lubrication force (third term). These three terms are of the order of 1, ϵ^{-1} and $\ln \epsilon^{-1}$, respectively. The second term is dominant for $\epsilon \ll 1$, so (3.8) is reduced to

$$\boldsymbol{F}_{ij}^{(p)} \approx \frac{\zeta_0}{8\epsilon} P_{ij} \cdot (\dot{\boldsymbol{r}}_{ij} - \dot{\gamma} y_{ij} \boldsymbol{e}_x) = \frac{\zeta_0}{8\epsilon} (\hat{\boldsymbol{r}}_{ij} \cdot \dot{\boldsymbol{r}}_{ij} - \dot{\gamma} r_{ij} \hat{y}_{ij} \hat{x}_{ij}) \hat{\boldsymbol{r}}_{ij}. \quad (3.9)$$

For hard spheres, the relative velocity of i and j is in the direction perpendicular to $\hat{\boldsymbol{r}}_{ij}$ in order not to overlap, i.e. $\hat{\boldsymbol{r}}_{ij} \cdot \dot{\boldsymbol{r}}_{ij} = 0$ or $P_{ij} \cdot \dot{\boldsymbol{r}}_{ij} = 0$ (cf. figure 2*a*). Then we obtain

$$\boldsymbol{F}_{ij}^{(p)} = -\tfrac{1}{2} \zeta_e \dot{\gamma} r_{ij} \hat{x}_{ij} \hat{y}_{ij} \hat{\boldsymbol{r}}_{ij}, \quad (3.10)$$

where we have defined

$$\zeta_e := \frac{\zeta_0}{4\epsilon} = \frac{3\pi\eta_0 d}{4\epsilon}. \quad (3.11)$$

Note that (3.10) is valid only at contact, i.e. $r_{ij} = d$, and $\boldsymbol{F}_{ij}^{(p)} = 0$ for $r_{ij} > d$ for hard spheres. That is, $\boldsymbol{F}_{ij}^{(p)} \propto \delta(r_{ij} - d)$. Thus we modify (3.10) by replacing r_{ij} with $d^2 \delta(r_{ij} - d)$,

$$\boldsymbol{F}_{ij}^{(p)} = -\tfrac{1}{2} \zeta_e \dot{\gamma} d^2 \delta(r_{ij} - d) \hat{x}_{ij} \hat{y}_{ij} \hat{\boldsymbol{r}}_{ij}. \quad (3.12)$$

Note that $\boldsymbol{F}_{ij}^{(p)} \propto \delta(r_{ij} - d)$ results in an important feature that the spatial correlations are expressed solely by (Donev *et al.* 2005)

$$g_0(\varphi) \sim (\varphi_J - \varphi)^{-1}, \quad (3.13)$$

where there is no dependence on its spatial derivative, $g'(r)$, because our dynamics inhibits the overlap of the contacting particles.

Furthermore, in order for $\boldsymbol{F}_{ij}^{(p)}$ to be a repulsive force, $\hat{x}_{ij} \hat{y}_{ij} < 0$ is necessary. Hence, we introduce a projection operator

$$\mathcal{P}(\hat{x}, \hat{y}) := -\hat{x}\hat{y}\Theta(-\hat{x}\hat{y}) > 0 \quad (3.14)$$

to assure this property,

$$\boldsymbol{F}_{ij}^{(p)} = \tfrac{1}{2} \zeta_e \dot{\gamma} d^2 \delta(r_{ij} - d) \mathcal{P}(\hat{x}_{ij}, \hat{y}_{ij}) \hat{\boldsymbol{r}}_{ij}. \quad (3.15)$$

Here, $\Theta(x)$ is Heaviside's step function, i.e. $\Theta(x) = 1$ for $x > 0$ and $\Theta(x) = 0$ otherwise. The projection operator in (3.15) implies that $\boldsymbol{F}_{ij}^{(p)}$ is non-zero only when the separation vector of the contacting two spheres $\boldsymbol{r}_{ij} := \boldsymbol{r}_i - \boldsymbol{r}_j$ is in the compression quadrant (cf. figure 1). This results from the approximation where we have neglected the first and third terms in the right-hand side of (3.8). In fact, these two terms are in general non-zero, irrespective of the direction of $\boldsymbol{r}_{ij}$. Hence, although the direction

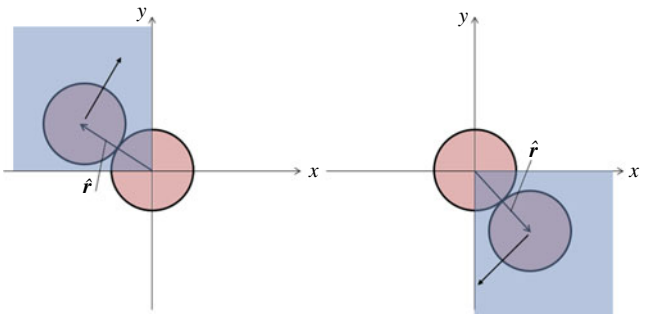

FIGURE 1. (Colour online) Dominant relative position of spheres in contact. The arrows perpendicular to $\hat{\boldsymbol{r}}$ show the direction of the velocity of the spheres.

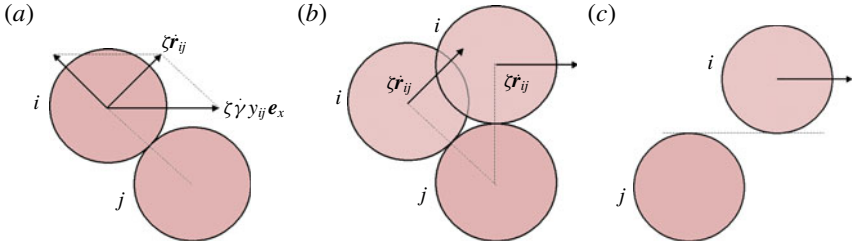

FIGURE 2. (Colour online) Dynamics of two spheres in contact: (*a*) instant of contact, (*b*) relative motion; two spheres in contact move relatively in the tangential direction until their departure, which occurs when they are aligned in the *y*-direction, (*c*) after departure.

of $\boldsymbol{r}_{ij}$ can be in any direction in dense suspensions, the dominant contribution of the interparticle force comes from configurations where $\boldsymbol{r}_{ij}$ is in the compression quadrant. To summarize, the equation of motion for dense hard-sphere suspensions is reduced to

$$\zeta_0(\dot{\boldsymbol{r}}_i - \dot{\gamma}y_i\boldsymbol{e}_x) + \sum_{j\neq i}\zeta^{(2)}_{lub,ij}(\dot{\boldsymbol{r}}_j - \dot{\gamma}y_j\boldsymbol{e}_x) = \sum_{j\neq i}\boldsymbol{F}^{(p)}_{ij}, \tag{3.16}$$

where the two-body interparticle force $\boldsymbol{F}^{(p)}_{ij}$ is given by (3.15), and the summation is over the contacting particles. Note that (3.16) is exact, under the assumption that the interparticle force is expressed as a superposition of two-body forces, equation (3.3), and hydrodynamic forces other than the lubrication force are neglected, equation (3.1).

In (2.9), not only the interparticle force $\boldsymbol{F}^{(p)}_i$ but also the inverse of the resistance matrix $\zeta^{(N)-1}_{ij}$ should be evaluated. We assume that $\zeta^{(N)-1}_{ij}$ can be approximated by the sum of the two-body mobility matrix $\overleftrightarrow{\mathcal{M}^{(2)}}$ as

$$\boldsymbol{v}_i = \dot{\boldsymbol{r}}_i - \dot{\gamma}y_i\boldsymbol{e}_x = \sum_{j=1}^{N}\zeta^{(N)-1}_{ij}\boldsymbol{F}^{(p)}_j \approx \sum_{j=1}^{N}\mathcal{M}^{(2)}_{ij}\boldsymbol{F}^{(p)}_j \tag{3.17}$$

for dense suspensions. Let us consider the two-body dynamics to evaluate the right-hand side of (3.17),

$$\begin{bmatrix}\boldsymbol{v}_i\\ \boldsymbol{v}_j\end{bmatrix} = \overleftrightarrow{\mathcal{M}^{(2)}}(\boldsymbol{r}_{ij})\begin{bmatrix}\boldsymbol{F}^{(p)}_i\\ \boldsymbol{F}^{(p)}_j\end{bmatrix} = \overleftrightarrow{\mathcal{M}^{(2)}}(\boldsymbol{r}_{ij})\begin{bmatrix}\boldsymbol{F}^{(p)}_{ij}\\ -\boldsymbol{F}^{(p)}_{ij}\end{bmatrix}, \tag{3.18}$$

where $\overleftrightarrow{\mathcal{M}}^{(2)}$ is explicitly given by (Rotne & Prager 1969)

$$\overleftrightarrow{\mathcal{M}^{(2)}}(\boldsymbol{r}_{ij}) = \frac{1}{3\pi\eta_0 d}\begin{bmatrix} \boldsymbol{I} & \boldsymbol{\Xi}(\boldsymbol{r}_{ij}) \\ \boldsymbol{\Xi}(\boldsymbol{r}_{ij}) & \boldsymbol{I} \end{bmatrix}, \tag{3.19}$$

$$\boldsymbol{\Xi}(\boldsymbol{r}_{ij}) := \left[\frac{3}{4}\frac{\mathrm{d}}{r_{ij}} - \left(\frac{\mathrm{d}}{2r_{ij}}\right)^3\right] P_{ij} + \left[\frac{3}{8}\frac{\mathrm{d}}{r_{ij}} + \frac{1}{2}\left(\frac{\mathrm{d}}{2r_{ij}}\right)^3\right] P'_{ij}. \tag{3.20}$$

Here, $P_{ij} := \hat{\boldsymbol{r}}_{ij}\hat{\boldsymbol{r}}_{ij}$ and $P'_{ij} := \boldsymbol{I} - \hat{\boldsymbol{r}}_{ij}\hat{\boldsymbol{r}}_{ij}$ are projection operators, as defined before. At contact, equation (3.18) is explicitly written by

$$\begin{bmatrix} \boldsymbol{v}_i \\ \boldsymbol{v}_j \end{bmatrix} = \frac{1}{3\pi\eta_0 d}\begin{bmatrix} \boldsymbol{F}_{ij}^{(p)} - \left[\frac{3}{4}\frac{\mathrm{d}}{r_{ij}} - \left(\frac{\mathrm{d}}{2r_{ij}}\right)^3\right]\boldsymbol{F}_{ij}^{(p)} \\ -\boldsymbol{F}_{ij}^{(p)} + \left[\frac{3}{4}\frac{\mathrm{d}}{r_{ij}} - \left(\frac{\mathrm{d}}{2r_{ij}}\right)^3\right]\boldsymbol{F}_{ij}^{(p)} \end{bmatrix} \approx \frac{1}{8\pi\eta_0 d}\begin{bmatrix} \boldsymbol{F}_{ij}^{(p)} \\ -\boldsymbol{F}_{ij}^{(p)} \end{bmatrix}, \tag{3.21}$$

where we have utilized the projection properties, $P_{ij}\cdot\boldsymbol{F}_{ij}^{(p)} = \boldsymbol{F}_{ij}^{(p)}$ and $P'_{ij}\cdot\boldsymbol{F}_{ij}^{(p)} = 0$ which follow from $\boldsymbol{F}_{ij}^{(p)} \propto \hat{\boldsymbol{r}}_{ij}$, and $r_{ij} \approx d$. Hence, equation (3.17) is evaluated as

$$\boldsymbol{v}_i = \sum_{j=1}^{N} \zeta_{ij}^{(N)-1}\boldsymbol{F}_j^{(p)} \approx \frac{1}{8\pi\eta_0 d}\sum_{j\neq i}\boldsymbol{F}_{ij}^{(p)}, \tag{3.22}$$

where the summation is over the contacting particles.

4. Approximate formulas for the viscosities and μ–J rheology

In § 3, we have derived approximate expressions for the interparticle force and the inverse of the resistance matrix, which appear in the right-hand side of the exact equation of the stress tensor, equation (2.9). Using these expressions, i.e. (3.15) and (3.22), an approximate equation for the stress tensor can be derived. The first term on the right-hand side of (2.9) is evaluated as

$$\begin{aligned} \sum_{i=1}^{N}\left\langle \sum_j \zeta_{ij}^{(N)-1} F_{j,\beta}^{(p)} F_{i,\alpha}^{(p)} \right\rangle &\approx \frac{1}{8\pi\eta_0 d}\sum_{i=1}^{N}\left\langle \sum_{j\neq i} F_{ij,\beta}^{(p)} \sum_{k\neq i} F_{ik,\alpha}^{(p)} \right\rangle \\ &= \frac{1}{4}\frac{\zeta_e^2}{8\pi\eta_0 d}\dot{\gamma}^2 d^4 \sum_{i=1}^{N}\left\langle \sum_{j\neq i}\sum_{k\neq i} \Delta_{ij}^{xy}\hat{r}_{ij,\beta}\Delta_{ik}^{xy}\hat{r}_{ik,\alpha} \right\rangle \\ &= \frac{1}{4}\zeta\dot{\gamma}^2 d^4 \sum_{i=1}^{N}\left\langle \sum_{j\neq i}\sum_{k\neq i} \Delta_{ij}^{xy}\hat{r}_{ij,\beta}\Delta_{ik}^{xy}\hat{r}_{ik,\alpha} \right\rangle, \end{aligned} \tag{4.1}$$

where we have introduced

$$\Delta_{ij}^{\alpha\beta} := -\delta(r_{ij} - d)\hat{r}_{ij,\alpha}\hat{r}_{ij,\beta}\Theta(-\hat{x}_{ij}\hat{y}_{ij}) \tag{4.2}$$

and

$$\zeta := \frac{\zeta_e^2}{8\pi\eta_0 d} = \frac{3}{32}\frac{\zeta_e}{\epsilon} = \frac{3}{128}\frac{\zeta_0}{\epsilon^2} \tag{4.3}$$

for abbreviation. For the second term on the right-hand side of (2.9) which includes a derivative of the interparticle force, special attention should be paid. Here, we only show the results (see appendix A for the detailed derivation):

$$\sum_{i,j}{}' \left\langle \sum_k \zeta_{ik}^{(N)-1} F_{k,\lambda}^{(p)} r_{j,\beta} \frac{\partial F_{j,\alpha}^{(p)}}{\partial r_{i,\lambda}} \right\rangle \approx \frac{1}{4}\zeta\dot{\gamma}^2 d^4 \sum_{i=1}^{N} \left\langle \sum_{j\neq i}\sum_{k\neq i} \Delta_{ij}^{xy}\hat{r}_{ij,\alpha}\Delta_{ik}^{xy}\hat{r}_{ik,\beta} + \Delta_{ik}^{xy}\Delta_{ij}^{\alpha\beta}(\hat{x}_{ik}\hat{y}_{ij}+\hat{y}_{ik}\hat{x}_{ij}) \right\rangle. \tag{4.4}$$

From (2.9), (4.1) and (4.4), we obtain an approximate equation for the stress evolution:

$$\frac{\mathrm{d}}{\mathrm{d}t}\sigma_{\alpha\beta} + \frac{1}{2}\dot{\gamma}(\delta_{\alpha x}\sigma_{y\beta}+\delta_{\beta x}\sigma_{y\alpha}) \approx -\zeta\dot{\gamma}^2\frac{d^4}{4V}\sum_{i=1}^{N}\sum_{j\neq i}\sum_{k\neq i}\langle\Delta_{ij}^{xy}\Delta_{ik}^{xy}\hat{r}_{ij,\alpha}\hat{r}_{ik,\beta}\rangle + (\alpha\leftrightarrow\beta)$$
$$-\zeta\dot{\gamma}^2\frac{d^4}{4V}\sum_{i=1}^{N}\sum_{j\neq i}\sum_{k\neq i}\langle\Delta_{ij}^{xy}\Delta_{ik}^{\alpha\beta}(\hat{x}_{ij}\hat{y}_{ik}+\hat{y}_{ij}\hat{x}_{ik})\rangle. \tag{4.5}$$

4.1. *Grad's 13-moment-like expansion*

To obtain the stress tensor from (4.5), it is still necessary to have the distribution function $f(\boldsymbol{\Gamma}, t)$ at hand to evaluate the statistical averages on the right-hand side. However, the exact expression of $f(\boldsymbol{\Gamma}, t)$ for many-body problems is unknown and thus we should resort to approximations. Here we adopt Grad's 13-moment-like expansion for $f(\boldsymbol{\Gamma}, t)$. This method is well established to approximate the distribution function in the kinetic theory of dilute or moderately dense gases (Grad 1949; Herdegen & Hess 1982; Jenkins & Richman 1985*b*,*a*; Tsao & Koch 1995; Sangani *et al.* 1996; Garzó 2002; Santos, Garzó & Dufty 2004; Kremer 2010; Garzó 2013; Chamorro, Reyes & Garzó 2015; Hayakawa & Takada 2016, 2017; Hayakawa *et al.* 2017). It is an expansion in terms of the heat and stress currents in addition to the five conserved currents for the collisional invariants. For simple shear without spatial inhomogeneity, the current for the heat and the conserved quantities are negligible, and hence the velocity distribution function is dominated by the stress current,

$$f(\boldsymbol{v}) \approx f_{eq}(\boldsymbol{v})\left[1+\frac{V}{2T_K}\Pi_{\alpha\beta}^{(K)}\tilde{\sigma}_{\alpha\beta}^{(K)}(\boldsymbol{v})\right], \tag{4.6}$$

where summation over repeated indices α, β is taken, e.g. $\sigma_{\alpha\alpha} := \mathrm{tr}(\sigma_{\alpha\beta}) = \sigma_{xx}+\sigma_{yy}+\sigma_{zz}$. Here, $\tilde{\sigma}_{\alpha\beta}^{(K)}(\boldsymbol{v}) := -mv_\alpha v_\beta/V$ is the microscopic kinetic stress, where m and $\boldsymbol{v}$ are the mass and velocity of the particle, $\Pi_{\alpha\beta}^{(K)} := \sigma_{\alpha\beta}^{(K)}/P^{(K)} + \delta_{\alpha\beta}$ is the normalized deviatoric stress, where $\sigma_{\alpha\beta}^{(K)} := \int \mathrm{d}\boldsymbol{v} f(\boldsymbol{v})\tilde{\sigma}_{\alpha\beta}^{(K)}(\boldsymbol{v})$ and $P^{(K)} := -\sigma_{\alpha\alpha}^{(K)}/3$ are the macroscopic kinetic stress and the pressure, $T_K := -\sigma_{\alpha\alpha}^{(K)}/(3n)$ is the kinetic temperature, where n is the average number density, and $f_{eq}(\boldsymbol{v})$ is the equilibrium distribution function. Note that the kinetic pressure satisfies the relation $P^{(K)} = nT_K$. This distribution function gives reasonably precise description of non-equilibrium gases, e.g. continuous as well as discontinuous shear thickening (Chamorro *et al.* 2015; Hayakawa & Takada 2016, 2017; Hayakawa *et al.* 2017). It is also notable

that (4.6) satisfies the Green–Kubo formula within the Bhatnagar–Gross–Krook (BGK) approximation (Hayakawa & Takada 2016), while it further incorporates the normal stress differences, which is not the case for the Green–Kubo formula.

The distribution function (4.6) cannot be directly applied to dense non-Brownian suspensions, where the Cauchy stress dominates the kinetic stress. A possible extension of this expansion for non-Brownian suspensions would be

$$f(\boldsymbol{\Gamma}, t) \approx f_{eq}(\boldsymbol{\Gamma}_v) f_{eq}(\boldsymbol{\Gamma}_r) \left[1 + \frac{V}{2T} \Pi_{\alpha\beta}(t) \tilde{\sigma}_{\alpha\beta}(\boldsymbol{\Gamma}_r)\right], \tag{4.7}$$

where $\boldsymbol{\Gamma} := \{\boldsymbol{\Gamma}_r, \boldsymbol{\Gamma}_v\}$ with $\boldsymbol{\Gamma}_r := \{\boldsymbol{r}_i\}_{i=1}^N$ and $\boldsymbol{\Gamma}_v := \{\boldsymbol{v}_i\}_{i=1}^N$, and the kinetic stress is replaced by the Cauchy stress. Here,

$$\Pi_{\alpha\beta} := \frac{\sigma_{\alpha\beta}}{P} + \delta_{\alpha\beta} \tag{4.8}$$

is the normalized deviatoric stress and the appropriate definition of the temperature T for non-Brownian suspensions will be discussed in § 4.4. Here it is postulated that the distribution function is factorized into peculiar velocity-dependent and position-dependent parts, where the peculiar velocity-dependent part can be approximated by Gaussian, $f_{eq}(\boldsymbol{\Gamma}_v)$, and the position-dependent part is approximated by an expansion around equilibrium, $f_{eq}(\boldsymbol{\Gamma}_r)$, with the stress current. This expansion around equilibrium is non-trivial for non-Brownian suspensions, where the equilibrium state is absent. Nonetheless, we will show in § 6 that the velocity distribution is nearly Gaussian and thus the factorization of (4.7) seems to be valid, and the expansion of the position distribution with the stress current is applicable for the evaluation of the stress.

From (4.7), the macroscopic average of an arbitrary observable $A(\boldsymbol{\Gamma}_r)$ which depends on $\boldsymbol{\Gamma}_r$ is given by

$$\langle A(\boldsymbol{\Gamma}_r(t))\rangle \approx \langle A(\boldsymbol{\Gamma}_r)\rangle_{eq} + \frac{V}{2T} \Pi_{\alpha\beta}(t) \langle A(\boldsymbol{\Gamma}_r) \tilde{\sigma}_{\alpha\beta}(\boldsymbol{\Gamma}_r)\rangle_{eq}, \tag{4.9}$$

where the first term on the right-hand side is the canonical term with

$$\langle \cdots \rangle_{eq} := \int \mathrm{d}\boldsymbol{\Gamma}_r f_{eq}(\boldsymbol{\Gamma}_r) \cdots \tag{4.10}$$

and the second term is its non-canonical correction. Note that (4.9) is formally equivalent to the multiple relaxation-time approximation of the Green–Kubo formula (Suzuki & Hayakawa 2015), where the dimensionless tensor $\Pi_{\alpha\beta}$ plays the role of the multiple relaxation times.

4.2. *Approximate expressions*

Let us evaluate the two averages on the right-hand side of (4.5) via the approximate formula (4.9). Detailed evaluation of the averages is shown in § B.1. These two averages are written as sums of terms of the form

$$\sum_{i=1}^{N} \sum_{j\neq i} \sum_{k\neq i} \langle X(\boldsymbol{r}_{ij}) Y(\boldsymbol{r}_{ik})\rangle, \tag{4.11}$$

where $X(\boldsymbol{r}_{ij})$ or $Y(\boldsymbol{r}_{ik})$ abbreviates term which depends on $\boldsymbol{r}_{ij}$ or $\boldsymbol{r}_{ik}$, respectively. For instance, for the first term on the right-hand side (4.5), $X(\boldsymbol{r}_{ij})$ and $Y(\boldsymbol{r}_{ik})$ are given by $X(\boldsymbol{r}_{ij}) = \hat{r}_{ij,\alpha}\Delta^{xy}_{ij}$, $Y(\boldsymbol{r}_{ik}) = \hat{r}_{ik,\beta}\Delta^{xy}_{ik}$, or $X(\boldsymbol{r}_{ij}) = \hat{r}_{ij,\beta}\Delta^{xy}_{ij}$, $Y(\boldsymbol{r}_{ik}) = \hat{r}_{ik,\alpha}\Delta^{xy}_{ik}$. Terms of the form (4.11) are evaluated by (4.9) as

$$\sum_{i=1}^{N}\sum_{j\neq i}\sum_{k\neq i}\langle X(\boldsymbol{r}_{ij})Y(\boldsymbol{r}_{ik})\rangle = \sum_{i=1}^{N}\sum_{j\neq i}\sum_{k\neq i}\left\{\langle X(\boldsymbol{r}_{ij})Y(\boldsymbol{r}_{ik})\rangle_{eq} + \frac{V}{2T}\Pi_{\rho\sigma}\langle X(\boldsymbol{r}_{ij})Y(\boldsymbol{r}_{ik})\tilde{\sigma}_{\rho\sigma}\rangle_{eq}\right\}. \tag{4.12}$$

Note that $\tilde{\sigma}_{\rho\sigma}$ depends on the relative coordinate, e.g. $\boldsymbol{r}_{lm}$, but either l or m must be identical to e.g. i; otherwise the correlation decouples and vanishes. Hence, the non-equilibrium term is given by

$$\sum_{i=1}^{N}\sum_{j\neq i}\sum_{k\neq i}\sum_{l\neq i}\langle X(\boldsymbol{r}_{ij})Y(\boldsymbol{r}_{ik})\tilde{\sigma}_{\rho\sigma}(\boldsymbol{r}_{il})\rangle_{eq}, \tag{4.13}$$

which can be decomposed into four-, three- and two-body correlations as

$$\sum_{i=1}^{N}\sum_{j\neq i}\sum_{k\neq i}\sum_{l\neq i}\langle X(\boldsymbol{r}_{ij})Y(\boldsymbol{r}_{ik})\tilde{\sigma}_{\rho\sigma}(\boldsymbol{r}_{il})\rangle_{eq} = \sum_{i,j,k,l}{}''' \langle X(\boldsymbol{r}_{ij})Y(\boldsymbol{r}_{ik})\tilde{\sigma}_{\rho\sigma}(\boldsymbol{r}_{il})\rangle_{eq} + \sum_{i,j,k}{}'' \langle X(\boldsymbol{r}_{ij})Y(\boldsymbol{r}_{ik})\tilde{\sigma}_{\rho\sigma}(\boldsymbol{r}_{ik})\rangle_{eq} + \sum_{i,j}{}' \langle X(\boldsymbol{r}_{ij})Y(\boldsymbol{r}_{ij})\tilde{\sigma}_{\rho\sigma}(\boldsymbol{r}_{ij})\rangle_{eq}. \tag{4.14}$$

Here, the four-, three- and two-body terms are given by

$$\sum_{i,j,k,l}{}''' \langle X(\boldsymbol{r}_{ij})Y(\boldsymbol{r}_{ik})\tilde{\sigma}_{\rho\sigma}(\boldsymbol{r}_{il})\rangle_{eq} = Nn^3\int \mathrm{d}^3\boldsymbol{r}\int \mathrm{d}^3\boldsymbol{r}'\int \mathrm{d}^3\boldsymbol{r}'' g^{(4)}(\boldsymbol{r},\boldsymbol{r}',\boldsymbol{r}'')X(\boldsymbol{r})Y(\boldsymbol{r}')\tilde{\sigma}_{\rho\sigma}(\boldsymbol{r}''), \tag{4.15}$$

$$\sum_{i,j,k}{}'' \langle X(\boldsymbol{r}_{ij})Y(\boldsymbol{r}_{ik})\tilde{\sigma}_{\rho\sigma}(\boldsymbol{r}_{ik})\rangle_{eq} = Nn^3\int \mathrm{d}^3\boldsymbol{r}\int \mathrm{d}^3\boldsymbol{r}' g^{(3)}(\boldsymbol{r},\boldsymbol{r}')X(\boldsymbol{r})Y(\boldsymbol{r}')\tilde{\sigma}_{\rho\sigma}(\boldsymbol{r}'), \tag{4.16}$$

$$\sum_{i,j(i\neq j)}{}' \langle X(\boldsymbol{r}_{ij})Y(\boldsymbol{r}_{ij})\tilde{\sigma}_{\rho\sigma}(\boldsymbol{r}_{ij})\rangle_{eq} = Nn^3\int \mathrm{d}^3\boldsymbol{r} g(r)X(\boldsymbol{r})Y(\boldsymbol{r})\tilde{\sigma}_{\rho\sigma}(\boldsymbol{r}), \tag{4.17}$$

respectively, where $g^{(4)}(\boldsymbol{r},\boldsymbol{r}',\boldsymbol{r}'')$ and $g^{(3)}(\boldsymbol{r},\boldsymbol{r}')$ are the quadruplet-correlation function (Hansen & McDonald 2006)

$$g^{(4)}(\boldsymbol{r},\boldsymbol{r}',\boldsymbol{r}'') := \frac{1}{Nn^3}\sum_{i,j,k,l}{}''' \langle\delta(\boldsymbol{r}-\boldsymbol{r}_{ij})\delta(\boldsymbol{r}'-\boldsymbol{r}_{ik})\delta(\boldsymbol{r}''-\boldsymbol{r}_{il})\rangle_{eq} \tag{4.18}$$

and the triplet-correlation function (Hansen & McDonald 2006)

$$g^{(3)}(\boldsymbol{r},\boldsymbol{r}') := \frac{1}{Nn^2}\sum_{i,j,k}{}'' \langle\delta(\boldsymbol{r}-\boldsymbol{r}_{ij})\delta(\boldsymbol{r}'-\boldsymbol{r}_{ik})\rangle_{eq}, \tag{4.19}$$

and the summations $\sum''_{i,j,k}$, and $\sum'''_{i,j,k,l}$ are performed over different particles. For instance, $\sum''_{i,j,k}$ is performed for i, j, k with $i \neq j$, $j \neq k$ and $k \neq i$. In the spatial integrations over $g(r)$, $g^{(3)}(\boldsymbol{r}, \boldsymbol{r}')$, or $g^{(4)}(\boldsymbol{r}, \boldsymbol{r}', \boldsymbol{r}'')$, it is crucial that these correlation functions are accompanied by the delta functions $\delta(r - d)$, $\delta(r - d)\delta(r' - d)$, or $\delta(r - d)\delta(r' - d)\delta(r'' - d)$, respectively. This feature can be explicitly traced back in (4.5), and is a consequence of the hard-core collision of the particles, equation (3.15). This implies that only the contact values of the correlation functions contribute. By virtue of this feature, we can conveniently approximate $g^{(3)}(\boldsymbol{r}, \boldsymbol{r}')$ and $g^{(4)}(\boldsymbol{r}, \boldsymbol{r}', \boldsymbol{r}'')$.

Let us consider $g^{(3)}(\boldsymbol{r}, \boldsymbol{r}')$ for illustration. First of all, we adopt the factorization approximation (Kirkwood 1935), $g^{(3)}(\boldsymbol{r}, \boldsymbol{r}') \approx g(r)g(r')g(|\boldsymbol{r} - \boldsymbol{r}'|)$. Although this approximation is not accurate in general, it has been argued that it is valid at contacts, where r, r', $|\boldsymbol{r} - \boldsymbol{r}'| \approx d$ (Alder 1964; Grouba, Zorin & Sevastianov 2004). Furthermore, we have shown in Suzuki & Hayakawa (2015) that only the radial contacts contribute to the divergence in the vicinity of the jamming point, i.e.

$$g^{(3)}(\boldsymbol{r}, \boldsymbol{r}') \approx g(r)g(r') \tag{4.20}$$

for $r, r' \approx d$. Similarly, $g^{(4)}(\boldsymbol{r}, \boldsymbol{r}', \boldsymbol{r}'')$ can be approximated as

$$g^{(4)}(\boldsymbol{r}, \boldsymbol{r}', \boldsymbol{r}'') \approx g(r)g(r')g(r'')g(|\boldsymbol{r} - \boldsymbol{r}'|)g(|\boldsymbol{r}' - \boldsymbol{r}''|)g(|\boldsymbol{r}'' - \boldsymbol{r}|) \approx g(r)g(r')g(r'') \tag{4.21}$$

for r, r', $r'' \approx d$, as far as divergence is concerned. We will examine the validity of the factorization approximation for the evaluation of the stress in § 6.

These approximations, together with $g(r)\delta(r - d) = g_0(\varphi)\delta(r - d)$, enable us to express the two averages on the right-hand side of (4.5) in terms of polynomials of the radial distribution function at contact, $g_0(\varphi)$. From tedious but straightforward calculation as shown in §§ B.1 and B.2, we reach the approximate equation of the stress

$$\begin{aligned}\frac{\mathrm{d}}{\mathrm{d}t}\sigma_{\alpha\beta} + \frac{1}{2}\dot{\gamma}(\delta_{\alpha x}\sigma_{y\beta} + \delta_{\beta x}\sigma_{y\alpha}) \approx \frac{\zeta\dot{\gamma}^2}{4d}\sum_{\ell=1}^{2}\{&-\varphi^{*3}g_0(\varphi)^2\mathcal{S}^{(\ell:c2)}_{\alpha\beta} - \varphi^{*2}g_0(\varphi)\mathcal{S}^{(\ell:c1)}_{\alpha\beta} \\ &+ \Lambda\Pi_{\rho\lambda}[\varphi^{*4}g_0(\varphi)^3\mathcal{S}^{(\ell:nc3)}_{\alpha\beta\rho\lambda} + \varphi^{*3}g_0(\varphi)^2\mathcal{S}^{(\ell:nc2)}_{\alpha\beta\rho\lambda} + \varphi^{*2}g_0(\varphi)\mathcal{S}^{(\ell:nc1)}_{\alpha\beta\rho\lambda}]\},\end{aligned} \tag{4.22}$$

where the two terms with coefficients $\mathcal{S}^{(\ell:c2)}_{\alpha\beta}$ and $\mathcal{S}^{(\ell:c1)}_{\alpha\beta}$ are the canonical contributions, and the three terms with coefficients $\mathcal{S}^{(\ell:nc3)}_{\alpha\beta\rho\lambda}$, $\mathcal{S}^{(\ell:nc2)}_{\alpha\beta\rho\lambda}$ and $\mathcal{S}^{(\ell:nc1)}_{\alpha\beta\rho\lambda}$ are the non-equilibrium corrections. The coefficients $\mathcal{S}^{(\ell:c1)}_{\alpha\beta}$, $\mathcal{S}^{(\ell:c2)}_{\alpha\beta}$ and $\mathcal{S}^{(\ell:nc3)}_{\alpha\beta\rho\lambda}$, $\mathcal{S}^{(\ell:nc2)}_{\alpha\beta\rho\lambda}$, $\mathcal{S}^{(\ell:nc1)}_{\alpha\beta\rho\lambda}$ are numbers which arise from angular integrals. Here, we have introduced a dimensionless scalar

$$\Lambda := \frac{\zeta\dot{\gamma}d^2}{4T}, \tag{4.23}$$

and $\varphi^* = 6\varphi/\pi = nd^3$ denotes the dimensionless number density.

4.3. *Implications of the symmetry*

A specific feature of non-Brownian suspensions under simple shear is the symmetry under the parity '$\hat{x} \to -\hat{x}$ and $\hat{y} \to -\hat{y}$', which follows from $\mathcal{P}(\hat{x}, \hat{y})$ introduced in (3.14). This implies that only the parity-even terms in (4.22) survive. Furthermore,

even though parity even, terms odd with respect to $\hat{z}$ vanish. These features can be summarized as follows,

$$\int \mathrm{d}\mathcal{S}\, \Theta(-\hat{x}\hat{y})\hat{x}^i\hat{y}^j\hat{z}^k \neq 0 \quad \text{if and only if } i+j=\text{even and } k=\text{even}, \tag{4.24}$$

where $\int \mathrm{d}\mathcal{S}\cdots$ expresses an angular integral with respect to $\hat{\boldsymbol{r}}$. As a consequence of this property we have

$$\int \mathrm{d}\mathcal{S}\Theta(-\hat{x}\hat{y})\hat{x}^i\hat{y}^j\hat{z}^k = 0 \quad \text{if } i+j+k=\text{odd}. \tag{4.25}$$

The terms proportional to $g_0(\varphi)^3$ in (4.22), which are cubic with respect to $\hat{\boldsymbol{r}}$, vanish because of (4.25),

$$\mathcal{S}^{(1:nc3)}_{\alpha\beta\rho\lambda} = \mathcal{S}^{(2:nc3)}_{\alpha\beta\rho\lambda} = 0. \tag{4.26}$$

The same observation holds for the canonical terms proportional to $g_0(\varphi)^2$, which are also cubic in $\hat{\boldsymbol{r}}$,

$$\mathcal{S}^{(1:c2)}_{\alpha\beta} = \mathcal{S}^{(2:c2)}_{\alpha\beta} = 0. \tag{4.27}$$

From (4.26) and (4.27), (4.22) reduces to

$$\begin{aligned}\frac{\mathrm{d}}{\mathrm{d}t}\sigma_{\alpha\beta} + \frac{1}{2}\dot{\gamma}(\delta_{\alpha x}\sigma_{y\beta} + \delta_{\beta x}\sigma_{y\alpha}) \approx \frac{\zeta\dot{\gamma}^2}{4d}\sum_{\ell=1}^{2}\{-\varphi^{*2}g_0(\varphi)\mathcal{S}^{(\ell:c1)}_{\alpha\beta} \\ + \Lambda\Pi_{\rho\lambda}[\varphi^{*3}g_0(\varphi)^2\mathcal{S}^{(\ell:nc2)}_{\alpha\beta\rho\lambda} + \varphi^{*2}g_0(\varphi)\mathcal{S}^{(\ell:nc1)}_{\alpha\beta\rho\lambda}]\},\end{aligned} \tag{4.28}$$

or, explicitly in components,

$$\frac{\mathrm{d}}{\mathrm{d}t}\begin{pmatrix}\sigma_{xy}\\ -3P\\ \sigma_{xx}\\ \sigma_{yy}\end{pmatrix} + \begin{pmatrix}\frac{1}{2}\sigma_{yy}\\ \sigma_{xy}\\ \sigma_{xy}\\ 0\end{pmatrix} \approx \frac{\zeta\dot{\gamma}}{4d}\varphi^{*2}g_0(\varphi)\left\{-\boldsymbol{\mathcal{B}} + \Lambda(\varphi^* g_0(\varphi)\boldsymbol{\mathcal{A}}^{(2)} + \boldsymbol{\mathcal{A}}^{(1)})\begin{pmatrix}\Pi_{xy}\\ \Pi_{xx}\\ \Pi_{yy}\end{pmatrix}\right\}, \tag{4.29}$$

where the matrices $\boldsymbol{\mathcal{A}}^{(m)}$ $(m=1,2)$ and the vector $\boldsymbol{\mathcal{B}}$ are given by (C 64)–(C 66). Note that $\Pi_{\alpha\beta}$ is given by (4.8) and hence (4.29) is a closed set of equations for P, σ_{xy}, σ_{xx} and σ_{yy}.

Note that (4.28) includes terms proportional to $g_0(\varphi)^2$ or $g_0(\varphi)$. Hence, we decompose the stress tensor as $\sigma_{\alpha\beta} = \sigma^{(2)}_{\alpha\beta} + \sigma^{(1)}_{\alpha\beta}$, where $\sigma^{(m)}_{\alpha\beta}$ is $O(g_0(\varphi)^m)$ $(m = 1, 2)$, because (3.13) suggests that it is separable near the jamming point. Then, equation (4.28) is cast into two equations, each for $\sigma^{(2)}_{\alpha\beta}$ and $\sigma^{(1)}_{\alpha\beta}$, respectively,

$$\frac{\mathrm{d}}{\mathrm{d}t}\sigma^{(2)}_{\alpha\beta} + \frac{1}{2}\dot{\gamma}(\delta_{\alpha x}\sigma^{(2)}_{\beta y} + \delta_{\beta x}\sigma^{(2)}_{\alpha y}) = \frac{\zeta\dot{\gamma}^2}{4d}\Lambda\varphi^{*3}g_0(\varphi)^2\Pi^{(2)}_{\rho\lambda}\sum_{\ell=1}^{2}\mathcal{S}^{(\ell:nc2)}_{\alpha\beta\rho\lambda}. \tag{4.30}$$

$$\frac{\mathrm{d}}{\mathrm{d}t}\sigma^{(1)}_{\alpha\beta} + \frac{1}{2}\dot{\gamma}(\delta_{\alpha x}\sigma^{(1)}_{\beta y} + \delta_{\beta x}\sigma^{(1)}_{\alpha y}) = \frac{\zeta\dot{\gamma}^2}{4d}\varphi^{*2}g_0(\varphi)\sum_{\ell=1}^{2}\{-\mathcal{S}^{(\ell:c1)}_{\alpha\beta} + \Lambda\Pi^{(1)}_{\rho\lambda}\mathcal{S}^{(\ell:nc1)}_{\alpha\beta\rho\lambda}\}. \tag{4.31}$$

Here, we have introduced

$$\Pi_{\alpha\beta}^{(m)} := \frac{\sigma_{\alpha\beta}^{(m)}}{P^{(m)}} + \delta_{\alpha\beta} \quad (m = 1, 2), \tag{4.32}$$

where $P^{(m)}$ is the component of the pressure of $O(g_0(\varphi)^m)$ $(m = 1, 2)$. The valid range of (4.30) and (4.31) from (4.28) is discussed in § D.2.

Another implication of the symmetry is that the uniform profile of the velocity distribution is maintained. This issue is discussed in appendix G.

4.4. *Interpretation of the temperature*

In contrast to the case of the kinetic theory of dilute and moderately dense gases, or even dense inertial suspensions near the jamming point, the determination method of the temperature T is not clear for non-Brownian suspensions. As discussed in § 4.1, in the kinetic theory, the temperature is determined by the equation of state $P^{(K)} = nT_K$, where $P^{(K)}$ and T_K are the kinetic pressure and the kinetic temperature, respectively. We attempt to introduce the temperature by the Cauchy stress, which dominates the kinetic stress in dense non-Brownian suspensions. Because T appears in the position-dependent part in (4.7), T should be defined by the position-dependent Cauchy stress. Note that T determines the magnitude of the non-equilibrium correction of the distribution function, equation (4.7). Accordingly, Λ introduced in (4.23) determines the non-equilibrium correction of the stress, equations (4.28) or (4.29). In this paper, let us introduce T by the equation of state

$$P^{(eq)} = nT[1 + 2\varphi g_0(\varphi)], \tag{4.33}$$

where $P^{(eq)}$ is the equilibrium part of the pressure determined from (4.28), (4.29) or (4.31) with $\Lambda = 0$. In other words, $P^{(eq)}$ can be estimated only by $f_{eq}(\boldsymbol{\Gamma}_r)$ in (4.7). The solution of (4.31) is given in (D 2), (D 3) in § D.1, from which we obtain $P^{(eq)}$ as ($P^{(1)}$ with $\Lambda = 0$)

$$P^{(eq)} = 0.0060 \times \frac{\zeta\dot{\gamma}}{4d}\varphi^{*2} g_0(\varphi) = 0.022 \times \frac{\zeta\dot{\gamma}}{4d}\varphi^2 g_0(\varphi), \tag{4.34}$$

where $\varphi^* = 6\varphi/\pi$. Thus, from (4.33) and (4.34), we obtain

$$T = 0.022 \times \frac{\zeta\dot{\gamma}}{4nd}\frac{\varphi^2 g_0(\varphi)}{1 + 2\varphi g_0(\varphi)} \approx 0.022 \times \frac{\zeta\dot{\gamma}d^2}{8nd^3}\varphi = 0.0014\zeta\dot{\gamma}d^2, \tag{4.35}$$

where we have approximated $1 + 2\varphi g_0(\varphi) \approx 2\varphi g_0(\varphi)$ in the second equality. This determines Λ as

$$\Lambda = \frac{\zeta\dot{\gamma}d^2}{4T} \approx 174, \tag{4.36}$$

which is independent of dimensional physical variables such as $\dot{\gamma}$, d or η_0, and is merely a number. This value is larger than the value $\Lambda = 0.04$ determined by fitting the absolute values of the shear and pressure viscosities to the result of molecular dynamics (MD) simulation (cf. §§ 4.5 and 5). This might be due to the fact that ζ in (4.36) is not equivalent to ζ_0 which sets the magnitude of the viscosities in MD simulation. In fact, ζ is given by (4.3) as $\zeta = 3\zeta_0/(128\epsilon^2)$, where $\epsilon \ll 1$ is

the magnitude of the separation of contacting particles. The ratio $\zeta/\zeta_0 = 174/0.04$ corresponds to $\epsilon \approx 0.002$, but since we cannot determine the magnitude of ϵ in our framework, we will leave Λ as a fitting parameter.

The important implication of (4.35) is

$$T \propto \zeta \dot{\gamma} d^2 \propto 3\pi d^3 \eta_0 \dot{\gamma}, \tag{4.37}$$

which is consistent with the 'effective temperature' of suspensions (Ono *et al.* 2002; Eisenmann *et al.* 2010) defined via the Stokes–Einstein relation, $D = T_{eff}/(3\pi\,\mathrm{d}\eta_0)$, where D is the diffusion coefficient. It has been shown by experiment (Leighton & Acrivos 1987*a*,*b*; Breedveld *et al.* 1998, 2002; Eisenmann *et al.* 2010) and simulation (Foss & Brady 1999; Heussinger *et al.* 2010; Olsson 2010) that $D \sim \mathrm{d}^2\dot{\gamma}$ holds below the jamming point and D exhibits only a weak dependence on the density, which suggests $T_{eff} = 3\pi d\eta_0 D \sim 3\pi d^3\eta_0\dot{\gamma}$.

4.5. *Viscosities and μ–J rheology in the steady state*

Let us analyse the rheology in the steady state, i.e. consider (4.28) with $\mathrm{d}\sigma_{\alpha\beta}/\mathrm{d}t = 0$. Then, equations (4.30) and (4.31) can be solved analytically. The analytic solutions for $\sigma^{(2)}_{\alpha\beta}$ and $\sigma^{(1)}_{\alpha\beta}$ are given by (D 1)–(D 4) in § D.1, together with (3.13):

$$\sigma^{(2)}_{\alpha\beta} \sim \frac{\zeta\dot{\gamma}}{d} g_0(\varphi)^2 \sim \frac{\zeta\dot{\gamma}}{d}\delta\varphi^{-2}, \tag{4.38}$$

$$\sigma^{(1)}_{\alpha\beta} \sim \frac{\zeta\dot{\gamma}}{d} g_0(\varphi) \sim \frac{\zeta\dot{\gamma}}{d}\delta\varphi^{-1}. \tag{4.39}$$

In particular, the normalized shear viscosity $\eta^*_s := \eta_s/\eta_0$ and pressure viscosity $\eta^*_n := \eta_n/\eta_0$ are given by

$$\eta^*_s \approx 0.0073\varphi^{*3}\delta\varphi^{-2} + 0.080\varphi^{*2}\delta\varphi^{-1}, \tag{4.40}$$

$$\eta^*_n \approx 0.045\varphi^{*3}\delta\varphi^{-2} + 0.0005\varphi^{*2}\delta\varphi^{-1} \approx 0.045\varphi^{*3}\delta\varphi^{-2}, \tag{4.41}$$

where $\Lambda = 0.04$ is adopted, which is determined by fitting the absolute values of η^*_s and η^*_n to the results of the MD simulation shown in the next section. The empirical formula $g_0(\varphi) = g_{CS}(\varphi_f)(\varphi_J - \varphi_f)/(\varphi_J - \varphi)$ with $\varphi_f = 0.49$ and $g_{CS}(\varphi) := (1 - \varphi/2)/(1 - \varphi)^3$ valid for $\varphi_f < \varphi < \varphi_J$ (Torquato 1995) is adopted, from which we obtain $g_0(\varphi) \approx 0.848\,\delta\varphi^{-1}$ for $\varphi_J = 0.639$. Although it is widely recognized that $\varphi_J \approx 0.64$ for monodisperse frictionless hard spheres without any solvent, it has been reported that the value of φ_J is not uniquely identified and depends on the protocols used to generate the jammed configurations (Ciamarra, Coniglio & de Candia 2010). In this work, we adopt $\varphi_J = 0.639$, which is obtained by the conjugate-gradient protocol (O'Hern *et al.* 2003). The numerical coefficients in (4.40) and (4.41) are determined analytically in rational forms, but we only show their approximate values in decimals for brevity.

It is evident from (4.40) and (4.41) that η^*_s and η^*_n exhibit

$$\eta^*_s \sim \eta^*_n \sim \delta\varphi^{-2} \tag{4.42}$$

near the jamming point. On the other hand, $O(\delta\varphi^{-1})$ term in η^*_n is small for finite $\delta\varphi$, while the corresponding term in η^*_s is significant. Noting $J = 1/\eta^*_n$, J and $\delta\varphi$ are uniquely invertible via (4.41) as

$$J^{1/2} \approx 4.74\varphi^{*-3/2}\delta\varphi, \tag{4.43}$$

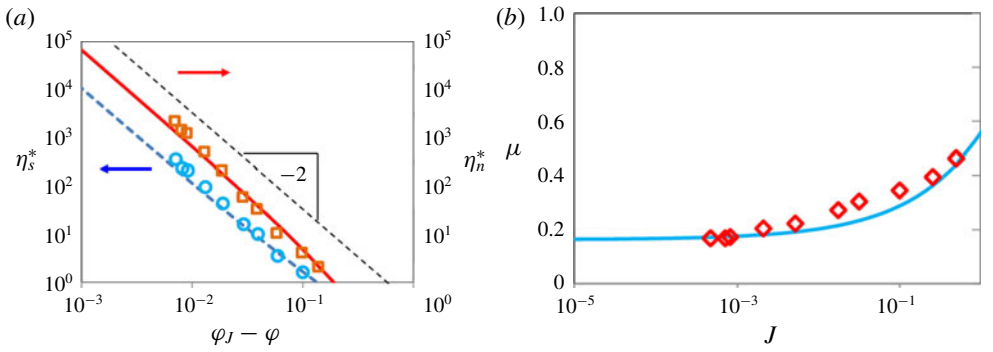

FIGURE 3. (Colour online) Comparison of theory with MD simulation. (*a*) The normalized shear viscosity $\eta_s^* = \eta_s/\eta_0$ and the pressure viscosity $\eta_n^* = \eta_n/\eta_0$, and (*b*) the stress ratio $\mu = \sigma_{xy}/P$. The results of the theory and MD for the shear (pressure) viscosity are shown in dashed (solid) lines and open circles (squares) in (*a*), and those for the stress ratio are shown in solid line and open diamonds in (*b*), respectively. The theoretical result adopts the fitting parameter $\Lambda = 0.04$. The result of MD is for $\varphi =$ 0.632, 0.631, 0.63, 0.626, 0.62, 0.61, 0.6, 0.58, 0.54 and 0.5.

or, equivalently,

$$\varphi = \varphi_J - 0.211\varphi^{*3/2}J^{1/2}. \tag{4.44}$$

From (4.40) and (4.41), we obtain the stress ratio μ as

$$\mu \approx 0.163 + 1.78\varphi^{*-1}\delta\varphi = 0.163 + 0.377\varphi^{*1/2}J^{1/2}. \tag{4.45}$$

Note that μ in the jamming limit, $\mu(J \to 0) = 0.163$, is independent of Λ.

5. Comparison with simulation and previous results

We compare our theory with the MD simulation and previous results. We adopt the algorithm for Brownian hard spheres (Scala, Voigtmann & Michele 2007) applied at zero thermal fluctuations for the MD simulation. By this choice the only source of the velocity fluctuation is the interparticle contacts. The resistance matrix is simplified to $\overleftrightarrow{\zeta}^{(N)} = \zeta_0 \boldsymbol{I}$, where $\zeta_0 := 3\pi d\,\eta_0$. The details of the simulation scheme is presented in appendix F.

We show the results for the normalized shear viscosity η_s^*, equation (4.40), pressure viscosity η_n^*, equation (4.41) and the stress ratio μ, equation (4.45), in figure 3. As is already mentioned, we adopt $\Lambda = 0.04$ as a fitting parameter for η_s^* and η_n^*. In the dense region, the theory predicts $\eta_s^* \sim \eta_n^* \sim \delta\varphi^{-2}$ in accordance with the MD result, and the stress ratio approaches $\mu(J \to 0) = 0.163$, which is also in good agreement with MD. Because there exists slight difference between η_s^* and η_n^* for finite $\delta\varphi$, we find that μ depends on J or $\delta\varphi$ (μ–J rheology). A reasonable agreement between our theory and MD is found, although the applicability for large J in our theory is questionable (see § D.2).

We compare our theory with previous results. It is notable that (4.43) and (4.45) are consistent with the experimental results $\delta\varphi \propto J^{1/2}$ and $\mu(J \to 0) \approx 0.32$ (Boyer *et al.* 2011). Discrepancy in the value of $\mu(J \to 0)$ might be caused by the friction or the hydrodynamic interaction between the particles. A comparison of the pressure viscosity with experimental results (Deboeuf *et al.* 2009; Dagois-Bohy *et al.* 2015) shows an agreement within a factor of 2 (see figure 4), and a comparison

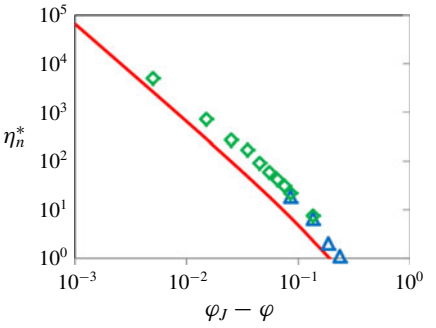

FIGURE 4. (Colour online) Comparison with experiments (Deboeuf *et al.* 2009; Dagois-Bohy *et al.* 2015). The results of the normalized pressure viscosity η_n^* are shown for our theory (solid line) and the experiments in Deboeuf *et al.* (2009) (open triangles) and Dagois-Bohy *et al.* (2015) (open diamonds). The theoretical result is for $\Lambda = 0.04$.

with empirical relations (Morris & Boulay 1999) also shows good agreement (see appendix E).

Next we discuss the results for the normal stress differences. The two normal stress differences, $N_1 = \sigma_{xx} - \sigma_{yy}$ and $N_2 = \sigma_{yy} - \sigma_{zz}$, are evaluated at $O(g_0(\varphi)^2)$ as

$$N_1 \approx -1.11\Lambda\Sigma^{(2)}, \tag{5.1}$$

$$N_2 \approx 0.576\Lambda\Sigma^{(2)}, \tag{5.2}$$

where $\Sigma^{(2)} := (\zeta\dot{\gamma}/4d)\varphi^{*3}g_0(\varphi)^2$. From these we see that $N_1 < 0$, $N_2 > 0$ and $N_1/N_2 \approx -1.9$, $N_2/P \approx 0.9$, which are independent of Λ. This is consistent with the experimental observation that $N_1 < 0$, $N_2 > 0$ and $N_1/N_2 = -2$ (Laun 1994). It should be noted, however, that the magnitudes and even the signs of the normal stress differences are controversial. For instance, Lootens *et al.* (2005) report that the sign of N_1 depends on the volume fraction, and Mari *et al.* (2014) exhibit $N_2 < 0$ and $|N_2| \gg |N_1|$, while Cwalina & Wagner (2014) assert N_1, $N_2 < 0$ and $|N_1| \approx |N_2|$. The pressure and the normal stress differences can be expressed in the form $P = \dot{\gamma}\eta_0\eta_n(1 + \lambda_2 + \lambda_3)/3$, $N_1 = -\dot{\gamma}\eta_0\eta_n(1 - \lambda_2)$, and $N_2 = -\dot{\gamma}\eta_0\eta_n(\lambda_2 - \lambda_3)$, where $\lambda_2 := \sigma_{yy}/\sigma_{xx}$ and $\lambda_3 := \sigma_{zz}/\sigma_{xx}$ (Morris & Boulay 1999). From (D 1), we obtain $\lambda_2 \approx 0.08$, $\lambda_3 \approx 0.56$, which are also independent of Λ. The value of λ_3 is close to the value $1/2$ determined in Morris & Boulay (1999). The value of λ_2 is left controversial as in Morris & Boulay (1999), but the assumed values such as 0.6, 0.8, or 1.0 are significantly larger than 0.08 in Morris & Boulay (1999).

Finally we clarify the difference between Brownian and non-Brownian suspensions. It is crucial in Brownian suspensions that the effective (long-time) self-diffusion constant $D_\infty(\varphi)$ vanishes at the jamming point, $D_\infty(\varphi) \sim \delta\varphi = \varphi_J - \varphi$, since the shear stress scales as $\sigma_{xy} \sim g_0(\varphi)/D_\infty(\varphi)$ (Brady 1993). In contrast, the above argument is not valid for non-Brownian suspensions. In fact, it is reported that $D_\infty(\varphi)$ increases as the density is increased and saturates at the jamming point (Leighton & Acrivos 1987*a*,*b*; Breedveld *et al.* 1998, 2002; Heussinger *et al.* 2010; Olsson 2010). This feature can be understood from the fact that, in non-Brownian suspensions, the source of the non-affine displacement is the contact interaction between the particles, rather than the fluctuating force from the solvent. It is obvious that the contact interaction is more significant in dense suspensions, which results in larger $D_\infty(\varphi)$. This feature

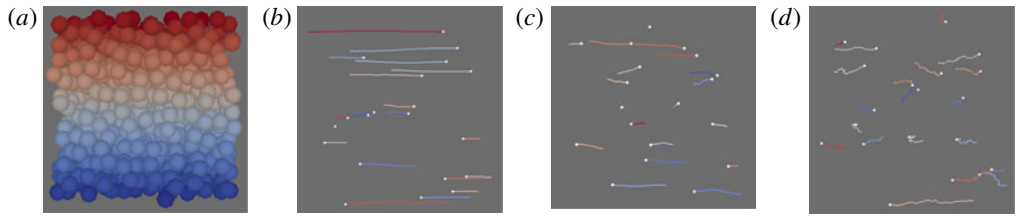

FIGURE 5. (Colour online) Trajectory of randomly sampled particles for $\varphi = 0.30, 0.60, 0.635$, from (*a*) to (*d*). The trajectory is ballistic for $\varphi = 0.30$, while it is diffusive for $\varphi = 0.635$.

can be seen in the trajectory of randomly sampled particles shown in figure 5. This clearly suggests that $\sigma_{xy} \sim \delta\varphi^{-2}$ is not the consequence of the diffusion constant in non-Brownian suspensions. Although the density dependence is similar, the underlying physics of the rheology is distinct for Brownian and non-Brownian suspensions.

6. Validation of the postulates

In this section we articulate the crucial postulates of our theory and report the results of the simulations performed for their verification. The postulates are

(i) the factorization of the distribution function into the peculiar velocity-dependent and position-dependent parts;
(ii) Grad's 13-moment-like expansion of the position-dependent distribution function, equation (4.7), which is an expansion around thermal equilibrium;
(iii) the factorization approximation of the multi-body correlations used in (4.20) and (4.21).

6.1. *Peculiar velocity distribution function*

The distribution of the peculiar velocity $\boldsymbol{v}_i = \dot{\boldsymbol{r}}_i - \dot{\gamma} y_i \boldsymbol{e}_x$ is measured by MD simulation. As shown in figure 6, the peculiar velocity distribution function is nearly Gaussian in spite of the absence of any inertial effect in the dynamics. This result implies that the factorization of the distribution function assumed in (4.7) is valid. The result of our simulation supports another theoretical assumption that the base state is nearly equilibrium.

6.2. *Grad's 13-moment-like expansion and factorization of multi-body correlations*

We validate the expansion of the distribution of the position with the stress current, equation (4.7). For this purpose, we consider the radial distribution function at the steady state, $g_{\dot{\gamma}}(\boldsymbol{r})$, which is anisotropic under shear. It is given by

$$g_{\dot{\gamma}}(\boldsymbol{r}) := \frac{1}{Nn}\left\langle \sum_i \sum_{j\neq i} \delta(\boldsymbol{r} - \boldsymbol{r}_{ij}) \right\rangle = \frac{1}{Nn}\int \mathrm{d}\boldsymbol{\Gamma} f(\boldsymbol{\Gamma}) \sum_i \sum_{j\neq i} \delta(\boldsymbol{r} - \boldsymbol{r}_{ij}). \tag{6.1}$$

From (4.7), after trivially integrating out $f_{eq}(\boldsymbol{\Gamma}_v)$, we obtain

$$g_{\dot{\gamma}}(\boldsymbol{r}) = g(r) + \frac{1}{Nn}\frac{V}{2T}\Pi_{\alpha\beta}\left\langle \sum_i \sum_{j\neq i} \delta(\boldsymbol{r} - \boldsymbol{r}_{ij})\tilde{\sigma}_{\alpha\beta} \right\rangle_{eq}, \tag{6.2}$$

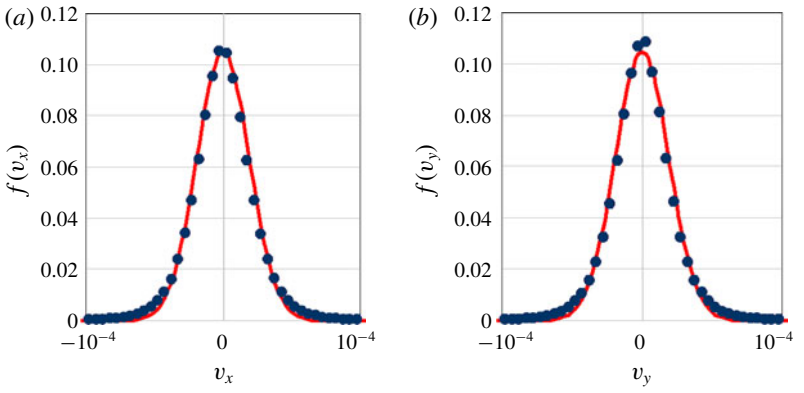

FIGURE 6. (Colour online) Distribution of the peculiar velocity measured by MD simulation (circles). The conditions are $\varphi = 0.63$, $N = 1000$, $\dot{\gamma}^* = 1 \times 10^{-5}$. The number of data averaged for each point is 10^5. The figure shows the x- and y-components. Also shown is the Gaussian distribution fitted to the measured data (solid line).

where $g(r)$ is the radial distribution function at equilibrium. By substituting the expression for the stress $\tilde{\sigma}_{\alpha\beta}$, equation (2.8) and that for the interparticle force $\boldsymbol{F}_{ij}^{(p)}$ therein, equation (3.8), we obtain

$$\begin{aligned} g_{\dot{\gamma}}(\boldsymbol{r}) &= g(r) - \frac{1}{Nn}\frac{\zeta_e \dot{\gamma} d^2}{8T} \Pi_{\alpha\beta} \left\langle \sum_i \sum_{j\neq i} \sum_{k\neq i} \delta(\boldsymbol{r} - \boldsymbol{r}_{ij}) r_{ik,\beta} \delta(r_{ik} - d) \mathcal{P}(\hat{x}_{ik}, \hat{y}_{ik}) \hat{r}_{ik,\alpha} \right\rangle_{eq} \\ &= g(r) - \frac{1}{Nn}\frac{\zeta_e \dot{\gamma} d^3}{8T} \Pi_{\alpha\beta} \left\langle \sum_i \sum_{j\neq i} \sum_{k\neq i} \delta(\boldsymbol{r} - \boldsymbol{r}_{ij}) \delta(r_{ik} - d) \mathcal{P}(\hat{x}_{ik}, \hat{y}_{ik}) \hat{r}_{ik,\alpha} \hat{r}_{ik,\beta} \right\rangle_{eq}. \end{aligned} \tag{6.3}$$

In the second equality, we have utilized $r_{ik,\beta}\delta(r_{ik} - d) = d\hat{r}_{ik,\beta}\delta(r_{ik} - d)$. Equation (6.3) is expressed in terms of the triplet-correlation function $g^{(3)}(\boldsymbol{r}, \boldsymbol{r}')$, equation (4.19), as

$$g_{\dot{\gamma}}(\boldsymbol{r}) = g(r) - n\frac{\zeta_e \dot{\gamma} d^3}{8T} \Pi_{\alpha\beta} \int \mathrm{d}^3\boldsymbol{r}' g^{(3)}(\boldsymbol{r}, \boldsymbol{r}') \delta(r' - d) \mathcal{P}(\hat{x}', \hat{y}') \hat{r}'_\alpha \hat{r}'_\beta. \tag{6.4}$$

We apply the factorization approximation to $g^{(3)}(\boldsymbol{r}, \boldsymbol{r}')$,

$$g^{(3)}(\boldsymbol{r}, \boldsymbol{r}') \approx g(r) g(r') [1 + h(|\boldsymbol{r} - \boldsymbol{r}'|)], \tag{6.5}$$

which leads to

$$\begin{aligned} g_{\dot{\gamma}}(\boldsymbol{r}) &\approx g(r) \left\{ 1 - n\frac{\zeta_e \dot{\gamma} d^3}{8T} \Pi_{\alpha\beta} \int \mathrm{d}^3\boldsymbol{r}' g(r') [1 + h(|\boldsymbol{r} - \boldsymbol{r}'|)] \delta(r' - d) \mathcal{P}(\hat{x}', \hat{y}') \hat{r}'_\alpha \hat{r}'_\beta \right\} \\ &= g(r) \left\{ 1 - n\frac{\zeta_e \dot{\gamma} d^5}{8T} g(d)\, \Pi_{\alpha\beta} \int \mathrm{d}\mathcal{S}' [1 + h(|\boldsymbol{r} - \boldsymbol{r}'|)] \mathcal{P}(\hat{x}', \hat{y}') \hat{r}'_\alpha \hat{r}'_\beta \right\}. \end{aligned} \tag{6.6}$$

Here, $h(r) = g(r) - 1$ is the pair-correlation function, and $\int \mathrm{d}\mathcal{S}' \cdots$ denotes angular integral with respect to $\hat{\boldsymbol{r}}'$.

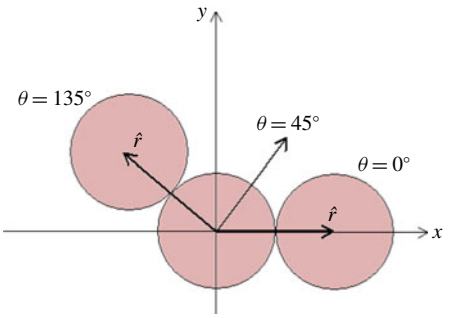

FIGURE 7. (Colour online) Definition of the angle of the separation vector. $\theta = 135°$ and $45°$ are the compressional and extensional directions of the shear, respectively: $\theta = 0°$ is the 'flow direction', which is the direction of the flow of the solvent.

Let us consider the angular dependence of the contact value of the radial distribution function in the (x, y)-plane. From (6.6), this is given by

$$g_{\dot\gamma}(d,\theta) \approx g(d)\left\{1 - n\frac{\zeta_e \dot\gamma d^5}{8T} g(d)\,\Pi_{\alpha\beta}\int \mathrm{d}\mathcal{S}'[1 + h(|\boldsymbol{r} - \boldsymbol{r}'|)]\mathcal{P}(\hat{x}', \hat{y}')\hat{r}'_\alpha \hat{r}'_\beta\right\}, \tag{6.7}$$

where θ is the angle of $\hat{\boldsymbol{r}}$ with respect to the x-axis, and $\theta = 135°$ and $45°$ are the directions of compression and extension, respectively (cf. figure 7). We adopt the approximate formula for the delta-function contribution of $h(r)$ (Donev *et al.* 2005),

$$h(r) \approx \frac{1}{4\varphi\delta}\left[\frac{6A}{\left(\dfrac{r/d-1}{\delta} + C\right)^4} + \frac{B}{\left(\dfrac{r/d-1}{\delta} + C\right)^2}\right], \tag{6.8}$$

where $\delta \approx (\varphi_J - \varphi)/(3\varphi_J)$ and $A = 3.43$, $B = 1.45$, $C = 2.25$. For the evaluation of the right-hand side of (6.7), we perform numerical integration.

The comparison of the both sides of (6.7) is shown in figure 8. The left-hand side is the radial distribution function at the steady state and measured by MD simulation (circles). The conditions for the simulation are described in the caption. The angular integration on the right-hand side has been evaluated as a double integral with respect to the two angles (ϕ_1, ϕ_2), where $\cos\phi_1 = \hat{\boldsymbol{r}} \cdot \hat{\boldsymbol{r}}'$ and ϕ_2 is the azimuthal angle of $\hat{\boldsymbol{r}}'$ around $\hat{\boldsymbol{r}}$. These angles are bounded in the range $\pi/3 < \phi_1 < \pi$ and $0 < \phi_2 < 2\pi$, respectively. The region $0 < \phi_1 < \pi/3$ is excluded to avoid overlap. The contact value of the equilibrium radial distribution function, $g(d)$, is given by $g_0(\varphi) \approx 0.848/(\varphi_J - \varphi)$ for $\varphi_J = 0.639$, which is approximately 100 for $\varphi = 0.63$. The result for the right-hand side shown in solid line in figure 8 is reduced to $1/3$ to fit the amplitude. We see that the peak in the compression direction ($\theta = 135°$) is captured by the theory, although the peak in the direction $\theta = 0°$ is not. The reason why the theory still reasonably predicts the stress is that the particles in contact with $\theta = 0°$ does not contribute to the stress, because they are driven with the same velocity by the uniform shear.

For further validation, we have measured the right-hand side of (4.7) directly by MD simulation. We measure the distribution of the microscopic stress $\tilde\sigma_{\alpha\beta}$ with respect to the angle of the separation vector $\boldsymbol{r}_{ij}$, which resides in the (x, y)-plane. To extract

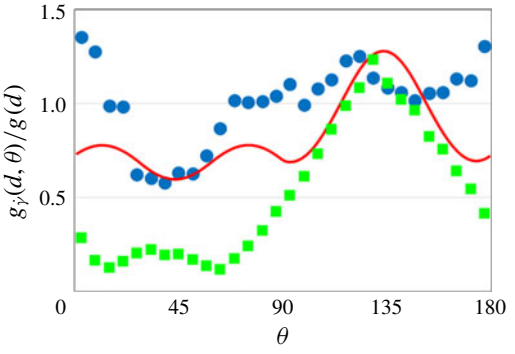

FIGURE 8. (Colour online) Angular distribution of the contact value of the radial distribution function at the steady state measured by MD simulation (circle). The conditions are $\varphi = 0.63$, $N = 1000$, $\dot{\gamma}^* = 1 \times 10^{-5}$. The number of data averaged for each point is 10^4. Also shown are the theoretical result of Grad's expansion (solid line) and the direct measurement of Grad's expansion (squares).

the contribution from the contacting pairs, we have assigned 1 to $f_{eq}(\boldsymbol{r}_{ij})$ when the two particles are in contact, and 0 otherwise. The factor of $(\pi/180)^2/Nn \times \Delta r \Delta\theta \Delta\phi$ is multiplied to obtain values which correspond to the radial distribution function. Here ϕ is the angle of $\boldsymbol{r}_{ij}$ around the x-axis and Δr, $\Delta\theta$, $\Delta\phi$ are the size of the bins in each direction. The result is shown in squares in figure 8. We see that the directly measured distribution has the same tendency with the theoretically evaluated distribution, i.e. both exhibit a peak in the compression direction, $\theta = 135°$, but the peak in $\theta = 0°$ is not visible.

It should be noticed that the directly measured distribution does not reflect the factorization approximation, equation (6.5). Hence, this result implies the validity of (6.5). As a check for the four-body correlation, we have measured the four-point susceptibility, χ_4, by MD simulation (cf. appendix I). The result is shown in figure 9. We see that no divergence is found in χ_4 near the jamming point. This implies that the divergence of the stress is determined by the divergence of the radial distribution function at contact, g_0. Thus, our theoretical treatment based on the factorization approximation is sufficient to discuss the singularities of the stress at the jamming point.

7. Discussion

First we discuss the hydrodynamic effects. We have formulated the theory by the resistance matrix $\overleftrightarrow{\zeta}^{(N)}$ to include the hydrodynamic effects. In our formulation, which focuses on the proximity effects of the particles, the far-field part of $\overleftrightarrow{\zeta}^{(N)}$ drops out, and the lubrication part $\overleftrightarrow{\zeta}^{(2)}_{lub}$ is taken into account. Although we have compared the theory and the MD simulation for the simplified case where $\overleftrightarrow{\zeta}^{(2)}_{lub}$ is proportional to the unit tensor, it is possible to do so for a more generic case. This is left for future work.

Next we discuss the effect of the contact force of the particles. In this work we have considered frictionless spheres, but it is reported that the exponent of the divergence λ depends on the friction between the particles; $\lambda = 1.6$ for frictionless spheres, while

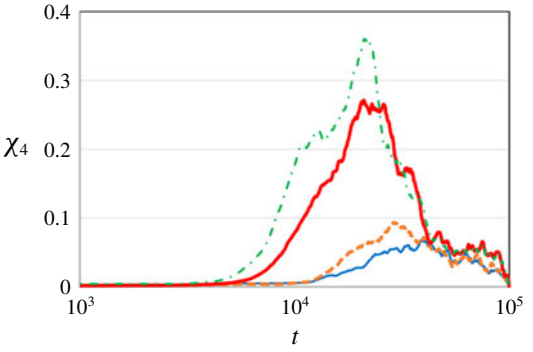

FIGURE 9. (Colour online) Four-point susceptibility measured by MD simulation. The conditions are $\varphi = 0.60 - 0.635$, $N = 1000$, $\dot{\gamma}^* = 1 \times 10^{-5}$. The number of data averaged for each point is 1000. The results are for $\varphi = 0.60$ (thin solid line), 0.62 (dashed line), 0.63 (thick solid line) and 0.635 (dot-dashed line).

$\lambda = 2.4$ in the strong friction limit (Mari *et al.* 2014). Note that the jamming density φ_J used in Mari *et al.* (2014) is 0.66, which reduces the exponent. Extension of this work to frictional particles is necessary to address this issue (Saitoh & Hayakawa 2019).

In the course of the derivation, we have assumed a separation between $O(g_0(\varphi))^2$ and $O(g_0(\varphi))$ terms as in (4.30) and (4.31). This assumption is valid when the magnitudes of $O(g_0(\varphi))^2$ and $O(g_0(\varphi))$ terms are well separated, which holds for larger Λ or φ closer to φ_J ($\delta\varphi$ closer to zero). For the case $\Lambda = 0.04$, this separation is reasonable only for $\delta\varphi < 0.001$, so the applicability below the jamming point must be perceived restricted than presented, as shown in § D.2.

Finally, we compare our theory with DeGiuli *et al.* (2015), which derives constitutive laws $\delta\varphi(J) \sim J^{b_\varphi}$ i.e. $\eta_n \sim \delta\varphi^{-1/b_\varphi}$ and $\mu(J) - \mu_0 \sim J^{b_\mu}$ with $b_\varphi = b_\mu \approx 0.35$, under the assumption that η_s and η_n diverges identically. The equality $b_\varphi = b_\mu$ suggests $\delta\varphi \sim \delta\mu$, which is consistent with our theory, equation (4.45), but the exponent of the divergence $1/b_\varphi \approx 2.83$ differs from our prediction of 2. Their exponent relies on $g'(r)$ for $r > d$, so it might be applicable to soft-core systems (Kawasaki *et al.* 2015). However, this is incompatible with hard spheres, because of (3.15). Note that their model does not consider the hydrodynamic interactions.

8. Concluding remarks

In this paper, we have derived approximate analytic formulas for the shear viscosity η_s, pressure viscosity η_n and the stress ratio μ for dense non-Brownian suspensions, valid at $\varphi \lesssim \varphi_J$. These formulas are derived from the microscopic overdamped equation of motion for suspended frictionless hard spheres, taking into account the proximity lubrication effect of the hydrodynamic interactions, and the approximate distribution function which is an extension of Grad's 13-moment-like expansion. We have performed MD simulations and confirmed that our theory successfully derives the relations $\eta_s/\eta_0 \sim \eta_n/\eta_0 \sim \delta\varphi^{-2}$ and $\mu - \mu_0 \sim \delta\varphi$, where $\delta\varphi = \varphi_J - \varphi$ and $\mu_0 \approx 0.16$.

Acknowledgements

The authors are grateful to S. Takada for providing the prototype of the program for the event-driven MD simulation. They are also grateful to K. Saitoh, A. Ikeda,

T. Kawasaki, Y. Oono, R. Mari and R. Seto for fruitful discussions on the subject. One of the authors (H.H.) appreciates useful comments by P. R. Nott and C. O'Hern. This work is partially supported by the Grant-in-Aid of MEXT for Scientific Research (grants no. 16H04025). The MD simulations for this work have been carried out at the computer facilities at the Yukawa Institute of Theoretical Physics, Kyoto University.

Appendix A. Force correlations

We derive explicit expressions for the second term on the right-hand side of (2.9), which includes a derivative of the interparticle forces. Note that collisions take place only when the interparticle distance is equal to the diameter in assemblies of hard spheres. Hence, the derivative acts only on the angular coordinates, e.g.

$$\begin{aligned}\frac{\partial F^{(p)}_{j,\alpha}}{\partial r_{i,\lambda}} &= \frac{1}{2}\zeta\dot{\gamma}d^2\sum_{k\neq j}\delta(r_{jk}-d)\frac{\partial}{\partial r_{i,\lambda}}[\mathcal{P}(\hat{x}_{jk},\hat{y}_{jk})\hat{r}_{jk,\alpha}]\\ &= \frac{1}{2}\zeta\dot{\gamma}d^2\sum_{k\neq j}\delta(r_{jk}-d)\Theta(-\hat{x}_{jk}\hat{y}_{jk})\frac{\partial}{\partial r_{i,\lambda}}[-\hat{x}_{jk}\hat{y}_{jk}\hat{r}_{jk,\alpha}].\end{aligned} \tag{A 1}$$

Here, the derivative of $\Theta(-\hat{x}\hat{y})=\Theta(\hat{x})\Theta(-\hat{y})+\Theta(-\hat{x})\Theta(\hat{y})$ vanishes since it yields $\hat{x}\delta(\hat{x})$ or $\hat{y}\delta(\hat{y})$. This is explicitly confirmed by

$$\hat{x}\hat{y}\hat{r}_\alpha\frac{\partial}{\partial\hat{r}_\lambda}\Theta(-\hat{x}\hat{y})=\hat{x}\hat{y}\hat{r}_\alpha[\delta_{\lambda x}\delta(\hat{x})\Theta(-\hat{y})-\delta_{\lambda y}\Theta(\hat{x})\delta(\hat{y})-\delta_{\lambda x}\delta(\hat{x})\Theta(\hat{y})+\delta_{\lambda y}\Theta(\hat{x})\delta(\hat{y})], \tag{A 2}$$

where each term includes $\hat{x}\delta(\hat{x})$ or $\hat{y}\delta(\hat{y})$. From (A 1), the third term on the right-hand side of (2.9) is evaluated as

$$\begin{aligned}&\sum_{i,j}\left\langle F^{(p)}_{i,\lambda}r_{j,\beta}\frac{\partial F^{(p)}_{j,\alpha}}{\partial r_{i,\lambda}}\right\rangle\\ &=\frac{1}{2}\zeta\sum_{i,j}\left\langle F^{(p)}_{i,\lambda}r_{j,\beta}\dot{\gamma}d^2\sum_{k\neq j}\delta(r_{jk}-d)\Theta(-\hat{x}_{jk}\hat{y}_{jk})\frac{\partial}{\partial r_{i,\lambda}}[-\hat{x}_{jk}\hat{y}_{jk}\hat{r}_{jk,\alpha}]\right\rangle\\ &=-\frac{1}{2}\zeta\sum_{i,j}\left\langle F^{(p)}_{i,\lambda}r_{j,\beta}\dot{\gamma}d\sum_{k\neq j}\tilde{\Delta}_{jk}\Theta_{jk}(\delta_{ij}-\delta_{ik})(\delta_{\lambda x}\hat{y}_{jk}\hat{r}_{jk,\alpha}+\delta_{\lambda y}\hat{x}_{jk}\hat{r}_{jk,\alpha}+\delta_{\lambda\alpha}\hat{x}_{jk}\hat{y}_{jk})\right\rangle\\ &=-\frac{1}{2}\zeta\dot{\gamma}d^2\sum_i\sum_{j\neq i}\langle F^{(p)}_{i,\lambda}\hat{r}_{ij,\beta}\tilde{\Delta}_{ij}\Theta_{ij}(\delta_{\lambda x}\hat{y}_{ij}\hat{r}_{ij,\alpha}+\delta_{\lambda y}\hat{x}_{ij}\hat{r}_{ij,\alpha}+\delta_{\lambda\alpha}\hat{x}_{ij}\hat{y}_{ij})\rangle\\ &=-\frac{1}{2}\zeta\dot{\gamma}d^2\sum_i\sum_{j\neq i}\langle F^{(p)}_{i,\lambda}\hat{r}_{ij,\beta}(\delta_{\lambda x}\Delta^{\alpha y}_{ij}+\delta_{\lambda y}\Delta^{\alpha x}_{ij}+\delta_{\lambda\alpha}\Delta^{xy}_{ij})\rangle,\end{aligned} \tag{A 3}$$

where $r_{j,\beta}$ is cast into a relative coordinate $r_{ij,\beta}$ in the third equality, and $\tilde{\Delta}_{ij}:=\delta(r_{ij}-d)$, $\Theta_{ij}:=\Theta(-\hat{x}_{ij}\hat{y}_{ij})$, $\Delta^{\alpha\beta}_{ij}:=\tilde{\Delta}_{ij}\hat{r}_{ij,\alpha}\hat{r}_{ij,\beta}\Theta_{ij}$ (cf. (4.2)). Note that relative coordinates, e.g. $r_{ij,\beta}$, are expressed in terms of normalized relative coordinates $\hat{r}_{ij,\beta}$ as $r_{ij}=d\hat{r}_{ij,\beta}$, due to the delta function $\delta(r_{ij}-d)$. If we further substitute $F^{(p)}_{i,\lambda}=\sum_{j\neq i}F^{(p)}_{ij,\lambda}$, where

$F^{(p)}_{ij,\lambda}$ is given by (3.15), we obtain

$$\begin{aligned}
&\sum_{i,j}\left\langle F^{(p)}_{i,\lambda} r_{j,\beta}\frac{\partial F^{(p)}_{j,\alpha}}{\partial r_{i,\lambda}}\right\rangle \\
&\quad=\frac{1}{4}\zeta^2\dot\gamma^2 d^4\sum_i\sum_{j\neq i}\sum_{k\neq i}\langle\tilde\Delta_{ik}\hat r_{ik,\lambda}\hat x_{ik}\hat y_{ik}\Theta_{ik}\hat r_{ij,\beta}(\delta_{\lambda x}\Delta^{\alpha y}_{ij}+\delta_{\lambda y}\Delta^{\alpha x}_{ij}+\delta_{\lambda\alpha}\Delta^{xy}_{ij})\rangle \\
&\quad=\frac{1}{4}\zeta^2\dot\gamma^2 d^4\sum_i\sum_{j\neq i}\sum_{k\neq i}\langle\Delta^{xy}_{ik}\hat r_{ik,\lambda}\hat r_{ij,\beta}(\delta_{\lambda x}\Delta^{\alpha y}_{ij}+\delta_{\lambda y}\Delta^{\alpha x}_{ij}+\delta_{\lambda\alpha}\Delta^{xy}_{ij})\rangle \\
&\quad=\frac{1}{4}\zeta^2\dot\gamma^2 d^4\sum_i\sum_{j\neq i}\sum_{k\neq i}\langle\Delta^{xy}_{ik}\hat r_{ij,\beta}(\hat x_{ik}\Delta^{\alpha y}_{ij}+\hat y_{ik}\Delta^{\alpha x}_{ij}+\hat r_{ik,\alpha}\Delta^{xy}_{ij})\rangle. \qquad (A\,4)
\end{aligned}$$

This can further be cast in the form

$$\begin{aligned}
&\sum_{i,j}\left\langle F^{(p)}_{i,\lambda} r_{j,\beta}\frac{\partial F^{(p)}_{j,\alpha}}{\partial r_{i,\lambda}}\right\rangle \\
&\quad=\frac{1}{4}\zeta^2\dot\gamma^2 d^4\sum_i\sum_{j\neq i}\sum_{k\neq i}\langle\Delta^{xy}_{ij}\Delta^{xy}_{ik}\hat r_{ij,\beta}\hat r_{ik,\alpha}+\Delta^{\alpha\beta}_{ij}\Delta^{xy}_{ik}(\hat x_{ij}\hat y_{ik}+\hat y_{ij}\hat x_{ik})\rangle \qquad (A\,5)
\end{aligned}$$

by the identities $\hat r_{ij,\beta}\Delta^{\alpha y}_{ij}=\hat y_{ij}\Delta^{\alpha\beta}_{ij}$ and $\hat r_{ij,\beta}\Delta^{\alpha x}_{ij}=\hat x_{ij}\Delta^{\alpha\beta}_{ij}$.

Appendix B. Approximation of the force correlations

First we derive approximate expressions for the force correlations which appear on the right-hand side of (4.5), by means of the approximate formula (4.9). Then we apply the factorization approximation to the multi-body correlations to obtain the final approximate expressions.

B.1. *Application of Grad's 13-moment-like expansion*

B.1.1. *Canonical terms*

Let us consider the first term on the right-hand side of (4.5) for illustration. The second term can be evaluated in parallel. The corresponding canonical term, i.e. the first term on the right-hand side of (4.9), includes three indices i, j, k for the particles. This can be decomposed into three- and two-body correlations as follows,

$$\begin{aligned}
&\sum_{i=1}^{N}\sum_{j\neq i}\sum_{k\neq i}\langle\Delta^{xy}_{ij}\Delta^{xy}_{ik}(\hat r_{ij,\alpha}\hat r_{ik,\beta}+\hat r_{ij,\beta}\hat r_{ik,\alpha})\rangle_{eq} \\
&\quad=\sum_{i,j,k}{}''\langle\Delta^{xy}_{ij}\Delta^{xy}_{ik}(\hat r_{ij,\alpha}\hat r_{ik,\beta}+\hat r_{ij,\beta}\hat r_{ik,\alpha})\rangle_{eq}+\frac{2}{d}\sum_{i,j}{}'\langle\tilde\Delta_{ij}\hat r_{ij,\alpha}\hat r_{ij,\beta}\hat x^2_{ij}\hat y^2_{ij}\Theta_{ij}\rangle_{eq}, \qquad (B\,1)
\end{aligned}$$

where $\tilde\Delta_{ij}:=\delta(r_{ij}-d)$, $\Theta_{ij}:=\Theta(-\hat x_{ij}\hat y_{ij})$ and $\Delta^{\alpha\beta}_{ij}$ is given by (4.2). Here, the summation $\sum''_{i,j,k}$ is performed over (i,j,k) where all the indices are different, i.e. $i\neq j$, $j\neq k$ and $k\neq i$, and the summation $\sum'_{i,j}$ is done for $i\neq j$. The two-body correlation

term (second term) is obtained by setting $j = k$ in the three-body correlation term (first term). Equation (B 1) can be further expressed as

$$\sum_{i=1}^{N}\sum_{j\neq i}\sum_{k\neq i}\langle \Delta_{ij}^{xy}\Delta_{ik}^{xy}(\hat{r}_{ij,\alpha}\hat{r}_{ik,\beta}+\hat{r}_{ij,\beta}\hat{r}_{ik,\alpha})\rangle_{eq}$$
$$= Nn(\varphi)^2\int \mathrm{d}^3\boldsymbol{r}\int \mathrm{d}^3\boldsymbol{r}' g^{(3)}(\boldsymbol{r},\boldsymbol{r}')\delta(r-d)\delta(r'-d)(\hat{r}_\alpha\hat{r}'_\beta+\hat{r}_\beta\hat{r}'_\alpha)\hat{x}\hat{y}\Theta_{\hat{r}}\hat{x}'\hat{y}'\Theta_{\hat{r}'}$$
$$+2N\frac{n(\varphi)}{d}\int \mathrm{d}^3\boldsymbol{r}\, g(r)\delta(r-d)\hat{r}_\alpha\hat{r}_\beta\hat{x}^2\hat{y}^2\Theta_{\hat{r}}, \tag{B 2}$$

where $\Theta_{\hat{r}} = \Theta(-\hat{x}\hat{y})$ and $g^{(3)}(\boldsymbol{r},\boldsymbol{r}')$ and $g(r)$ are the triplet- and pair-correlation functions, respectively (cf. (4.19)). Similarly, the canonical term for the second term on the right-hand side of (4.5) is given by

$$\sum_{i=1}^{N}\sum_{j\neq i}\sum_{k\neq i}\langle \Delta_{ij}^{\alpha\beta}\Delta_{ik}^{xy}(\hat{x}_{ij}\hat{y}_{ik}+\hat{y}_{ij}\hat{x}_{ik})\rangle_{eq}$$
$$= Nn(\varphi)^2\int \mathrm{d}^3\boldsymbol{r}\int \mathrm{d}^3\boldsymbol{r}'\, g^{(3)}(\boldsymbol{r},\boldsymbol{r}')\delta(r-d)\delta(r'-d)(\hat{x}\hat{y}'+\hat{y}\hat{x}')\hat{r}_\alpha\hat{r}_\beta\Theta_{\hat{r}}\hat{x}'\hat{y}'\Theta_{\hat{r}'}$$
$$+2N\frac{n(\varphi)}{\mathrm{d}}\int \mathrm{d}^3\boldsymbol{r}\, g(r)\delta(r-d)\hat{r}_\alpha\hat{r}_\beta\hat{x}^2\hat{y}^2\Theta_{\hat{r}}. \tag{B 3}$$

B.1.2. *Non-canonical terms*

Similarly to the canonical terms, let us consider the first term on the right-hand side of (4.5) for illustration. The second term can be evaluated in parallel. We consider the corresponding non-canonical term, i.e. the second term on the right-hand side of (4.9). This term includes five indices i, j, k, l, m for the particles as follows,

$$\frac{V}{2T}\Pi_{\rho\lambda}\sum_{i=1}^{N}\sum_{j\neq i}\sum_{k\neq i}\langle \Delta_{ij}^{xy}\Delta_{ik}^{xy}\hat{r}_{ij,\alpha}\hat{r}_{ik,\beta}\tilde{\sigma}_{\rho\lambda}\rangle_{eq}+(\alpha\leftrightarrow\beta)$$
$$= -\frac{1}{2T}\Pi_{\rho\lambda}\sum_{i=1}^{N}\sum_{j\neq i}\sum_{k\neq i}\langle \Delta_{ij}^{xy}\Delta_{ik}^{xy}\hat{r}_{ij,\alpha}\hat{r}_{ik,\beta}\sum_{l} r_{l,\lambda}F_{l,\rho}^{(p)}\rangle_{eq}+(\alpha\leftrightarrow\beta)$$
$$= -\frac{\zeta\dot{\gamma}d^2}{2T}\Pi_{\rho\lambda}\sum_{i=1}^{N}\sum_{j\neq i}\sum_{k\neq i}\sum_{l,m}\langle \Delta_{ij}^{xy}\Delta_{ik}^{xy}\Delta_{lm}^{xy}\hat{r}_{ij,\alpha}\hat{r}_{ik,\beta}r_{l,\lambda}\hat{r}_{lm,\rho}\rangle_{eq}+(\alpha\leftrightarrow\beta), \tag{B 4}$$

where we have substituted $F_{l,\rho}^{(p)} = \sum_{m\neq l}F_{lm,\rho}^{(p)}$ with $F_{lm,\rho}^{(p)}$ given by (3.15) in the second equality and $\Delta_{ij}^{\alpha\beta} := \delta(r_{ij}-d)\hat{r}_{ij,\alpha}\hat{r}_{ij,\beta}\Theta(-\hat{x}_{ij}\hat{y}_{ij})$ (cf. (4.2)). If the particles l, m differ from any of the particle i, j or k, the correlation decouples and vanishes due to $\langle\tilde{\sigma}_{\rho\lambda}\rangle_{eq} = 0$. Hence, particle l or m must be equal to at least one of the particles i, j or k. Let us choose l to be equal to i, and redefine m as l,

$$\frac{V}{2T}\Pi_{\rho\lambda}\sum_{i=1}^{N}\sum_{j\neq i}\sum_{k\neq i}\langle \Delta_{ij}^{xy}\Delta_{ik}^{xy}\hat{r}_{ij,\alpha}\hat{r}_{ik,\beta}\tilde{\sigma}_{\rho\lambda}\rangle_{eq}+(\alpha\leftrightarrow\beta)$$
$$= -\frac{\zeta\dot{\gamma}d^2}{2T}\Pi_{\rho\lambda}\sum_{i=1}^{N}\sum_{j\neq i}\sum_{k\neq i}\sum_{l}\langle \Delta_{ij}^{xy}\Delta_{ik}^{xy}\Delta_{il}^{xy}\hat{r}_{ij,\alpha}\hat{r}_{ik,\beta}r_{i,\lambda}\hat{r}_{il,\rho}\rangle_{eq}+(\alpha\leftrightarrow\beta). \tag{B 5}$$

This term includes four indices i, j, k, l for the particles, and can be decomposed into four-, three- and two-body correlations.

The four-body correlation corresponds to the case where all the indices i, j, k, l are different from one another. It can be expressed by the quadruplet-correlation function $g^{(4)}(\boldsymbol{r}, \boldsymbol{r}', \boldsymbol{r}'')$, equation (4.18), as

$$\begin{aligned}
&\text{(four-body correlation)}\\
&= -\frac{\zeta\dot\gamma d^3}{4T}\Pi_{\rho\lambda}\sum_{i,j,k,l}{}''' \langle \Delta_{ij}^{xy}\Delta_{ik}^{xy}\Delta_{il}^{xy}\hat r_{ij,\alpha}\hat r_{ik,\beta}\hat r_{il,\lambda}\hat r_{il,\rho}\rangle_{eq} + (\alpha\leftrightarrow\beta)\\
&= -N\frac{\zeta\dot\gamma d^3}{4T}\Pi_{\rho\lambda}n(\varphi)^3\int \mathrm{d}^3\boldsymbol{r}\int \mathrm{d}^3\boldsymbol{r}'\int \mathrm{d}^3\boldsymbol{r}''\, g^{(4)}(\boldsymbol{r},\boldsymbol{r}',\boldsymbol{r}'')\delta(r-d)\delta(r'-d)\delta(r''-d)\\
&\quad\times \hat r_\alpha\hat r'_\beta\hat r''_\lambda\hat r''_\rho\hat x\hat y\Theta_{\hat r}\hat x'\hat y'\Theta_{\hat r'}\hat x''\hat y''\Theta_{\hat r''} + (\alpha\leftrightarrow\beta),
\end{aligned}\tag{B 6}$$

where the summation $\sum'''_{i,j,k,l}$ is performed over (i, j, k, l) with all the indices different from one other. Note that $r_{i,\lambda}$ is converted to $r_{il,\lambda}$ by virtue of the odd parity with respect to the exchange $i \leftrightarrow l$. This conversion allows us to express this term only in relative coordinates.

The three-body correlation is obtained by setting l equal to j or k in (B 6). Let us choose l to be equal to j,

$$\begin{aligned}
&\text{(three-body correlation)}\\
&= -\frac{\zeta\dot\gamma d}{2T}\Pi_{\rho\lambda}\sum_{i,j,k}{}'' \langle \tilde\Delta_{ij}\Delta_{ik}^{xy}\hat r_{ij,\alpha}\hat r_{ik,\beta}r_{i,\lambda}\hat r_{ij,\rho}\hat x_{ij}^2\hat y_{ij}^2\Theta_{ij}\rangle_{eq} + (\alpha\leftrightarrow\beta).
\end{aligned}\tag{B 7}$$

Here, $r_{i,\lambda}$ should be converted to $r_{ij,\lambda}$ or $r_{ik,\lambda}$, in order for this term to be expressed only in relative coordinates. By noting that this term is even with respect to the exchange $i \leftrightarrow j$ and odd with respect to $i \leftrightarrow k$, $r_{ij,\lambda}$ vanishes and $r_{ik,\lambda}$ survives. Hence, we obtain

$$\begin{aligned}
&\text{(three-body correlation)}\\
&= -\frac{\zeta\dot\gamma d^2}{4T}\Pi_{\rho\lambda}\sum_{i,j,k}{}'' \langle \tilde\Delta_{ij}\Delta_{ik}^{xy}\hat r_{ij,\alpha}\hat r_{ij,\rho}\hat r_{ik,\beta}\hat r_{ik,\lambda}\hat x_{ij}^2\hat y_{ij}^2\Theta_{ij}\rangle_{eq} + (\alpha\leftrightarrow\beta)\\
&= -N\frac{\zeta\dot\gamma d^2}{4T}\Pi_{\rho\lambda}n(\varphi)^2\int \mathrm{d}^3\boldsymbol{r}\int \mathrm{d}^3\boldsymbol{r}'\, g^{(3)}(\boldsymbol{r},\boldsymbol{r}')\delta(r-d)\delta(r'-d)\hat r_\alpha\hat r_\rho\hat r'_\beta\hat r'_\lambda\hat x^2\hat y^2\Theta_{\hat r}\hat x'\hat y'\Theta_{\hat r'}\\
&\quad + (\alpha\leftrightarrow\beta).
\end{aligned}\tag{B 8}$$

Finally, the two-body correlation is obtained by setting $k = j$ in the expression for the three-body correlation. This is given by

$$\begin{aligned}
&\text{(two-body correlation)}\\
&= -\frac{\zeta\dot\gamma d}{4T}\Pi_{\rho\lambda}\sum_{i,j}{}' \langle \tilde\Delta_{ij}\hat r_{ij,\alpha}\hat r_{ij,\beta}\hat r_{ij,\rho}\hat r_{ij,\lambda}\hat x_{ij}^3\hat y_{ij}^3\Theta_{ij}\rangle_{eq} + (\alpha\leftrightarrow\beta)\\
&= -N\frac{\zeta\dot\gamma d}{4T}\Pi_{\rho\lambda}n(\varphi)\int \mathrm{d}^3\boldsymbol{r} g(r)\delta(r-d)\hat r_\alpha\hat r_\beta\hat r_\rho\hat r_\lambda\hat x^3\hat y^3\Theta_{\hat r} + (\alpha\leftrightarrow\beta)\\
&= -N\frac{\zeta\dot\gamma d}{2T}\Pi_{\rho\lambda}n(\varphi)\int \mathrm{d}^3\boldsymbol{r} g(r)\delta(r-d)\hat r_\alpha\hat r_\beta\hat r_\rho\hat r_\lambda\hat x^3\hat y^3\Theta_{\hat r}.
\end{aligned}\tag{B 9}$$

From (B 6), (B 8) and (B 9), we obtain

$$\begin{aligned}
&\frac{V}{2T}\Pi_{\rho\lambda}\sum_{i=1}^{N}\sum_{j\neq i}\sum_{k\neq i}\langle\Delta_{ij}^{xy}\Delta_{ik}^{xy}\hat{r}_{ij,\alpha}\hat{r}_{ik,\beta}\tilde{\sigma}_{\rho\lambda}\rangle_{eq}+(\alpha\leftrightarrow\beta)\\
&\quad\approx -N\frac{\zeta\dot{\gamma}d^3}{4T}\Pi_{\rho\lambda}n(\varphi)^3\int\mathrm{d}^3\boldsymbol{r}\int\mathrm{d}^3\boldsymbol{r}'\int\mathrm{d}^3\boldsymbol{r}''g^{(4)}(\boldsymbol{r},\boldsymbol{r}',\boldsymbol{r}'')\delta(r-d)\delta(r'-d)\delta(r''-d)\\
&\qquad\times\hat{r}_\alpha\hat{r}'_\beta\hat{r}''_\lambda\hat{r}''_\rho\hat{x}\hat{y}\Theta_{\hat{r}}\hat{x}'\hat{y}'\Theta_{\hat{r}'}\hat{x}''\hat{y}''\Theta_{\hat{r}''}+(\alpha\leftrightarrow\beta)\\
&\qquad-N\frac{\zeta\dot{\gamma}d^2}{4T}\Pi_{\rho\lambda}n(\varphi)^2\\
&\times\int\mathrm{d}^3\boldsymbol{r}\int\mathrm{d}^3\boldsymbol{r}'g^{(3)}(\boldsymbol{r},\boldsymbol{r}')\delta(r-d)\delta(r'-d)\hat{r}_\alpha\hat{r}_\rho\hat{r}'_\beta\hat{r}'_\lambda\hat{x}^2\hat{y}^2\Theta_{\hat{r}}\hat{x}'\hat{y}'\Theta_{\hat{r}'}+(\alpha\leftrightarrow\beta)\\
&\qquad-N\frac{\zeta\dot{\gamma}d}{2T}\Pi_{\rho\lambda}n(\varphi)\int\mathrm{d}^3\boldsymbol{r}\,g(r)\delta(r-d)\hat{r}_\alpha\hat{r}_\beta\hat{r}_\rho\hat{r}_\lambda\hat{x}^3\hat{y}^3\Theta_{\hat{r}}.
\end{aligned}\tag{B 10}$$

Similarly, the canonical term for the second term on the right-hand side of (4.5) is given by

$$\begin{aligned}
&\frac{V}{2T}\Pi_{\rho\lambda}\sum_{i=1}^{N}\sum_{j\neq i}\sum_{k\neq i}\langle\Delta_{ij}^{\alpha\beta}\Delta_{ik}^{xy}(\hat{x}_{ij}\hat{y}_{ik}+\hat{y}_{ij}\hat{x}_{ik})\tilde{\sigma}_{\rho\lambda}\rangle_{eq}\\
&\quad\approx -N\frac{\zeta\dot{\gamma}d^3}{4T}\Pi_{\rho\lambda}n(\varphi)^3\int\mathrm{d}^3\boldsymbol{r}\int\mathrm{d}^3\boldsymbol{r}'\int\mathrm{d}^3\boldsymbol{r}''g^{(4)}(\boldsymbol{r},\boldsymbol{r}',\boldsymbol{r}'')\delta(r-d)\delta(r'-d)\delta(r''-d)\\
&\qquad\times(\hat{x}\hat{y}'+\hat{y}\hat{x}')\hat{r}''_\lambda\hat{r}''_\rho\hat{r}_\alpha\hat{r}_\beta\Theta_{\hat{r}}\hat{x}'\hat{y}'\Theta_{\hat{r}'}\hat{x}''\hat{y}''\Theta_{\hat{r}''}+(\alpha\leftrightarrow\beta)\\
&\qquad-N\frac{\zeta\dot{\gamma}d^2}{4T}\Pi_{\rho\lambda}n(\varphi)^2\\
&\qquad\times\int\mathrm{d}^3\boldsymbol{r}\int\mathrm{d}^3\boldsymbol{r}'g^{(3)}(\boldsymbol{r},\boldsymbol{r}')\delta(r-d)\delta(r'-d)(\hat{x}\hat{y}'+\hat{y}\hat{x}')\hat{r}_\rho\hat{r}'_\lambda\hat{x}\hat{y}\hat{r}_\alpha\hat{r}_\beta\Theta_{\hat{r}}\hat{x}'\hat{y}'\Theta_{\hat{r}'}\\
&\qquad-N\frac{\zeta\dot{\gamma}d}{2T}\Pi_{\rho\lambda}n(\varphi)\int\mathrm{d}^3\boldsymbol{r}g(r)\delta(r-d)\hat{r}_\alpha\hat{r}_\beta\hat{r}_\rho\hat{r}_\lambda\hat{x}^3\hat{y}^3\Theta_{\hat{r}}.
\end{aligned}\tag{B 11}$$

B.2. *Factorization approximation*

The first and second terms on the right-hand side of (4.5) are expressed as spatial integrations of the correlation functions $g^{(4)}(\boldsymbol{r},\boldsymbol{r}',\boldsymbol{r}'')$, $g^{(3)}(\boldsymbol{r},\boldsymbol{r}')$ and $g(r)$ by means of the approximate formula (4.9), as is shown in (B 2), (B 3), (B 10) and (B 11). To proceed, it is necessary to adopt approximations for $g^{(4)}(\boldsymbol{r},\boldsymbol{r}',\boldsymbol{r}'')$ and $g^{(3)}(\boldsymbol{r},\boldsymbol{r}')$, which are difficult to evaluate. As explained in § 4.2, we adopt the following approximations which are valid for the evaluation of divergences in the vicinity of the jamming point,

$$g^{(4)}(\boldsymbol{r},\boldsymbol{r}',\boldsymbol{r}'')\approx g(r)g(r')g(r'')\quad(r,r',r''\approx d),\tag{B 12}$$

$$g^{(3)}(\boldsymbol{r},\boldsymbol{r}')\approx g(r)g(r')\quad(r,r'\approx d).\tag{B 13}$$

We apply (B 12) and (B 13) to (B 2), (B 3), (B 10) and (B 11), and utilize $g(r)\delta(r-d)=g_0(\varphi)\delta(r-d)$ in this section.

B.2.1. *Canonical terms*

By applying (B 13) to (B 2), the radial integrations can be performed straightforwardly. Thus we obtain

$$\begin{aligned}
&\sum_{i=1}^{N}\sum_{j\neq i}\sum_{k\neq i}\langle \Delta_{ij}^{xy}\Delta_{ik}^{xy}(\hat{r}_{ij,\alpha}\hat{r}_{ik,\beta}+\hat{r}_{ij,\beta}\hat{r}_{ik,\alpha})\rangle_{eq}\\
&\quad\approx \frac{N}{d^2}\varphi^{*2}g_0(\varphi)^2\int \mathrm{d}\mathcal{S}\int \mathrm{d}\mathcal{S}'(\hat{r}_\alpha\hat{r}'_\beta+\hat{r}_\beta\hat{r}'_\alpha)\hat{x}\hat{y}\Theta_{\hat{r}}\hat{x}'\hat{y}'\Theta_{\hat{r}'}+2\frac{N}{d^2}\varphi^* g_0(\varphi)\\
&\qquad\times\int \mathrm{d}\mathcal{S}\hat{r}_\alpha\hat{r}_\beta\hat{x}^2\hat{y}^2\Theta_{\hat{r}}\\
&\quad=\frac{N}{d^2}\{\varphi^{*2}g_0(\varphi)^2\mathcal{S}_{\alpha\beta}^{(1:c2)}+\varphi^* g_0(\varphi)\mathcal{S}_{\alpha\beta}^{(1:c1)}\},
\end{aligned}\tag{B 14}$$

where $\varphi^*=n(\varphi)d^3=6\varphi/\pi$ is the dimensionless average number density and the angular integrals $\mathcal{S}_{\alpha\beta}^{(1:c2)}$ and $\mathcal{S}_{\alpha\beta}^{(1:c1)}$ are given by

$$\mathcal{S}_{\alpha\beta}^{(1:c2)}=\int \mathrm{d}\mathcal{S}\int \mathrm{d}\mathcal{S}'\,\hat{x}\hat{y}\hat{x}'\hat{y}'(\hat{r}_\alpha\hat{r}'_\beta+\hat{r}_\beta\hat{r}'_\alpha)\Theta_{\hat{r}}\Theta_{\hat{r}'},\tag{B 15}$$

$$\mathcal{S}_{\alpha\beta}^{(1:c1)}=2\int \mathrm{d}\mathcal{S}\hat{x}^2\hat{y}^2\hat{r}_\alpha\hat{r}_\beta\Theta_{\hat{r}}.\tag{B 16}$$

Here, $\int \mathrm{d}\mathcal{S}\cdots$ and $\int \mathrm{d}\mathcal{S}'\cdots$ are angular integrals with respect to $\hat{\boldsymbol{r}}$ and $\hat{\boldsymbol{r}}'$, respectively. Equation (B 3) can be evaluated similarly. The result is synthesized as follows,

$$(\text{canonical})=-\frac{\zeta\dot{\gamma}}{4d}\sum_{\ell=1}^{2}\{\varphi^{*3}g_0(\varphi)^2\mathcal{S}_{\alpha\beta}^{(\ell:c2)}+\varphi^{*2}g_0(\varphi)\mathcal{S}_{\alpha\beta}^{(\ell:c1)}\},\tag{B 17}$$

where the angular integrals $\mathcal{S}_{\alpha\beta}^{(2:c2)}$, $\mathcal{S}_{\alpha\beta}^{(2:c1)}$ are given by

$$\mathcal{S}_{\alpha\beta}^{(2:c2)}=\int \mathrm{d}\mathcal{S}\int \mathrm{d}\mathcal{S}'\hat{r}_\alpha\hat{r}_\beta\hat{x}'\hat{y}'(\hat{x}\hat{y}'+\hat{y}\hat{x}')\Theta_{\hat{r}}\Theta_{\hat{r}'},\tag{B 18}$$

$$\mathcal{S}_{\alpha\beta}^{(2:c1)}=\mathcal{S}_{\alpha\beta}^{(1:c1)}.\tag{B 19}$$

B.2.2. *Non-canonical terms*

By applying (B 12) and (B 13) to (B 10), the radial integrations can be performed straightforwardly. Thus we obtain

$$\begin{aligned}
&\frac{V}{2T}\Pi_{\rho\lambda}\sum_{i=1}^{N}\sum_{j\neq i}\sum_{k\neq i}\langle \Delta_{ij}^{xy}\Delta_{ik}^{xy}\hat{r}_{ij,\alpha}\hat{r}_{ik,\beta}\tilde{\sigma}_{\rho\lambda}\rangle_{eq}+(\alpha\leftrightarrow\beta)\\
&\quad\approx -N\frac{\zeta\dot{\gamma}}{4T}\Pi_{\rho\lambda}\varphi^{*3}g_0(\varphi)^3\\
&\qquad\times\int \mathrm{d}\mathcal{S}\int \mathrm{d}\mathcal{S}'\int \mathrm{d}\mathcal{S}''\hat{r}_\alpha\hat{r}'_\beta\hat{r}''_\lambda\hat{r}''_\rho\hat{x}\hat{y}\Theta_{\hat{r}}\hat{x}'\hat{y}'\Theta_{\hat{r}'}\hat{x}''\hat{y}''\Theta_{\hat{r}''}+(\alpha\leftrightarrow\beta)\\
&\qquad-N\frac{\zeta\dot{\gamma}}{4T}\Pi_{\rho\lambda}\varphi^{*2}g_0(\varphi)^2\int \mathrm{d}\mathcal{S}\int \mathrm{d}\mathcal{S}'\hat{r}_\alpha\hat{r}_\rho\hat{r}'_\beta\hat{r}'_\lambda\hat{x}^2\hat{y}^2\Theta_{\hat{r}}\hat{x}'\hat{y}'\Theta_{\hat{r}'}+(\alpha\leftrightarrow\beta)
\end{aligned}$$

$$-N\frac{\zeta\dot{\gamma}}{2T}\Pi_{\rho\lambda}\varphi^{*}g_0(\varphi)\int \mathrm{d}\mathcal{S}\hat{r}_\alpha\hat{r}_\beta\hat{r}_\lambda\hat{r}_\rho\hat{x}^3\hat{y}^3\Theta_{\hat{r}}$$

$$=-N\frac{\zeta\dot{\gamma}}{4T}\Pi_{\rho\lambda}[\varphi^{*3}g_0(\varphi)^3\mathcal{S}^{(1:nc3)}_{\alpha\beta\rho\lambda}+\varphi^{*2}g_0(\varphi)^2\mathcal{S}^{(1:nc2)}_{\alpha\beta\rho\lambda}+\varphi^{*}g_0(\varphi)\mathcal{S}^{(1:nc1)}_{\alpha\beta\rho\lambda}]. \quad \text{(B 20)}$$

Here, the angular integrals are given by

$$\mathcal{S}^{(1:nc3)}_{\alpha\beta\rho\lambda}=\int \mathrm{d}\mathcal{S}\int \mathrm{d}\mathcal{S}'\int \mathrm{d}\mathcal{S}''\hat{r}_\alpha\hat{r}'_\beta\hat{r}''_\lambda\hat{r}''_\rho\hat{x}\hat{y}\Theta_{\hat{r}}\hat{x}'\hat{y}'\Theta_{\hat{r}'}\hat{x}''\hat{y}''\Theta_{\hat{r}''}+(\alpha\leftrightarrow\beta), \quad \text{(B 21)}$$

$$\mathcal{S}^{(1:nc2)}_{\alpha\beta\rho\lambda}=\int \mathrm{d}\mathcal{S}\int \mathrm{d}\mathcal{S}'\hat{r}_\alpha\hat{r}_\rho\hat{r}'_\beta\hat{r}'_\lambda\hat{x}^2\hat{y}^2\Theta_{\hat{r}}\hat{x}'\hat{y}'\Theta_{\hat{r}'}+(\alpha\leftrightarrow\beta), \quad \text{(B 22)}$$

$$\mathcal{S}^{(1:nc1)}_{\alpha\beta\rho\lambda}=2\int \mathrm{d}\mathcal{S}\hat{r}_\alpha\hat{r}_\beta\hat{r}_\lambda\hat{r}_\rho\hat{x}^3\hat{y}^3\Theta_{\hat{r}}. \quad \text{(B 23)}$$

Equation (B 11) can be evaluated similarly. The result is synthesized as follows,

(non-canonical)

$$=\frac{\zeta\dot{\gamma}}{4d}\frac{\zeta\dot{\gamma}d^2}{4T}\Pi_{\rho\lambda}\sum_{\ell=1}^{2}\{[\varphi^{*4}g_0(\varphi)^3\mathcal{S}^{(\ell:nc3)}_{\alpha\beta\rho\lambda}+\varphi^{*3}g_0(\varphi)^2\mathcal{S}^{(\ell:nc2)}_{\alpha\beta\rho\lambda}+\varphi^{*2}g_0(\varphi)\mathcal{S}^{(\ell:nc1)}_{\alpha\beta\rho\lambda}]\}, \quad \text{(B 24)}$$

where the angular integrals $\mathcal{S}^{(2:nc3)}_{\alpha\beta\rho\lambda}$, $\mathcal{S}^{(2:nc2)}_{\alpha\beta\rho\lambda}$, $\mathcal{S}^{(2:nc1)}_{\alpha\beta\rho\lambda}$ are given by

$$\mathcal{S}^{(2:nc3)}_{\alpha\beta\rho\lambda}=\int \mathrm{d}\mathcal{S}\int \mathrm{d}\mathcal{S}'\int \mathrm{d}\mathcal{S}''\hat{r}_\alpha\hat{r}_\beta\hat{x}'\hat{y}'(\hat{x}\hat{y}'+\hat{y}\hat{x}')\hat{x}''\hat{y}''\hat{r}''_\lambda\hat{r}''_\rho\Theta_{\hat{r}}\Theta_{\hat{r}'}\Theta_{\hat{r}''}, \quad \text{(B 25)}$$

$$\mathcal{S}^{(2:nc2)}_{\alpha\beta\rho\lambda}=\int \mathrm{d}\mathcal{S}\int \mathrm{d}\mathcal{S}'\hat{x}\hat{y}\hat{r}_\alpha\hat{r}_\beta\hat{r}_\rho(\hat{x}\hat{y}'+\hat{y}\hat{x}')\hat{x}'\hat{y}'\hat{r}'_\lambda\Theta_{\hat{r}}\Theta_{\hat{r}'}, \quad \text{(B 26)}$$

$$\mathcal{S}^{(2:nc1)}_{\alpha\beta\rho\lambda}=\mathcal{S}^{(1:nc1)}_{\alpha\beta\rho\lambda}. \quad \text{(B 27)}$$

Appendix C. Evaluation of the coefficients of the coupled equations

We explicitly evaluate the angular integrals $\mathcal{S}^{(\ell:nc2)}_{\alpha\beta\rho\lambda}$, $\mathcal{S}^{(\ell:c1)}_{\alpha\beta}$ and $\mathcal{S}^{(\ell:nc1)}_{\alpha\beta\rho\lambda}$, which appear in (4.30) and (4.31). These integrals enter as coefficients in the coupled equations for the stress tensor components. Eventually, equations (4.30) and (4.31) are cast in the form

$$\frac{\mathrm{d}}{\mathrm{d}t}\begin{pmatrix}\sigma^{(2)}_{xy}\\ \sigma^{(2)}_{\alpha\alpha}\\ \sigma^{(2)}_{xx}\\ \sigma^{(2)}_{yy}\end{pmatrix}+\dot{\gamma}\begin{pmatrix}\frac{1}{2}\sigma^{(2)}_{yy}\\ \sigma^{(2)}_{xy}\\ \sigma^{(2)}_{xy}\\ 0\end{pmatrix}=\Lambda\frac{\zeta\dot{\gamma}^2}{4d}\varphi^{*3}g_0(\varphi)^2\boldsymbol{\mathcal{A}}^{(2)}\begin{pmatrix}\Pi^{(2)}_{xy}\\ \Pi^{(2)}_{xx}\\ \Pi^{(2)}_{yy}\end{pmatrix}, \quad \text{(C 1)}$$

$$\frac{\mathrm{d}}{\mathrm{d}t}\begin{pmatrix}\sigma^{(1)}_{xy}\\ \sigma^{(1)}_{\alpha\alpha}\\ \sigma^{(1)}_{xx}\\ \sigma^{(1)}_{yy}\end{pmatrix}+\dot{\gamma}\begin{pmatrix}\frac{1}{2}\sigma^{(1)}_{yy}\\ \sigma^{(1)}_{xy}\\ \sigma^{(1)}_{xy}\\ 0\end{pmatrix}=\frac{\zeta\dot{\gamma}^2}{4d}\varphi^{*2}g_0(\varphi)\left\{-\boldsymbol{\mathcal{B}}+\Lambda\boldsymbol{\mathcal{A}}^{(1)}\begin{pmatrix}\Pi^{(1)}_{xy}\\ \Pi^{(1)}_{xx}\\ \Pi^{(1)}_{yy}\end{pmatrix}\right\}, \quad \text{(C 2)}$$

respectively. Here, the elements of the vector $\boldsymbol{\mathcal{B}}:=(\mathcal{B}_{xy},\mathcal{B}_{\alpha\alpha},\mathcal{B}_{xx},\mathcal{B}_{yy})^{\mathrm{T}}$ and the matrices

$$\boldsymbol{\mathcal{A}}^{(m)}:=\begin{pmatrix}\mathcal{A}^{(m)}_{xy;xy} & \mathcal{A}^{(m)}_{xy;xx} & \mathcal{A}^{(m)}_{xy;yy}\\ \mathcal{A}^{(m)}_{\alpha\alpha;xy} & \mathcal{A}^{(m)}_{\alpha\alpha;xx} & \mathcal{A}^{(m)}_{\alpha\alpha;yy}\\ \mathcal{A}^{(m)}_{xx;xy} & \mathcal{A}^{(m)}_{xx;xx} & \mathcal{A}^{(m)}_{xx;yy}\\ \mathcal{A}^{(m)}_{yy;xy} & \mathcal{A}^{(m)}_{yy;xx} & \mathcal{A}^{(m)}_{yy;yy}\end{pmatrix} \quad (m=1,2) \quad \text{(C 3)}$$

are given by the angular integrals. In this section, we evaluate the elements of $\boldsymbol{\mathcal{B}}$ and $\boldsymbol{\mathcal{A}}^{(m)}$ $(m=1,2)$. In the course of the evaluation, there appears integrals of the form

$$\mathcal{A}_{pqr;stu} := \int \mathrm{d}\mathcal{S} \int \mathrm{d}\mathcal{S}' \Theta_{\hat{r}} \Theta_{\hat{r}'} \hat{x}^p \hat{y}^q \hat{z}^r \hat{x}'^s \hat{y}'^t \hat{z}'^u, \tag{C 4}$$

$$\mathcal{B}_{pqr} := \int \mathrm{d}\mathcal{S} \Theta_{\hat{r}} \hat{x}^p \hat{y}^q \hat{z}^r, \tag{C 5}$$

where $\int \mathrm{d}\mathcal{S} \cdots$ and $\int \mathrm{d}\mathcal{S}' \cdots$ denote angular integrals with respect to $\hat{\boldsymbol{r}}$ and $\hat{\boldsymbol{r}}'$, respectively. The values for $\mathcal{A}_{pqr;stu}$ and $\mathcal{B}_{pqr}$ for various combinations of (p, q, r) and/or (s, t, u) are collected in appendix H.

C.1. *Equation for the shear stress*

We consider the case $(\alpha, \beta) = (x, y)$ in (4.30) and (4.31). Let us begin with the evaluation of the non-canonical term with $l=1$,

$$\Pi^{(2)}_{\rho\lambda} \mathcal{S}^{(1:nc2)}_{xy\rho\lambda} = \Pi^{(2)}_{\rho\lambda} \int \mathrm{d}\mathcal{S} \int \mathrm{d}\mathcal{S}' \hat{x}^2 \hat{y}^2 \hat{r}_\rho (\hat{x}\hat{y}' + \hat{y}\hat{x}') \hat{x}' \hat{y}' \hat{r}'_\lambda \Theta_{\hat{r}} \Theta_{\hat{r}'}, \tag{C 6}$$

$$\Pi^{(1)}_{\rho\lambda} \mathcal{S}^{(1:nc1)}_{xy\rho\lambda} = 2\Pi^{(1)}_{\rho\lambda} \int \mathrm{d}\mathcal{S} \hat{x}^4 \hat{y}^4 \hat{r}_\rho \hat{r}_\lambda \Theta_{\hat{r}}. \tag{C 7}$$

Recalling the implications of the symmetry, equations (4.24) and (4.25), we obtain

$$\begin{aligned} \Pi^{(2)}_{\rho\lambda} \mathcal{S}^{(1:nc2)}_{xy\rho\lambda} &= (\mathcal{A}_{420;220} + \mathcal{A}_{330;310}) \Pi^{(2)}_{xx} + (\mathcal{A}_{330;130} + \mathcal{A}_{240;220}) \Pi^{(2)}_{yy} \\ &\quad + (\mathcal{A}_{420;130} + 2\mathcal{A}_{330;220} + \mathcal{A}_{240;310}) \Pi^{(2)}_{xy}, \end{aligned} \tag{C 8}$$

$$\begin{aligned} \Pi^{(1)}_{\rho\lambda} \mathcal{S}^{(1:nc1)}_{xy\rho\lambda} &= 2\mathcal{B}_{640} \Pi^{(1)}_{xx} + 2\mathcal{B}_{460} \Pi^{(1)}_{yy} + 2\mathcal{B}_{442} \Pi^{(1)}_{zz} + 4\mathcal{B}_{550} \Pi^{(1)}_{xy} \\ &= 2(\mathcal{B}_{640} - \mathcal{B}_{442}) \Pi^{(1)}_{xx} + 2(\mathcal{B}_{460} - \mathcal{B}_{442}) \Pi^{(1)}_{yy} + 4\mathcal{B}_{550} \Pi^{(1)}_{xy}. \end{aligned} \tag{C 9}$$

Here, we have utilized the relation $\Pi_{zz} = -(\Pi_{xx} + \Pi_{yy})$. Similarly, the term for $l=2$ can be evaluated as

$$\Pi^{(2)}_{\rho\lambda} \mathcal{S}^{(2:nc2)}_{xy\rho\lambda} = \Pi^{(2)}_{\rho\lambda} \int \mathrm{d}\mathcal{S} \int \mathrm{d}\mathcal{S}' \hat{x}^2 \hat{y}^2 \hat{r}_\rho (\hat{x}\hat{y}' + \hat{y}\hat{x}') \hat{x}' \hat{y}' \hat{r}'_\lambda \Theta_{\hat{r}} \Theta_{\hat{r}'} = \Pi^{(2)}_{\rho\lambda} \mathcal{S}^{(1:nc2)}_{xy\rho\lambda}, \tag{C 10}$$

$$\Pi^{(1)}_{\rho\lambda} \mathcal{S}^{(2:nc1)}_{xy\rho\lambda} = \Pi^{(1)}_{\rho\lambda} \mathcal{S}^{(1:nc1)}_{xy\rho\lambda}. \tag{C 11}$$

The coefficients of the canonical term in (4.31) are evaluated as

$$\mathcal{S}^{(1:c1)}_{xy} = 2 \int \mathrm{d}\mathcal{S} \hat{x}^3 \hat{y}^3 \Theta_{\hat{r}} = 2\mathcal{B}_{330} = -\tfrac{16}{105}, \tag{C 12}$$

$$\mathcal{S}^{(2:c1)}_{xy} = \mathcal{S}^{(1:c1)}_{xy} = -\tfrac{16}{105}. \tag{C 13}$$

Hence, from (C 8) and (C 10), we obtain

$$\frac{\mathrm{d}}{\mathrm{d}t} \sigma^{(2)}_{xy} = -\frac{1}{2} \sigma^{(2)}_{yy} + \frac{\zeta \dot{\gamma}}{4d} \Lambda \varphi^{*3} g_0(\varphi)^2 [\mathcal{A}^{(2)}_{xy;xx} \Pi^{(2)}_{xx} + \mathcal{A}^{(2)}_{xy;yy} \Pi^{(2)}_{yy} + \mathcal{A}^{(2)}_{xy;xy} \Pi^{(2)}_{xy}], \tag{C 14}$$

and from (C 9) and (C 11), we obtain

$$\frac{\mathrm{d}}{\mathrm{d}t}\sigma_{xy}^{(1)} = -\frac{1}{2}\sigma_{yy}^{(1)} + \frac{\zeta\dot{\gamma}}{4d}\varphi^{*2}g_0(\varphi)\left\{-\frac{32}{105} + \Lambda[\mathcal{A}_{xy;xx}^{(1)}\Pi_{xx}^{(1)} + \mathcal{A}_{xy;yy}^{(1)}\Pi_{yy}^{(1)} + \mathcal{A}_{xy;xy}^{(1)}\Pi_{xy}^{(1)}]\right\}, \tag{C 15}$$

where the coefficients are evaluated as

$$\mathcal{A}_{xy;xx}^{(2)} = 2(\mathcal{A}_{420;220} + \mathcal{A}_{330;310}) = \frac{12\pi^2 + 128}{1575}, \tag{C 16}$$

$$\mathcal{A}_{xy;yy}^{(2)} = \mathcal{A}_{xy;xx}^{(2)} = \frac{12\pi^2 + 128}{1575}, \tag{C 17}$$

$$\mathcal{A}_{xy;xy}^{(2)} = 4(\mathcal{A}_{420;130} + \mathcal{A}_{330;220}) = -\frac{32\pi}{315}, \tag{C 18}$$

and

$$\mathcal{A}_{xy;xx}^{(1)} = 4(\mathcal{B}_{640} - \mathcal{B}_{442}) = \frac{16\pi}{1155}, \tag{C 19}$$

$$\mathcal{A}_{xy;yy}^{(1)} = \mathcal{A}_{xy;xx}^{(1)} = \frac{16\pi}{1155}, \tag{C 20}$$

$$\mathcal{A}_{xy;xy}^{(1)} = 8\mathcal{B}_{550} = -\tfrac{1024}{10395}. \tag{C 21}$$

C.2. *Equation for the pressure*

We take the trace with respect to the indices (α, β) in (4.30) and (4.31). The non-canonical term with $l = 1$ is evaluated, by virtue of the symmetry, equations (4.24) and (4.25), and with the aid of $\Pi_{zz} = -(\Pi_{xx} + \Pi_{yy})$, as follows,

$$\begin{aligned}
\Pi_{\rho\lambda}^{(2)}\mathcal{S}_{\alpha\alpha\rho\lambda}^{(1:nc2)} &= 2\Pi_{\rho\lambda}^{(2)}\int \mathrm{d}\mathcal{S}\int \mathrm{d}\mathcal{S}'\hat{x}^2\hat{y}^2\hat{r}_\alpha\hat{r}_\rho\hat{x}'\hat{y}'\hat{r}'_\alpha\hat{r}'_\lambda\Theta_{\hat{r}}\Theta_{\hat{r}'} \\
&= 2(\mathcal{A}_{420;310} + \mathcal{A}_{330;220})\Pi_{xx}^{(2)} + 2(\mathcal{A}_{330;220} + \mathcal{A}_{240;130})\Pi_{yy}^{(2)} + 2\mathcal{A}_{222;112}\Pi_{zz}^{(2)} \\
&\quad + 2(\mathcal{A}_{420;220} + 2\mathcal{A}_{330;310} + \mathcal{A}_{240;220})\Pi_{xy}^{(2)} \\
&= 2(\mathcal{A}_{420;310} + \mathcal{A}_{330;220} - \mathcal{A}_{222;112})\Pi_{xx}^{(2)} + 2(\mathcal{A}_{330;220} + \mathcal{A}_{240;130} - \mathcal{A}_{222;112})\Pi_{yy}^{(2)} \\
&\quad + 2(\mathcal{A}_{420;220} + 2\mathcal{A}_{330;310} + \mathcal{A}_{240;220})\Pi_{xy}^{(2)},
\end{aligned} \tag{C 22}$$

$$\begin{aligned}
\Pi_{\rho\lambda}^{(1)}\mathcal{S}_{\alpha\alpha\rho\lambda}^{(1:nc1)} &= 2\Pi_{\rho\lambda}^{(1)}\int \mathrm{d}\mathcal{S}\hat{x}^3\hat{y}^3\hat{r}_\rho\hat{r}_\lambda\Theta_{\hat{r}} \\
&= 2\mathcal{B}_{530}\Pi_{xx}^{(1)} + 2\mathcal{B}_{350}\Pi_{yy}^{(1)} + 2\mathcal{B}_{332}\Pi_{zz}^{(1)} + 4\mathcal{B}_{440}\Pi_{xy}^{(1)} \\
&= 2(\mathcal{B}_{530} - \mathcal{B}_{332})\Pi_{xx}^{(1)} + 2(\mathcal{B}_{350} - \mathcal{B}_{332})\Pi_{yy}^{(1)} + 4\mathcal{B}_{440}\Pi_{xy}^{(1)}.
\end{aligned} \tag{C 23}$$

Similarly, the term for $l = 2$ are evaluated as

$$\begin{aligned}\Pi^{(2)}_{\rho\lambda}\mathcal{S}^{(2:nc2)}_{\alpha\alpha\rho\lambda} &= \Pi^{(2)}_{\rho\lambda}\int \mathrm{d}\mathcal{S}\int \mathrm{d}\mathcal{S}'\hat{x}\hat{y}\hat{r}_\rho(\hat{x}\hat{y}'+\hat{y}\hat{x}')\hat{x}'\hat{y}'\hat{r}'_\lambda\Theta_{\hat{r}}\Theta_{\hat{r}'}\\ &= (\mathcal{A}_{310;220}+\mathcal{A}_{220;310})\Pi^{(2)}_{xx}+(\mathcal{A}_{220;130}+\mathcal{A}_{130;220})\Pi^{(2)}_{yy}\\ &\quad+(\mathcal{A}_{310;130}+2\mathcal{A}_{220;220}+\mathcal{A}_{130;310})\Pi^{(2)}_{xy}, \qquad (C\,24)\end{aligned}$$

$$\Pi^{(1)}_{\rho\lambda}\mathcal{S}^{(2:nc1)}_{\alpha\alpha\rho\lambda} = \Pi^{(1)}_{\rho\lambda}\mathcal{S}^{(1:nc1)}_{\alpha\alpha\rho\lambda}. \qquad (C\,25)$$

The coefficients of the canonical term in (4.31) are evaluated as

$$\mathcal{S}^{(1:c1)}_{\alpha\alpha} = 2\int \mathrm{d}\mathcal{S}\,\hat{x}^2\hat{y}^2\Theta_{\hat{r}} = 2\mathcal{B}_{220} = \frac{2\pi}{15}, \qquad (C\,26)$$

$$\mathcal{S}^{(2:c1)}_{\alpha\alpha} = \mathcal{S}^{(1:c1)}_{\alpha\alpha} = \frac{2\pi}{15}. \qquad (C\,27)$$

Hence, from (C 22) and (C 24), we obtain

$$\frac{\mathrm{d}}{\mathrm{d}t}\sigma^{(2)}_{\alpha\alpha} = -\sigma^{(2)}_{xy}+\frac{\zeta\dot{\gamma}}{4d}\Lambda\,\varphi^{*3}g_0(\varphi)^2[\mathcal{A}^{(2)}_{\alpha\alpha;xx}\Pi^{(2)}_{xx}+\mathcal{A}^{(2)}_{\alpha\alpha;yy}\Pi^{(2)}_{yy}+\mathcal{A}^{(2)}_{\alpha\alpha;xy}\Pi^{(2)}_{xy}], \qquad (C\,28)$$

and from (C 23) and (C 25), we obtain

$$\frac{\mathrm{d}}{\mathrm{d}t}\sigma^{(1)}_{\alpha\alpha} = -\sigma^{(1)}_{xy}+\frac{\zeta\dot{\gamma}}{4d}\varphi^{*2}g_0(\varphi)\left\{\frac{4\pi}{15}+\Lambda[\mathcal{A}^{(2)}_{\alpha\alpha;xx}\Pi^{(1)}_{xx}+\mathcal{A}^{(2)}_{\alpha\alpha;yy}\Pi^{(1)}_{yy}+\mathcal{A}^{(2)}_{\alpha\alpha;xy}\Pi^{(1)}_{xy}]\right\}, \qquad (C\,29)$$

where the coefficients are evaluated as

$$\mathcal{A}^{(2)}_{\alpha\alpha;xx} = 2(\mathcal{A}_{420;310}+\mathcal{A}_{330;220}-\mathcal{A}_{222;112}+\mathcal{A}_{310;220}) = -\frac{184\pi}{1575}, \qquad (C\,30)$$

$$\mathcal{A}^{(2)}_{\alpha\alpha;yy} = \mathcal{A}^{(2)}_{\alpha\alpha;xx} = -\frac{184\pi}{1575}, \qquad (C\,31)$$

$$\mathcal{A}^{(2)}_{\alpha\alpha;xy} = 4(\mathcal{A}_{420;220}+\mathcal{A}_{330;310})+2(\mathcal{A}_{310;310}+\mathcal{A}_{220;220}) = \frac{52\pi^2+604}{1575}, \qquad (C\,32)$$

and

$$\mathcal{A}^{(1)}_{\alpha\alpha;xx} = 4(\mathcal{B}_{530}-\mathcal{B}_{332}) = -\tfrac{32}{315} \qquad (C\,33)$$

$$\mathcal{A}^{(1)}_{\alpha\alpha;yy} = \mathcal{A}^{(1)}_{\alpha\alpha;xx} = -\tfrac{32}{315}, \qquad (C\,34)$$

$$\mathcal{A}^{(1)}_{\alpha\alpha;xy} = 8\mathcal{B}_{440} = \frac{8\pi}{105}. \qquad (C\,35)$$

C.3. *Equation for the* (x, x) *component*

We consider the $(\alpha, \beta) = (x, x)$ components in (4.30) and (4.31). The non-canonical terms for $l = 1$ are evaluated, by virtue of the symmetry, equations (4.24) and (4.25), and with the aid of $\Pi_{zz} = -(\Pi_{xx}+\Pi_{yy})$, as

$$\begin{aligned}\Pi^{(2)}_{\rho\lambda}\mathcal{S}^{(1:nc2)}_{xx\rho\lambda} &= 2\Pi^{(2)}_{\rho\lambda}\int \mathrm{d}\mathcal{S}\int \mathrm{d}\mathcal{S}'\hat{x}^3\hat{y}^2\hat{r}_\rho\hat{x}'^2\hat{y}'\hat{r}'_\lambda\Theta_{\hat{r}}\Theta_{\hat{r}'}\\ &= 2\mathcal{A}_{420;310}\Pi^{(2)}_{xx}+2\mathcal{A}_{330;220}\Pi^{(2)}_{yy}+2(\mathcal{A}_{420;220}+\mathcal{A}_{330;310})\Pi^{(2)}_{xy}, \qquad (C\,36)\end{aligned}$$

$$\begin{aligned}\Pi^{(1)}_{\rho\lambda}\mathcal{S}^{(1:nc1)}_{xx\rho\lambda} &= 2\Pi^{(1)}_{\rho\lambda}\int \mathrm{d}\mathcal{S}\hat{x}^5\hat{y}^3\hat{r}_\rho\hat{r}_\lambda\Theta_{\hat{r}}\\ &= 2\mathcal{B}_{730}\Pi^{(1)}_{xx} + 2\mathcal{B}_{550}\Pi^{(1)}_{yy} + 2\mathcal{B}_{532}\Pi^{(1)}_{zz} + 4\mathcal{B}_{640}\Pi^{(1)}_{xy}\\ &= 2(\mathcal{B}_{730}-\mathcal{B}_{532})\Pi^{(1)}_{xx} + 2(\mathcal{B}_{550}-\mathcal{B}_{532})\Pi^{(1)}_{yy} + 4\mathcal{B}_{640}\Pi^{(1)}_{xy}. \end{aligned} \tag{C 37}$$

Similarly, the terms for $l=2$ are evaluated as

$$\begin{aligned}\Pi^{(2)}_{\rho\lambda}\mathcal{S}^{(2:nc2)}_{xx\rho\lambda} &= \Pi^{(2)}_{\rho\lambda}\int \mathrm{d}\mathcal{S}\int \mathrm{d}\mathcal{S}'\hat{x}^3\hat{y}\hat{r}_\rho(\hat{x}\hat{y}'+\hat{y}\hat{x}')\hat{x}'\hat{y}'\hat{r}'_\lambda\Theta_{\hat{r}}\Theta_{\hat{r}'}\\ &= (\mathcal{A}_{510;220}+\mathcal{A}_{420;310})\Pi^{(2)}_{xx} + (\mathcal{A}_{420;130}+\mathcal{A}_{330;220})\Pi^{(2)}_{yy}\\ &\quad + (\mathcal{A}_{510;130}+2\mathcal{A}_{420;220}+\mathcal{A}_{330;310})\Pi^{(2)}_{xy}, \end{aligned} \tag{C 38}$$

$$\Pi^{(1)}_{\rho\lambda}\mathcal{S}^{(2:nc1)}_{xx\rho\lambda} = \Pi^{(1)}_{\rho\lambda}\mathcal{S}^{(1:nc1)}_{xx\rho\lambda}. \tag{C 39}$$

The coefficients of the canonical terms in (4.31) are evaluated as

$$\mathcal{S}^{(1:c1)}_{xx} = 2\int \mathrm{d}\mathcal{S}\hat{x}^4\hat{y}^2\Theta_{\hat{r}} = 2\mathcal{B}_{420} = \frac{2\pi}{35}, \tag{C 40}$$

$$\mathcal{S}^{(2:c1)}_{xx} = \mathcal{S}^{(1:c1)}_{xx} = \frac{2\pi}{35}. \tag{C 41}$$

Hence, from (C 36) and (C 38), we obtain

$$\frac{\mathrm{d}}{\mathrm{d}t}\sigma^{(2)}_{xx} = -\sigma^{(2)}_{xy} + \frac{\zeta\dot{\gamma}}{4d}\Lambda\varphi^{*3}g_0(\varphi)^2[\mathcal{A}^{(2)}_{xx;xx}\Pi^{(2)}_{xx} + \mathcal{A}^{(2)}_{xx;yy}\Pi^{(2)}_{yy} + \mathcal{A}^{(2)}_{xx;xy}\Pi^{(2)}_{xy}], \tag{C 42}$$

and from (C 37) and (C 39), we obtain

$$\frac{\mathrm{d}}{\mathrm{d}t}\sigma^{(1)}_{xx} = -\sigma^{(1)}_{xy} + \frac{\zeta\dot{\gamma}}{4d}\varphi^{*2}g_0(\varphi)\left\{\frac{4\pi}{35} + \Lambda[\mathcal{A}^{(1)}_{xx;xx}\Pi^{(1)}_{xx} + \mathcal{A}^{(1)}_{xx;yy}\Pi^{(1)}_{yy} + \mathcal{A}^{(1)}_{xx;xy}\Pi^{(1)}_{xy}]\right\}, \tag{C 43}$$

where the coefficients are evaluated as

$$\mathcal{A}^{(2)}_{xx;xx} = 3\mathcal{A}_{420;310} + \mathcal{A}_{510;220} = -\frac{104\pi}{1575}, \tag{C 44}$$

$$\mathcal{A}^{(2)}_{xx;yy} = 3\mathcal{A}_{330;220} + \mathcal{A}_{420;130} = -\frac{8\pi}{175}, \tag{C 45}$$

$$\mathcal{A}^{(2)}_{xx;xy} = 4\mathcal{A}_{420;220} + 3\mathcal{A}_{330;310} + \mathcal{A}_{510;130} = \frac{24\pi^2+320}{1575}, \tag{C 46}$$

and

$$\mathcal{A}^{(1)}_{xx;xx} = 4(\mathcal{B}_{730}-\mathcal{B}_{532}) = -\tfrac{128}{2079}, \tag{C 47}$$

$$\mathcal{A}^{(1)}_{xx;yy} = 4(\mathcal{B}_{550}-\mathcal{B}_{532}) = -\tfrac{128}{3465}, \tag{C 48}$$

$$\mathcal{A}^{(1)}_{xx;xy} = 8\mathcal{B}_{640} = \frac{8\pi}{231}. \tag{C 49}$$

C.4. *Equation for the* (y, y) *component*

Finally, we consider the $(\alpha, \beta) = (y, y)$ components in (4.30) and (4.31). The non-canonical terms for $l=1$ are evaluated by virtue of the symmetry, equations (4.24)

and (4.25), and with the aid of $\Pi_{zz} = -(\Pi_{xx} + \Pi_{yy})$, as

$$\begin{aligned}\Pi^{(2)}_{\rho\lambda}\mathcal{S}^{(1:nc2)}_{yy\rho\lambda} &= 2\Pi^{(2)}_{\rho\lambda}\int \mathrm{d}\mathcal{S}\int \mathrm{d}\mathcal{S}'\hat{x}^2\hat{y}^3\hat{r}_\rho\hat{x}'\hat{y}'^2\hat{r}'_\lambda\Theta_{\hat{r}}\Theta_{\hat{r}'}\\ &= 2\mathcal{A}_{330;220}\Pi^{(2)}_{xx} + 2\mathcal{A}_{240;130}\Pi^{(2)}_{yy} + 2(\mathcal{A}_{330;130}+\mathcal{A}_{240;220})\Pi^{(2)}_{xy}, \end{aligned} \tag{C 50}$$

$$\begin{aligned}\Pi^{(1)}_{\rho\lambda}\mathcal{S}^{(1:nc1)}_{yy\rho\lambda} &= 2\Pi^{(1)}_{\rho\lambda}\int \mathrm{d}\mathcal{S}\hat{x}^3\hat{y}^5\hat{r}_\rho\hat{r}_\lambda\Theta_{\hat{r}}\\ &= 2\mathcal{B}_{550}\Pi^{(1)}_{xx} + 2\mathcal{B}_{370}\Pi^{(1)}_{yy} + 2\mathcal{B}_{352}\Pi^{(1)}_{zz} + 4\mathcal{B}_{460}\Pi^{(1)}_{xy}\\ &= 2(\mathcal{B}_{550}-\mathcal{B}_{352})\Pi^{(1)}_{xx} + 2(\mathcal{B}_{370}-\mathcal{B}_{352})\Pi^{(1)}_{yy} + 4\mathcal{B}_{460}\Pi^{(1)}_{xy}. \end{aligned} \tag{C 51}$$

Similarly, the terms for $l=2$ are evaluated as

$$\begin{aligned}\Pi^{(2)}_{\rho\lambda}\mathcal{S}^{(2:nc2)}_{yy\rho\lambda} &= \Pi^{(2)}_{\rho\lambda}\int \mathrm{d}\mathcal{S}\int \mathrm{d}\mathcal{S}'\hat{x}\hat{y}^3\hat{r}_\rho(\hat{x}\hat{y}'+\hat{y}\hat{x}')\hat{x}'\hat{y}'\hat{r}'_\lambda\Theta_{\hat{r}}\Theta_{\hat{r}'}\\ &= (\mathcal{A}_{330;220}+\mathcal{A}_{240;310})\Pi^{(2)}_{xx} + (\mathcal{A}_{240;130}+\mathcal{A}_{150;220})\Pi^{(2)}_{yy}\\ &\quad + (\mathcal{A}_{330;130}+2\mathcal{A}_{240;220}+\mathcal{A}_{150;310})\Pi^{(2)}_{xy}, \end{aligned} \tag{C 52}$$

$$\Pi^{(1)}_{\rho\lambda}\mathcal{S}^{(2:nc1)}_{yy\rho\lambda} = \Pi^{(1)}_{\rho\lambda}\mathcal{S}^{(1:nc1)}_{yy\rho\lambda}. \tag{C 53}$$

The coefficients of the canonical terms in (4.31) are evaluated as

$$\mathcal{S}^{(1:c1)}_{yy} = 2\int \mathrm{d}\mathcal{S}\hat{x}^2\hat{y}^4\Theta_{\hat{r}} = 2\mathcal{B}_{240} = \frac{2\pi}{35}, \tag{C 54}$$

$$\mathcal{S}^{(2:c1)}_{yy} = \mathcal{S}^{(1:c1)}_{yy} = \frac{2\pi}{35}. \tag{C 55}$$

Hence, from (C 50) and (C 52), we obtain

$$\frac{\mathrm{d}}{\mathrm{d}t}\sigma^{(2)}_{yy} = \frac{\zeta\dot{\gamma}}{4d}\Lambda\,\varphi^{*3}g_0(\varphi)^2[\mathcal{A}^{(2)}_{yy;xx}\Pi^{(2)}_{xx} + \mathcal{A}^{(2)}_{yy;yy}\Pi^{(2)}_{yy} + \mathcal{A}^{(2)}_{yy;xy}\Pi^{(2)}_{xy}], \tag{C 56}$$

and from (C 51) and (C 53), we obtain

$$\frac{\mathrm{d}}{\mathrm{d}t}\sigma^{(1)}_{yy} = \frac{\zeta\dot{\gamma}}{4d}\varphi^{*2}g_0(\varphi)\left\{\frac{4\pi}{35} + \Lambda[\mathcal{A}^{(1)}_{yy;xx}\Pi^{(1)}_{xx} + \mathcal{A}^{(1)}_{yy;yy}\Pi^{(1)}_{yy} + \mathcal{A}^{(1)}_{yy;xy}\Pi^{(1)}_{xy}]\right\}, \tag{C 57}$$

where the coefficients are evaluated as

$$\mathcal{A}^{(2)}_{yy;xx} = 3\mathcal{A}_{330;220} + \mathcal{A}_{240;310} = -\frac{8\pi}{175}, \tag{C 58}$$

$$\mathcal{A}^{(2)}_{yy;yy} = 3\mathcal{A}_{240;130} + \mathcal{A}_{150;220} = -\frac{104\pi}{1575}, \tag{C 59}$$

$$\mathcal{A}^{(2)}_{yy;xy} = 3\mathcal{A}_{330;130} + 4\mathcal{A}_{240;220} + \mathcal{A}_{150;310} = \frac{24\pi^2+320}{1575}, \tag{C 60}$$

and

$$\mathcal{A}^{(1)}_{yy;xx} = 4(\mathcal{B}_{550}-\mathcal{B}_{352}) = -\tfrac{128}{3465}, \tag{C 61}$$

$$\mathcal{A}^{(1)}_{yy;yy} = 4(\mathcal{B}_{370}-\mathcal{B}_{352}) = -\tfrac{128}{2079}, \tag{C 62}$$

$$\mathcal{A}^{(1)}_{yy;xy} = 8\mathcal{B}_{460} = \frac{8\pi}{231}. \tag{C 63}$$

C.5. *Summary*

From §§ C.1–C.4, the elements of the matrices $\boldsymbol{\mathcal{A}}^{(m)}$ $(m = 1, 2)$ and the vector $\boldsymbol{\mathcal{B}}$ are evaluated as follows,

$$\boldsymbol{\mathcal{A}}^{(2)} = \begin{pmatrix} -\dfrac{32\pi}{315} & \dfrac{12\pi^2+128}{1575} & \dfrac{12\pi^2+128}{1575} \\ \dfrac{52\pi^2+604}{1575} & -\dfrac{184\pi}{1575} & -\dfrac{184\pi}{1575} \\ \dfrac{24\pi^2+320}{1575} & -\dfrac{104\pi}{1575} & -\dfrac{8\pi}{175} \\ \dfrac{24\pi^2+320}{1575} & -\dfrac{8\pi}{175} & -\dfrac{104\pi}{1575} \end{pmatrix} \approx \begin{pmatrix} -0.319 & 0.156 & 0.156 \\ 0.709 & -0.367 & -0.367 \\ 0.354 & -0.207 & -0.144 \\ 0.354 & -0.144 & -0.207 \end{pmatrix}, \tag{C 64}$$

$$\boldsymbol{\mathcal{A}}^{(1)} = \begin{pmatrix} -\dfrac{1024}{10395} & \dfrac{16\pi}{1155} & \dfrac{16\pi}{1155} \\ \dfrac{8\pi}{105} & -\dfrac{32}{315} & -\dfrac{32}{315} \\ \dfrac{8\pi}{231} & -\dfrac{128}{2079} & -\dfrac{128}{3465} \\ \dfrac{8\pi}{231} & -\dfrac{128}{3465} & -\dfrac{128}{2079} \end{pmatrix} \approx \begin{pmatrix} 0.0435 & 0.0435 & -0.0985 \\ -0.102 & -0.102 & 0.239 \\ -0.0616 & -0.0369 & 0.109 \\ -0.0369 & -0.0616 & 0.109 \end{pmatrix}, \tag{C 65}$$

$$\boldsymbol{\mathcal{B}} = \begin{pmatrix} -\dfrac{32}{105} \\ \dfrac{4\pi}{15} \\ \dfrac{4\pi}{35} \\ \dfrac{4\pi}{35} \end{pmatrix} \approx \begin{pmatrix} -0.305 \\ 0.838 \\ 0.359 \\ 0.359 \end{pmatrix}. \tag{C 66}$$

Appendix D. Solution of the coupled equations

D.1. *Analytic solutions of the steady equations*

We show the analytic solutions of the steady equations for (4.30) and (4.31), or (C 1) and (C 2), in this section. The solution of (4.30) or (C 1) is given by

$$\begin{pmatrix} P^{(2)} \\ \sigma_{xy}^{(2)} \\ \sigma_{xx}^{(2)} \\ \sigma_{yy}^{(2)} \\ \sigma_{zz}^{(2)} \end{pmatrix} = P^{(2)} \begin{pmatrix} 1 \\ \Pi_{xy}^{(2)} \\ \Pi_{xx}^{(2)} - 1 \\ \Pi_{yy}^{(2)} - 1 \\ -(\Pi_{xx}^{(2)} + \Pi_{yy}^{(2)} + 1) \end{pmatrix} \approx \begin{pmatrix} 0.659 \\ 0.107 \\ -1.21 \\ -0.097 \\ -0.673 \end{pmatrix} \Lambda \frac{\zeta\dot{\gamma}}{4d} \varphi^{*3} g_0(\varphi)^2, \tag{D 1}$$

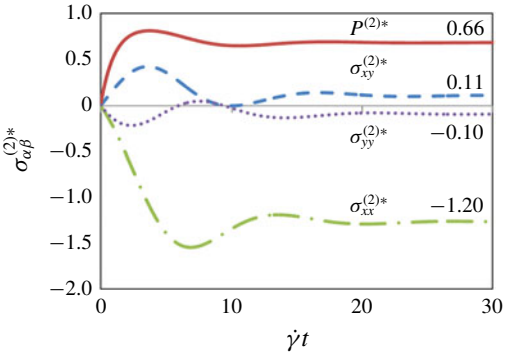

FIGURE 10. (Colour online) Transient numerical solution for $\sigma_{xy}^{(2)*} := \sigma_{xy}^{(2)}/(\Lambda\Sigma^{(2)})$, $\sigma_{xx}^{(2)*} := \sigma_{xx}^{(2)}/(\Lambda\Sigma^{(2)})$, $\sigma_{yy}^{(2)*} := \sigma_{yy}^{(2)}/(\Lambda\Sigma^{(2)})$ and $P^{(2)*} := P^{(2)}/(\Lambda\Sigma^{(2)})$ with $\Sigma^{(2)} := (\zeta\dot{\gamma}/4d)\varphi^{*3}g_0(\varphi)^2$, for the case $\xi = 0.001$.

which coincides with the asymptotic numerical solution of the transient equation, supplemented with a relaxation term of the pressure for numerical stability (see figure 10 and § D.2). The solution of (4.31) or (C 2) is given by

$$\begin{pmatrix} P^{(1)} \\ \sigma_{xy}^{(1)} \\ \sigma_{xx}^{(1)} \\ \sigma_{yy}^{(1)} \\ \sigma_{zz}^{(1)} \end{pmatrix} = P^{(1)*} \begin{pmatrix} 1 \\ \Pi_{xy}^{(1)} \\ \Pi_{xx}^{(1)} - 1 \\ \Pi_{yy}^{(1)} - 1 \\ -(\Pi_{xx}^{(1)} + \Pi_{yy}^{(1)} + 1) \end{pmatrix} \frac{\zeta\dot{\gamma}}{4d}\varphi^{*2}g_0(\varphi), \tag{D 2}$$

where $P^{(1)*}$, $\Pi_{xx}^{(1)}$, $\Pi_{yy}^{(1)}$ and $\Pi_{xy}^{(1)}$ are given in terms of Λ by

$$P^{(1)*} \approx \frac{0.0203}{3.38 - 0.363\Lambda}, \tag{D 3}$$

$$\begin{aligned} \begin{pmatrix} \Pi_{xx}^{(1)} \\ \Pi_{yy}^{(1)} \\ \Pi_{xy}^{(1)} \end{pmatrix} &\approx \frac{1}{\Lambda(0.000469P^{(1)*} + 3.17 \times 10^{-5})} \\ &\quad \times \begin{pmatrix} (0.00521 - 0.00100\Lambda)P^{(1)*} + 0.000168 \\ 0.000469\Lambda P^{(1)*} + 8.59 \times 10^{-5} \\ (0.00332 - 7.58 \times 10^{-5}\Lambda)P^{(1)*} + 0.000210 \end{pmatrix}. \end{aligned} \tag{D 4}$$

The derivation of the solution is shown in §§ D.1.1 and D.1.2. Note that Λ introduced in (4.23) is merely a constant, as discussed in § 4.5. In (D 1), (D 3) and (D 4), the numerical coefficients are determined analytically in rational forms, but only their approximate values in decimals are shown for brevity.

D.1.1. *Order* $O(g_0(\varphi)^2)$

Let us solve the set of equations of $O(g_0(\varphi)^2)$, equation (C 1), with time derivatives set to zero. We cast these equations into the form

$$\boldsymbol{A}^{(2)}(P^{(2)*}) \begin{pmatrix} \Pi_{xy}^{(2)} \\ \Pi_{xx}^{(2)} \\ \Pi_{yy}^{(2)} \end{pmatrix} = \begin{pmatrix} -P^{(2)*} \\ 0 \\ 0 \end{pmatrix}, \tag{D 5}$$

$$\boldsymbol{A}^{(2)}(P^{(2)*}) = \begin{pmatrix} 2\mathcal{A}^{(2)}_{xy;xy} & 2\mathcal{A}^{(2)}_{xy;xx} & 2\mathcal{A}^{(2)}_{xy;yy} - P^{(2)*} \\ \mathcal{A}^{(2)}_{\alpha\alpha;xy} - \mathcal{A}^{(2)}_{xx;xy} & \mathcal{A}^{(2)}_{\alpha\alpha;xx} - \mathcal{A}^{(2)}_{xx;xx} & \mathcal{A}^{(2)}_{\alpha\alpha;yy} - \mathcal{A}^{(2)}_{xx;yy} \\ \mathcal{A}^{(2)}_{yy;xy} & \mathcal{A}^{(2)}_{yy;xx} & \mathcal{A}^{(2)}_{yy;yy} \end{pmatrix}$$
$$= \begin{pmatrix} -0.638 & 0.313 & 0.313 - P^{(2)*} \\ 0.356 & -0.160 & -0.223 \\ 0.354 & -0.144 & -0.207 \end{pmatrix}, \tag{D 6}$$

where we have defined

$$P^{(2)*} := \frac{P^{(2)}}{\Lambda \Sigma^{(2)}}, \tag{D 7}$$

$$\Sigma^{(2)} := \frac{\zeta \dot{\gamma}}{4d} \varphi^{*3} g_0(\varphi)^2. \tag{D 8}$$

This can be solved as

$$\begin{pmatrix} \Pi^{(2)}_{xy} \\ \Pi^{(2)}_{xx} \\ \Pi^{(2)}_{yy} \end{pmatrix} = \boldsymbol{A}^{(2)}(P^{(2)*})^{-1} \begin{pmatrix} -P^{(2)*} \\ 0 \\ 0 \end{pmatrix} = -\frac{P^{(2)*}}{\det \boldsymbol{A}^{(2)}(P^{(2)*})} \begin{pmatrix} A^{(2)}_{xy} \\ A^{(2)}_{xx} \\ A^{(2)}_{yy} \end{pmatrix}$$
$$= -\frac{P^{(2)*}}{A^{(2)} P^{(2)*} + B^{(2)}} \begin{pmatrix} A^{(2)}_{xy} \\ A^{(2)}_{xx} \\ A^{(2)}_{yy} \end{pmatrix}, \tag{D 9}$$

where the numerical factors are given by

$$A^{(2)}_{xy} = 0.00102, \quad A^{(2)}_{yy} = 0.00533, \quad A^{(2)}_{xx} = -0.00518, \tag{D 10a–c}$$

$$A^{(2)} = -0.00532, \quad B^{(2)} = -0.00061. \tag{D 11a,b}$$

From (D 6) and (D 9), the numerical factors in (D 10) and (D 11) are determined in rational forms. However, the expressions are extremely complicated, so we only show their approximate values in decimals. All the decimals which appear in the remainder are also approximations of rational forms. From (C 1) and (D 9), we obtain

$$P^{(2)} = \Lambda \Sigma^{(2)} \left(\mathcal{A}^{(2)}_{xx;xy} + \frac{\Pi^{(2)}_{xx}}{\Pi^{(2)}_{xy}} \mathcal{A}^{(2)}_{xx;xx} + \frac{\Pi^{(2)}_{yy}}{\Pi^{(2)}_{xy}} \mathcal{A}^{(2)}_{xx;yy} \right)$$
$$= \Lambda \Sigma^{(2)} \left(\mathcal{A}^{(2)}_{xx;xy} + \frac{A^{(2)}_{xx}}{A^{(2)}_{xy}} \mathcal{A}^{(2)}_{xx;xx} + \frac{A^{(2)}_{yy}}{A^{(2)}_{xy}} \mathcal{A}^{(2)}_{xx;yy} \right)$$
$$\approx 0.659 \Lambda \Sigma^{(2)}, \tag{D 12}$$

which in turn determines $\Pi^{(2)}_{xx}$, $\Pi^{(2)}_{yy}$ and $\Pi^{(2)}_{xy}$ by (D 9). The stress components are determined as

$$\sigma^{(2)}_{xy} = P^{(2)} \Pi^{(2)}_{xy} \approx 0.107 \Lambda \Sigma^{(2)}, \tag{D 13}$$

$$\sigma^{(2)}_{xx} = P^{(2)} (\Pi^{(2)}_{xx} - 1) \approx -1.21 \Lambda \Sigma^{(2)}, \tag{D 14}$$

$$\sigma^{(2)}_{yy} = P^{(2)} (\Pi^{(2)}_{yy} - 1) \approx -0.097 \Lambda \Sigma^{(2)}, \tag{D 15}$$

$$\sigma_{zz}^{(2)} = P^{(2)}(\Pi_{zz}^{(2)} - 1) = -P^{(2)}(\Pi_{xx}^{(2)} + \Pi_{yy}^{(2)} + 1) \approx -0.673\Lambda\Sigma^{(2)}, \tag{D 16}$$

$$\mu_0 = \mu(\delta\varphi \to 0) = \frac{\sigma_{xy}^{(2)}}{P^{(2)}} = 0.163. \tag{D 17}$$

Note that the magnitudes of $\sigma_{\alpha\beta}^{(2)}$ with $(\alpha, \beta) = (x, y), (x, x), (y, y), (z, z)$ are proportional to Λ, and the stress ratio μ_0 is independent of Λ.

D.1.2. *Order* $O(g_0(\varphi))$

Next we solve the set of equations of $O(g_0(\varphi))$, equation (C 2), with time derivatives set to zero. This can be cast into the form

$$\boldsymbol{A}^{(1)}(P^{(1)*}) \begin{pmatrix} \Pi_{xy}^{(1)} \\ \Pi_{xx}^{(1)} \\ \Pi_{yy}^{(1)} \end{pmatrix} = \begin{pmatrix} 2\mathcal{B}_{xy}^* - P^{(1)*} \\ \mathcal{B}_{\alpha\alpha}^* - \mathcal{B}_{xx}^* \\ \mathcal{B}_{yy}^* \end{pmatrix}, \tag{D 18}$$

$$\begin{aligned} \boldsymbol{A}^{(1)}(P^{(1)*}) &= \begin{pmatrix} 2\mathcal{A}_{xy;xy}^{(1)} & 2\mathcal{A}_{xy;xx}^{(1)} & 2\mathcal{A}_{xy;yy}^{(1)} - P^{(1)*} \\ \mathcal{A}_{\alpha\alpha;xy}^{(1)} - \mathcal{A}_{xx;xy}^{(1)} & \mathcal{A}_{\alpha\alpha;xx}^{(1)} - \mathcal{A}_{xx;xx}^{(1)} & \mathcal{A}_{\alpha\alpha;yy}^{(1)} - \mathcal{A}_{xx;yy}^{(1)} \\ \mathcal{A}_{yy;xy}^{(1)} & \mathcal{A}_{yy;xx}^{(1)} & \mathcal{A}_{yy;yy}^{(1)} \end{pmatrix} \\ &= \begin{pmatrix} -0.197 & 0.0870 & 0.0870 - P^{(1)*} \\ 0.131 & -0.0400 & -0.0646 \\ 0.109 & -0.0369 & -0.0616 \end{pmatrix}, \end{aligned} \tag{D 19}$$

where we have defined

$$P^{(1)*} := \frac{P^{(1)}}{\Lambda\Sigma^{(1)}}, \tag{D 20}$$

$$\Sigma^{(1)} := \frac{\zeta\dot{\gamma}}{4d}\varphi^{*2}g_0(\varphi), \tag{D 21}$$

$$\mathcal{B}_{\alpha\alpha}^* := \frac{\mathcal{B}_{\alpha\alpha}}{\Lambda}, \quad \mathcal{B}_{xx}^* := \frac{\mathcal{B}_{xx}}{\Lambda}, \quad \mathcal{B}_{yy}^* := \frac{\mathcal{B}_{yy}}{\Lambda}, \quad \mathcal{B}_{xy}^* := \frac{\mathcal{B}_{xy}}{\Lambda}. \tag{D 22a–d}$$

This can be solved in parallel to (D 9) as

$$\begin{aligned} \begin{pmatrix} \Pi_{xy}^{(1)} \\ \Pi_{xx}^{(1)} \\ \Pi_{yy}^{(1)} \end{pmatrix} &= \boldsymbol{A}^{(1)}(P^{(1)*})^{-1} \begin{pmatrix} 2\mathcal{B}_{xy}^* - P^{(1)*} \\ \mathcal{B}_{\alpha\alpha}^* - \mathcal{B}_{xx}^* \\ \mathcal{B}_{yy}^* \end{pmatrix} \\ &= \frac{1}{\det \boldsymbol{A}^{(1)}(P^{(1)*})} \begin{pmatrix} \Lambda^{-1}(A_{xy}^{(1)}P^{(1)*} + B_{xy}^{(1)}) - C_{xy}^{(1)}P^{(1)*} \\ \Lambda^{-1}(A_{xx}^{(1)}P^{(1)*} + B_{xx}^{(1)}) - C_{xx}^{(1)}P^{(1)*} \\ \Lambda^{-1}(A_{yy}^{(1)}P^{(1)*} + B_{yy}^{(1)}) - C_{yy}^{(1)}P^{(1)*} \end{pmatrix} \\ &= \frac{1}{A^{(1)}P^{(1)*} + B^{(1)}} \begin{pmatrix} \Lambda^{-1}(A_{xy}^{(1)}P^{(1)*} + B_{xy}^{(1)}) - C_{xy}^{(1)}P^{(1)*} \\ \Lambda^{-1}(A_{xx}^{(1)}P^{(1)*} + B_{xx}^{(1)}) - C_{xx}^{(1)}P^{(1)*} \\ \Lambda^{-1}(A_{yy}^{(1)}P^{(1)*} + B_{yy}^{(1)}) - C_{yy}^{(1)}P^{(1)*} \end{pmatrix}, \end{aligned} \tag{D 23}$$

where the numerical factors are given by

$$A_{xy}^{(1)} = 0.00332, \quad B_{xy}^{(1)} = 0.000210, \quad C_{xy}^{(1)} = 7.58 \times 10^{-5}, \tag{D 24a–c}$$

$$A_{xx}^{(1)} = 0.00521, \quad B_{xx}^{(1)} = 0.000168, \quad C_{xx}^{(1)} = 0.00100, \tag{D 25a–c}$$

$$A_{yy}^{(1)} = 0, \quad B_{yy}^{(1)} = 8.59 \times 10^{-5}, \quad C_{yy}^{(1)} = -0.000469, \tag{D 26a–c}$$

$$A^{(1)} = 0.000469, \quad B^{(1)} = 3.17 \times 10^{-5}. \tag{D 27a,b}$$

From (C 2) and (D 23), we obtain

$$\begin{aligned} P^{(1)*} &= -\frac{\mathcal{B}_{xx}^{*}}{\Pi_{xy}^{(1)}} + \mathcal{A}_{xx;xy}^{(1)} + \frac{\Pi_{xx}^{(1)}}{\Pi_{xy}^{(1)}}\mathcal{A}_{xx;xx}^{(1)} + \frac{\Pi_{yy}^{(1)}}{\Pi_{xy}^{(1)}}\mathcal{A}_{xx;yy}^{(1)} \\ &= -\frac{A^{(1)}P^{(1)*} + B^{(1)}}{(A_{xy}^{(1)} - \Lambda C_{xy}^{(1)})P^{(1)*} + B_{xy}^{(1)}}\mathcal{B}_{xx} + \mathcal{A}_{xx;xy}^{(1)} \\ &\quad + \frac{(A_{xx}^{(1)} - \Lambda C_{xx}^{(1)})P^{(1)*} + B_{xx}^{(1)}}{(A_{xy}^{(1)} - \Lambda C_{xy}^{(1)})P^{(1)*} + B_{xy}^{(1)}}\mathcal{A}_{xx;xx}^{(1)} + \frac{(A_{yy}^{(1)} - \Lambda C_{yy}^{(1)})P^{(1)*} + B_{yy}^{(1)}}{(A_{xy}^{(1)} - \Lambda C_{xy}^{(1)})P^{(1)*} + B_{xy}^{(1)}}\mathcal{A}_{xx;yy}^{(1)}, \end{aligned} \tag{D 28}$$

from which $P^{(1)*}$ is determined as

$$P^{(1)*} = \frac{X + \sqrt{X^2 + 4Y}}{2}, \tag{D 29}$$

$$X := \frac{\mathcal{A}_{xx;xx}^{(1)}(A_{xx}^{(1)} - \Lambda C_{xx}^{(1)}) + \mathcal{A}_{xx;yy}^{(1)}(A_{yy}^{(1)} - \Lambda C_{yy}^{(1)}) + \mathcal{A}_{xx;xy}^{(1)}(A_{xy}^{(1)} - \Lambda C_{xy}^{(1)}) - A^{(1)}\mathcal{B}_{xx} - B_{xy}^{(1)}}{A_{xy}^{(1)} - \Lambda C_{xy}^{(1)}}, \tag{D 30}$$

$$Y := \frac{\mathcal{A}_{xx;xx}^{(1)}B_{xx}^{(1)} + \mathcal{A}_{xx;yy}^{(1)}B_{yy}^{(1)} + \mathcal{A}_{xx;xy}^{(1)}B_{xy}^{(1)} - B^{(1)}\mathcal{B}_{xx}}{A_{xy}^{(1)} - \Lambda C_{xy}^{(1)}}. \tag{D 31}$$

Evaluation of the numerators of X and Y yields

$$X \approx \frac{3.63 \times 10^{-5}\Lambda - 3.38 \times 10^{-4}}{A_{xy}^{(1)} - \Lambda C_{xy}^{(1)}}, \tag{D 32}$$

$$Y \approx \frac{2.03 \times 10^{-6}}{A_{xy}^{(1)} - \Lambda C_{xy}^{(1)}}, \tag{D 33}$$

which implies $X < 0$, $Y > 0$ and $|X| \gg |Y|$. Hence, we obtain

$$P^{(1)*} \approx \frac{|Y|}{|X|} = \frac{0.0203}{3.38 - 0.363\Lambda}, \tag{D 34}$$

$$P^{(1)} = P^{(1)*}\Sigma^{(1)} = \frac{0.0203}{3.38 - 0.363\Lambda}\Sigma^{(1)}, \tag{D 35}$$

which in turn determines $\Pi_{xx}^{(1)}$, $\Pi_{yy}^{(1)}$ and $\Pi_{xy}^{(1)}$ by (D 23). The stress components are determined as in (D 13)–(D 16). For instance, for $\Lambda = 0.04$, we obtain

$$P^{(1)} \approx 1.20 \times 10^{-4}\Sigma^{(1)}, \tag{D 36}$$

$$\sigma_{xy}^{(1)} \approx 0.0399\Sigma^{(1)}, \tag{D 37}$$

$$\sigma_{xx}^{(1)} \approx 0.0345\Sigma^{(1)}, \tag{D 38}$$

$$\sigma_{yy}^{(1)} \approx 0.0148\Sigma^{(1)}, \tag{D 39}$$

$$\sigma_{zz}^{(1)} \approx -0.0497\Sigma^{(1)}. \tag{D 40}$$

D.2. *Numerical solutions of the transient equations*

Let us solve the transient equations of $O(g_0(\varphi)^2)$, equation (4.30), numerically. For this purpose, we choose the stress components $\sigma_{\alpha\beta}^{(2)}$ rather than the deviatoric stress components $\Pi_{\alpha\beta}^{(2)}$ as independent variables. Equation (4.30) is expressed solely in terms of $\sigma_{\alpha\beta}^{(2)}$ as

$$\frac{\mathrm{d}}{\mathrm{d}t}\sigma_{xy}^{(2)} = -\frac{1}{2}\dot{\gamma}\sigma_{yy}^{(2)} + \dot{\gamma}\Lambda\frac{\Sigma^{(2)}}{P^{(2)}}[\mathcal{A}_{xy;xx}^{(2)}\sigma_{xx}^{(2)} + \mathcal{A}_{xy;yy}^{(2)}\sigma_{yy}^{(2)} + \mathcal{A}_{xy;xy}^{(2)}\sigma_{xy}^{(2)}] + \dot{\gamma}\Lambda\Sigma^{(2)}(\mathcal{A}_{xy;xx}^{(2)} + \mathcal{A}_{xy;yy}^{(2)}), \tag{D 41}$$

$$\frac{\mathrm{d}}{\mathrm{d}t}P^{(2)} = \frac{1}{3}\dot{\gamma}\sigma_{xy}^{(2)} - \frac{1}{3}\dot{\gamma}\Lambda\frac{\Sigma^{(2)}}{P^{(2)}}[\mathcal{A}_{\alpha\alpha;xx}^{(2)}\sigma_{xx}^{(2)} + \mathcal{A}_{\alpha\alpha;yy}^{(2)}\sigma_{yy}^{(2)} + \mathcal{A}_{\alpha\alpha;xy}^{(2)}\sigma_{xy}^{(2)}] - \frac{1}{3}\dot{\gamma}\Lambda\Sigma^{(2)}(\mathcal{A}_{\alpha\alpha;xx}^{(2)} + \mathcal{A}_{\alpha\alpha;yy}^{(2)}), \tag{D 42}$$

$$\frac{\mathrm{d}}{\mathrm{d}t}\sigma_{xx}^{(2)} = -\dot{\gamma}\sigma_{xy}^{(2)} + \dot{\gamma}\Lambda\frac{\Sigma^{(2)}}{P^{(2)}}[\mathcal{A}_{xx;xx}^{(2)}\sigma_{xx}^{(2)} + \mathcal{A}_{xx;yy}^{(2)}\sigma_{yy}^{(2)} + \mathcal{A}_{xx;xy}^{(2)}\sigma_{xy}^{(2)}] + \dot{\gamma}\Lambda\Sigma^{(2)}(\mathcal{A}_{xx;xx}^{(2)} + \mathcal{A}_{xx;yy}^{(2)}), \tag{D 43}$$

$$\frac{\mathrm{d}}{\mathrm{d}t}\sigma_{yy}^{(2)} = \dot{\gamma}\Lambda\frac{\Sigma^{(2)}}{P^{(2)}}[\mathcal{A}_{yy;xx}^{(2)}\sigma_{xx}^{(2)} + \mathcal{A}_{yy;yy}^{(2)}\sigma_{yy}^{(2)} + \mathcal{A}_{yy;xy}^{(2)}\sigma_{xy}^{(2)}] + \dot{\gamma}\Lambda\Sigma^{(2)}(\mathcal{A}_{yy;xx}^{(2)} + \mathcal{A}_{yy;yy}^{(2)}), \tag{D 44}$$

where $\Sigma^{(2)}$ is defined as

$$\Sigma^{(2)} := \frac{\zeta\dot{\gamma}}{4d}\varphi^{*3}g_0(\varphi)^2 > 0. \tag{D 45}$$

The first terms on the right-hand side of (D 41)–(D 43) correspond to the heating due to shear, and the terms proportional to $\Sigma^{(2)}$ are the relaxation terms which originate from dissipation.

It should be noted that (D 42) is singular in the sense that the self-relaxation term proportional to $P^{(2)}$ is absent from the right-hand side. In contrast, the other equations for $\sigma_{xy}^{(2)}$, $\sigma_{xx}^{(2)}$ and $\sigma_{yy}^{(2)}$ include self-relaxation terms proportional to themselves. This singularity in (D 42) causes instability in the numerical integration. To avoid this problem, we add a self-relaxation term to the right-hand side of (D 42), which vanishes in the steady state, as

$$\frac{\mathrm{d}}{\mathrm{d}t}P^{(2)} = \frac{1}{3}\dot{\gamma}\sigma_{xy}^{(2)} + \frac{1}{3}\dot{\gamma}\Lambda\frac{\Sigma^{(2)}}{P^{(2)}}[0.367\sigma_{xx}^{(2)} + 0.367\sigma_{yy}^{(2)} - 0.709\sigma_{xy}^{(2)}] - \xi(P^{(2)} - P_{ss}^{(2)}) + 0.245\dot{\gamma}\Lambda\Sigma^{(2)}, \tag{D 46}$$

where $P_{ss}^{(2)} = 0.659\Lambda\Sigma^{(2)}$ is the steady solution and $\xi > 0$ is a viscous constant. The numerical solution of the coupled equations (D 41), (D 43), (D 44) and (D 46) is shown in figure 10, for the case $\xi = 0.001$ and initial conditions $\sigma_{xy}^{(2)}(t=0) = \sigma_{xx}^{(2)}(t=0) = \sigma_{yy}^{(2)}(t=0) = 0$, $P^{(2)}(t=0) = 0.01\Lambda\Sigma^{(2)}$. We confirm that the asymptotic steady values coincide with the analytical solutions, equation (D 1).

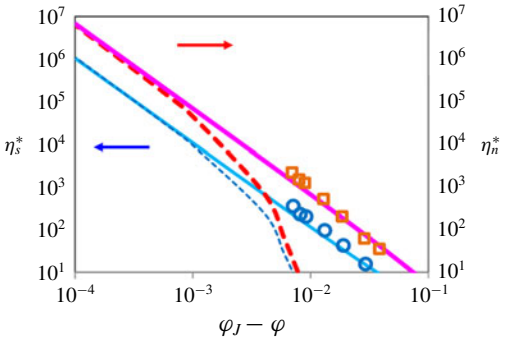

FIGURE 11. (Colour online) Shear and pressure viscosities for the case $\Lambda = 0.04$. The thick-solid line, thick-dashed line, open squares are the results of the pressure viscosity with splitting, without splitting and of MD. The thin-solid line, thin-dashed line, open circles are the results of the shear viscosity with splitting, without splitting and of MD.

Next, we numerically solve the transient equations without splitting into $O(g_0(\varphi)^2)$ and $O(g_0(\varphi))$, i.e. (4.28) or (4.29). We choose $\sigma_{\alpha\beta}$ as independent variables as in (D 41)–(D 44), and attach a self-relaxation term to the pressure equation as in (D 46). We will not explicitly write down the equations and present the result in figure 11. We see that the result with splitting deviates from that without splitting for $\delta\varphi = \varphi_J - \varphi > 10^{-3}$.

Appendix E. Comparison with empirical relations

We compare our theory with empirical relations which describe experimental results well. The empirical equations for the normalized pressure and shear viscosities are, respectively, given by

$$\eta_n^{*(MB)} = K_n \left(\frac{\varphi/\varphi_J}{1 - \varphi/\varphi_J} \right)^2, \tag{E 1}$$

$$\eta_s^{*(MB)} = K_s \left(\frac{\varphi/\varphi_J}{1 - \varphi/\varphi_J} \right)^2 + 2.5 \left(\frac{\varphi_J}{1 - \varphi/\varphi_J} \right) + 1, \tag{E 2}$$

where the upper script (MB) is named after the authors, and the coefficients are given by $K_n = 0.75$ and $K_s = 0.1$ (Morris & Boulay 1999). In figure 12, we present the results of (E 1) and (E 2), together with our theoretical results. For comparison, the results of (E 1) and (E 2) are multiplied by 0.3 for comparison. In the dense region, where the first term on the right-hand side of (E 2) is dominant, we obtain

$$\mu^{(MB)}(\delta\varphi \to 0) = \frac{\eta_s^{*(MB)}(\delta\varphi \to 0)}{\eta_n^{*(MB)}(\delta\varphi \to 0)} = \frac{K_s}{K_n} = 0.133. \tag{E 3}$$

This is in a relatively good agreement with the result of the present theory, 0.163. For lower densities, from (E 1) and (E 2), we obtain

$$\mu^{(MB)} = \frac{\eta_s^{*(MB)}}{\eta_n^{*(MB)}} = \frac{K_s}{K_n} + \frac{2.5}{K_n(\varphi/\varphi_J)^2}\delta\varphi + \frac{1}{K_n\varphi^2}\delta\varphi^2 \approx 0.133 + \frac{3.33}{(\varphi/\varphi_J)^2}\delta\varphi, \tag{E 4}$$

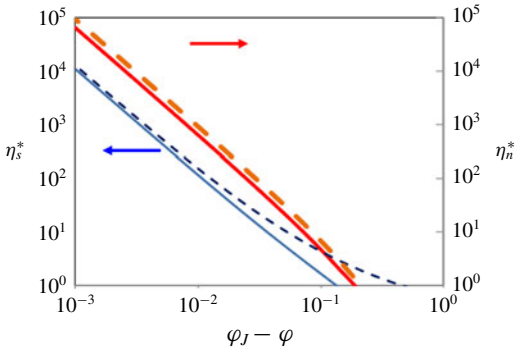

FIGURE 12. (Colour online) Comparison with the empirical relation (Morris & Boulay 1999). The results of the normalized shear and pressure viscosities are shown in thin-dashed line and thick-dashed line, respectively. The results are multiplied by 0.3 for comparison to the theoretical results for $\Lambda = 0.04$ shown in figure 3, which are also displayed.

where we have neglected the $O(\delta\varphi^2)$ term in the last equality. Specifically, for $10^{-2} < \delta\varphi < 10^{-1}$ and $\varphi_J = 0.639$, we obtain

$$0.133 + 3.44\delta\varphi < \mu^{(MB)} < 0.133 + 4.68\delta\varphi. \tag{E 5}$$

This is also in a relatively good agreement with our theory, $\mu \approx 0.163 + 1.78\varphi^{*-1}\delta\varphi$ (cf. (4.45)).

Appendix F. Details of the event-driven MD simulation

The scheme of the event-driven MD simulation is discussed. It is based on the scheme for Brownian hard spheres (Scala *et al.* 2007), which solves the overdamped equation of motion,

$$\zeta \dot{\boldsymbol{r}}_i = \boldsymbol{F}_i^{(p)} + \zeta\dot{\gamma} y_i \boldsymbol{e}_x + \boldsymbol{F}_i^{(r)}. \tag{F 1}$$

Here, $\zeta = 3\pi d\,\eta_0$ is the scalar resistance and $\boldsymbol{F}_i^{(r)}$ is the random fluctuation force exerted by the solvent, which is assumed to be Gaussian,

$$\langle \boldsymbol{F}_i^{(r)}(t)\boldsymbol{F}_i^{(r)}(t')\rangle = 2D_0\zeta^2\delta(t-t'). \tag{F 2}$$

The diffusion constant is related to ζ as $D_0 = T_{eq}/\zeta$ via the fluctuation-dissipation theorem, where T_{eq} is the equilibrium temperature of the solvent. The units of length and time are chosen as d and d^2/D_0. If we require that the physical mass of the particle m does not appear explicitly in the overdamped dynamics of (F 1), the only combination with the dimension of mass is $\zeta d^2/D_0$, and hence we choose this as the unit of mass. The algorithm consists of three steps:

(i) for each time step $t_n = n\Delta t$ $(n = 0, 1, \ldots)$, random velocities $\boldsymbol{v}_i^{(r)} = (\Delta\boldsymbol{r}_i - \langle\Delta\boldsymbol{r}\rangle)/\Delta t$ are sampled for $i = 1, \ldots, N$ according to the Maxwellian distribution $f(\boldsymbol{v}) = (m_v/(2\pi T_{eq}))^{-3/2}\exp(-m_v\boldsymbol{v}^2/(2T_{eq}))$, where m_v is the 'virtual mass' related to D_0 as $D_0 = T_{eq}\Delta t/(2m_v)$;
(ii) add uniform shear velocity $\dot{\gamma} y_i \boldsymbol{e}_x$ to the random velocity;

(iii) evolve between t_n and t_{n+1} by the event-driven MD.

Note that m_v is a virtual quantity introduced in the Maxwellian distribution, so as to ensure the diffusive motion of the particles. In fact, from $D_0 = T_{eq}/\zeta$ and $D_0 = T_{eq}\Delta t/(2m_v)$, m_v is determined as

$$m_v = \zeta\,\Delta t/2 = \zeta d^2\Delta t^*/(2D_0), \tag{F 3}$$

which depends on $\Delta t = \Delta t^* d^2/D_0$ and hence is not physical. (We attach $*$ to dimensionless quantities.)

We modify the above scheme to adapt to non-Brownian hard spheres. We can eliminate the Brownian motion by taking the limit $D_0 \to 0$, or $T_{eq} \to 0$, with $m_v = \zeta\,\Delta t/2$ fixed. By this choice, for each time step $t_n = n\Delta t$, the velocity of the particles is set to the uniform shear velocity $\dot\gamma y_i \boldsymbol{e}_x$, and the dynamics is evolved between t_n and t_{n+1} by the event-driven MD. However, taking the limit $D_0 \to 0$ requires us to choose other units for the time and mass, which are uniquely determined to be $\dot\gamma^{-1}$ and $\zeta/\dot\gamma$, respectively. This implies that Δt and m_v should be scaled as

$$\Delta t = \dot\gamma^{-1}\Delta t^* \tag{F 4}$$

and

$$m_v = (\zeta/\dot\gamma)(\Delta t^*/2). \tag{F 5}$$

Although the physical mass m exists in real suspensions, the overdamped approximation, equation (F 1), superficially replaces m with the virtual mass m_v, which is given by (F 3) for the Brownian and (F 5) for the non-Brownian suspensions, respectively.

After equilibration from an initial configuration without overlapping of the spheres, we start the sampling. The average of the stress tensor is evaluated by

$$\sigma_{\alpha\beta} = \sigma^{(K)}_{\alpha\beta} + \sigma^{(C)}_{\alpha\beta}, \tag{F 6}$$

where

$$\sigma^{(K)}_{\alpha\beta} = -\frac{1}{V}\left\langle \sum_{i=1}^{N} \frac{1}{m_v} p_{i,\alpha} p_{i,\beta} \right\rangle = -\frac{1}{V}\left\langle \sum_{i=1}^{N} m_v v_{i,\alpha} v_{i,\beta} \right\rangle \tag{F 7}$$

is the average kinetic stress and

$$\sigma^{(C)}_{\alpha\beta} = -\frac{1}{V}\left\langle \sum_{i=1}^{N} \frac{1}{2t_m} \sum_{coll} r_{ij,\alpha} p_{ij,\beta} \right\rangle = -\frac{1}{V}\left\langle \sum_{i=1}^{N} \frac{m_v}{2t_m} \sum_{coll} r_{ij,\alpha} v_{ij,\beta} \right\rangle \tag{F 8}$$

is the average contact stress, with

$$\boldsymbol{p}_i = m_v \boldsymbol{v}_i = m_v(\dot{\boldsymbol{r}}_i - \dot\gamma y_i \boldsymbol{e}_x) \tag{F 9}$$

the peculiar momentum. In (F 8), t_m is a time interval which is introduced to evaluate the force from the momentum transfer as $\boldsymbol{F}_{ij} = \boldsymbol{p}_{ij}/t_m$, and the summation $\sum_{coll}$ is performed over all the colliding pairs (i, j). The parameters are set as $N = 1000$, $\Delta t^* = 0.001$ and $t^*_m = 10\Delta t^* = 0.01$. By the choice $t^*_m \propto \Delta t^*$, equation (F 8) is insensitive to Δt^*. Furthermore, we have verified that $\sigma^{(C)}_{\alpha\beta}$ is insensitive to the choice of t^*_m. We have confirmed that the results are almost insensitive to the shear rate, which exemplifies the Newtonian behaviour (cf. figure 13). We have also confirmed that, although the magnitude of $\sigma^{(K)}_{\alpha\beta}$ is proportional to Δt^*, it does not exhibit any divergence in approaching the jamming point, which validates (2.8). We have compared the result of the event-driven MD simulation with that of soft-sphere MD simulation ($\dot\gamma^* = 10^{-7}$) and found reasonable agreement between them (cf. figure 14).

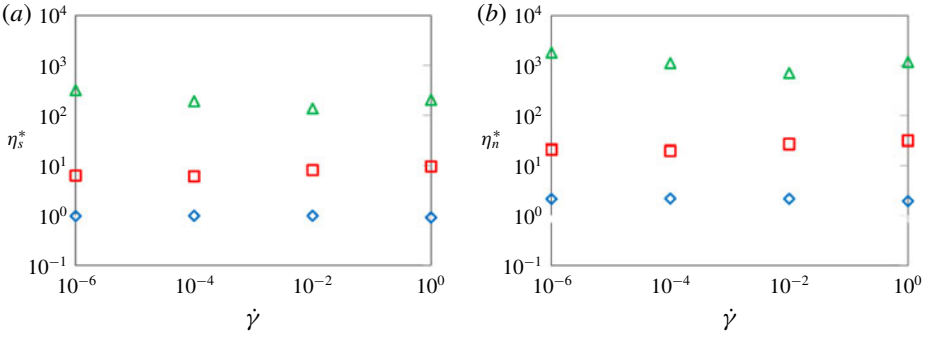

FIGURE 13. (Colour online) (*a*) Shear-rate dependence of the shear viscosity and (*b*) the pressure viscosity. The results for $\varphi = 0.50$, 0.60, 0.63 are shown in open diamonds, squares and triangles, respectively.

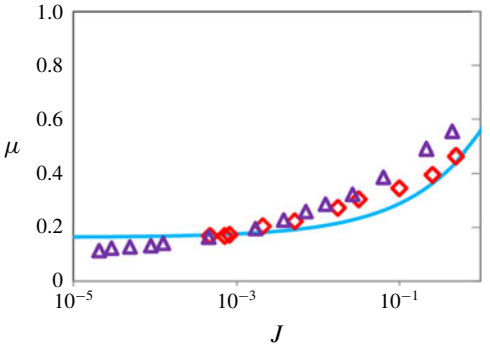

FIGURE 14. (Colour online) Comparison of the theoretical result with those of hard-sphere and soft-sphere MD simulations. The results of the theory, hard-sphere MD and soft-sphere MD are shown in solid line, open diamonds and crosses, respectively.

Appendix G. Implication of the symmetry

Here we discuss another implication of the symmetry. From (2.1), the velocity distribution of the particles deviates from the uniform profile of that of the solvent, $\dot{\gamma} y_i \boldsymbol{e}_x$, if the average force is non-vanishing, $\langle \boldsymbol{F}_i^{(p)} \rangle \neq 0$. However, this is actually not the case. From (3.15) and (4.9), we have

$$\begin{aligned}\langle \boldsymbol{F}_i^{(p)} \rangle &= \sum_{j \neq i} \langle \boldsymbol{F}_{ij}^{(p)} \rangle = -\frac{1}{2} \zeta_e \dot{\gamma} d^2 \sum_{j \neq i} \langle \hat{\boldsymbol{r}}_{ij} \delta(r_{ij} - d) \hat{x}_{ij} \hat{y}_{ij} \Theta(-\hat{x}_{ij} \hat{y}_{ij}) \rangle \\ &= -\frac{1}{2} \zeta_e \dot{\gamma} d^2 \sum_{j \neq i} \left\{ \langle \Delta_{ij} \hat{\boldsymbol{r}}_{ij} \hat{x}_{ij} \hat{y}_{ij} \Theta_{ij} \rangle_{eq} + \frac{V}{2T} \Pi_{\alpha\beta} \langle \Delta_{ij} \hat{\boldsymbol{r}}_{ij} \hat{x}_{ij} \hat{y}_{ij} \Theta_{ij} \tilde{\sigma}_{\alpha\beta} \rangle_{eq} \right\}, \end{aligned} \tag{G 1}$$

where $\Delta_{ij} := \delta(r_{ij} - d)$ and $\Theta_{ij} := \Theta(-\hat{x}_{ij}\hat{y}_{ij})$. From (4.25) it is obvious that the first canonical term vanishes (cubic in $\hat{\boldsymbol{r}}_{ij}$). By noting that $\tilde{\sigma}_{\alpha\beta}$ is quartic in $\hat{\boldsymbol{r}}$, the second non-canonical term also vanishes. Hence, the linear profile of the velocity of the particles is preserved in the steady state.

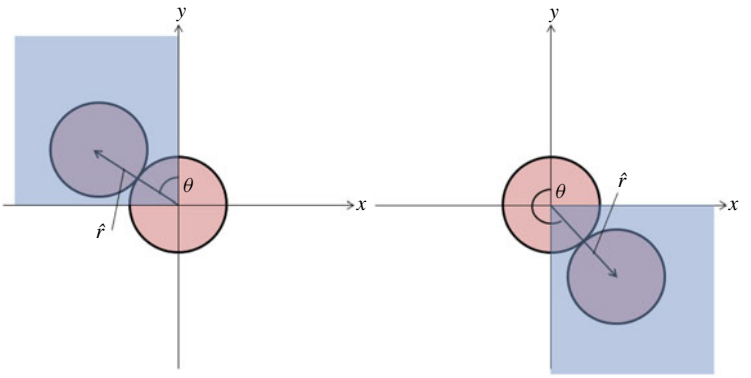

FIGURE 15. (Colour online) Spherical coordinate for the angular integral.

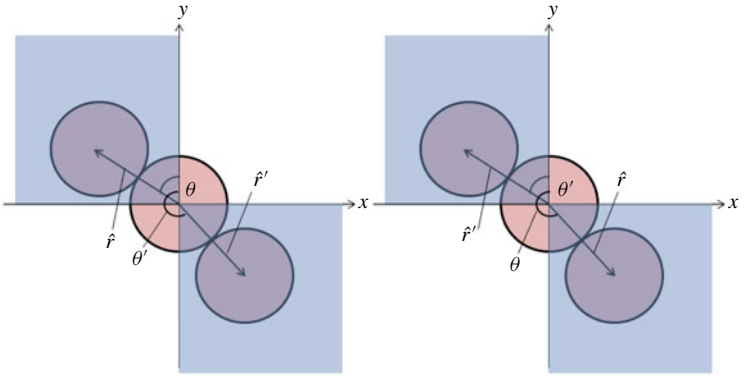

FIGURE 16. (Colour online) Possible configurations for the double angular integrals.

Appendix H. Angular integrals

We collect the results of the angular integrals $\mathcal{A}_{pqr;stu}$ and $\mathcal{B}_{pqr}$, defined in (C 4) and (C 5). Let us introduce the following spherical coordinate (cf. figure 15),

$$\hat{z} = \sin\theta\cos\phi, \tag{H 1}$$

$$\hat{x} = \sin\theta\sin\phi, \tag{H 2}$$

$$\hat{y} = \cos\theta. \tag{H 3}$$

Then, equation (C 5) is parametrized as

$$\begin{aligned}\mathcal{B}_{pqr} &= \int \mathrm{d}\mathcal{S}(\Theta(\hat{y})\Theta(-\hat{x}) + \Theta(-\hat{y})\Theta(\hat{x}))\hat{x}^p\hat{y}^q\hat{z}^r \\ &= \left\{\int_0^1 \mathrm{d}(\cos\theta)\int_{-\pi}^0 \mathrm{d}\phi + \int_{-1}^0 \mathrm{d}(\cos\theta)\int_0^\pi \mathrm{d}\phi\right\}\hat{x}^p\hat{y}^q\hat{z}^r.\end{aligned} \tag{H 4}$$

Equation (C 4) is a double angular integral with respect to $\hat{\boldsymbol{r}}$ and $\hat{\boldsymbol{r}}'$, which can be classified into the two cases depicted in figure 16. Accordingly, it is parametrized as

follows,

$$\mathcal{A}_{pqr;stu} = \left\{ \int_0^1 \mathrm{d}(\cos\theta) \int_{-\pi}^0 \mathrm{d}\phi \int_{-1}^0 \mathrm{d}(\cos\theta') \int_0^\pi \mathrm{d}\phi' + \int_{-1}^0 \mathrm{d}(\cos\theta) \int_0^\pi \mathrm{d}\phi \int_0^1 \mathrm{d}(\cos\theta') \int_{-\pi}^0 \mathrm{d}\phi' \right\} \times \hat{x}^p \hat{y}^q \hat{z}^r \hat{x}'^s \hat{y}'^t \hat{z}'^u. \tag{H 5}$$

Note that only the integrands which are even with respect to the parity transformation '$\hat{x} \to -\hat{x}$ and $\hat{y} \to -\hat{y}$' survive (cf. (4.22)). For parity-even terms, equation (H 5) reduces to

$$\mathcal{A}_{pqr;stu} = 2 \int_0^1 \mathrm{d}(\cos\theta) \int_{-\pi}^0 \mathrm{d}\phi \int_{-1}^0 \mathrm{d}(\cos\theta') \int_0^\pi \mathrm{d}\phi' \hat{x}^p \hat{y}^q \hat{z}^r \hat{x}'^s \hat{y}'^t \hat{z}'^u. \tag{H 6}$$

Hence, equation (C 4) is expressed as

$$\mathcal{A}_{pqr;stu} = 2\mathcal{B}_{pqr}\mathcal{C}_{stu}, \tag{H 7}$$

$$\mathcal{B}_{pqr} = \int_0^1 \mathrm{d}(\cos\theta) \int_{-\pi}^0 \mathrm{d}\phi\, \hat{x}^p \hat{y}^q \hat{z}^r = \int_0^1 \mathrm{d}(\cos\theta) \int_{-\pi}^0 \mathrm{d}\phi\, \cos^q\theta \sin^{p+r}\theta \sin^p\phi \cos^r\phi, \tag{H 8}$$

$$\mathcal{C}_{stu} = \int_{-1}^0 \mathrm{d}(\cos\theta') \int_0^\pi \mathrm{d}\phi' \hat{x}'^s \hat{y}'^t \hat{z}'^u = \int_{-1}^0 \mathrm{d}(\cos\theta') \int_0^\pi \mathrm{d}\phi' \cos^t\theta \sin^{s+u}\theta \sin^s\phi \cos^u\phi. \tag{H 9}$$

Furthermore, $\mathcal{B}_{pqr} = \mathcal{C}_{pqr}$ holds, so we finally obtain

$$\mathcal{A}_{pqr;stu} = 2\mathcal{B}_{pqr}\mathcal{B}_{stu}. \tag{H 10}$$

It should be noted that $\mathcal{B}_{pqr} = \mathcal{B}_{qpr}$ holds from symmetry. We collect the results of $\mathcal{B}_{pqr}$ necessary for our purpose below:

$$\mathcal{B}_{730} = \mathcal{B}_{370} = \int_0^1 \mathrm{d}(\cos\theta) \int_{-\pi}^0 \mathrm{d}\phi\, \cos^3\theta \sin^7\theta \sin^7\phi = -\tfrac{64}{3465}, \tag{H 11}$$

$$\mathcal{B}_{710} = \mathcal{B}_{170} = \int_0^1 \mathrm{d}(\cos\theta) \int_{-\pi}^0 \mathrm{d}\phi\, \cos\theta \sin^7\theta \sin^7\phi = -\tfrac{32}{315}, \tag{H 12}$$

$$\mathcal{B}_{640} = \mathcal{B}_{460} = \int_0^1 \mathrm{d}(\cos\theta) \int_{-\pi}^0 \mathrm{d}\phi\, \cos^4\theta \sin^6\theta \sin^6\phi = \frac{\pi}{231}, \tag{H 13}$$

$$\mathcal{B}_{620} = \mathcal{B}_{260} = \int_0^1 \mathrm{d}(\cos\theta) \int_{-\pi}^0 \mathrm{d}\phi\, \cos^2\theta \sin^6\theta \sin^6\phi = \frac{\pi}{63}, \tag{H 14}$$

$$\mathcal{B}_{550} = \int_0^1 \mathrm{d}(\cos\theta) \int_{-\pi}^0 \mathrm{d}\phi\, \cos^5\theta \sin^5\theta \sin^5\phi = -\tfrac{128}{10395}, \tag{H 15}$$

$$\mathcal{B}_{530} = \mathcal{B}_{350} = \int_0^1 \mathrm{d}(\cos\theta) \int_{-\pi}^0 \mathrm{d}\phi\, \cos^3\theta \sin^5\theta \sin^5\phi = -\tfrac{32}{945}, \tag{H 16}$$

$$\mathcal{B}_{510} = \mathcal{B}_{150} = \int_0^1 \mathrm{d}(\cos\theta) \int_{-\pi}^0 \mathrm{d}\phi\, \cos\theta \sin^5\theta \sin^5\phi = -\tfrac{16}{105}, \tag{H 17}$$

$$\mathcal{B}_{440} = \int_0^1 \mathrm{d}(\cos\theta) \int_{-\pi}^0 \mathrm{d}\phi \cos^4\theta \sin^4\theta \sin^4\phi = \frac{\pi}{105}, \tag{H 18}$$

$$\mathcal{B}_{420} = \mathcal{B}_{240} = \int_0^1 \mathrm{d}(\cos\theta) \int_{-\pi}^0 \mathrm{d}\phi \cos^2\theta \sin^4\theta \sin^4\phi = \frac{\pi}{35}, \tag{H 19}$$

$$\mathcal{B}_{330} = \int_0^1 \mathrm{d}(\cos\theta) \int_{-\pi}^0 \mathrm{d}\phi \cos^3\theta \sin^3\theta \sin^3\phi = -\tfrac{8}{105}, \tag{H 20}$$

$$\mathcal{B}_{310} = \mathcal{B}_{130} = \int_0^1 \mathrm{d}(\cos\theta) \int_{-\pi}^0 \mathrm{d}\phi \cos\theta \sin^3\theta \sin^3\phi = -\tfrac{4}{15}, \tag{H 21}$$

$$\mathcal{B}_{220} = \int_0^1 \mathrm{d}(\cos\theta) \int_{-\pi}^0 \mathrm{d}\phi \cos^2\theta \sin^2\theta \sin^2\phi = \frac{\pi}{15}, \tag{H 22}$$

$$\mathcal{B}_{040} = \int_0^1 \mathrm{d}(\cos\theta) \int_{-\pi}^0 \mathrm{d}\phi \cos^4\theta = \frac{\pi}{5}, \tag{H 23}$$

$$\mathcal{B}_{020} = \int_0^1 \mathrm{d}(\cos\theta) \int_{-\pi}^0 \mathrm{d}\phi \cos^2\theta = \frac{\pi}{3}, \tag{H 24}$$

$$\mathcal{B}_{442} = \int_0^1 \mathrm{d}(\cos\theta) \int_{-\pi}^0 \mathrm{d}\phi \cos^4\theta \sin^6\theta \sin^4\phi \cos^2\phi = \frac{\pi}{1155}, \tag{H 25}$$

$$\mathcal{B}_{242} = \mathcal{B}_{422} = \int_0^1 \mathrm{d}(\cos\theta) \int_{-\pi}^0 \mathrm{d}\phi \cos^4\theta \sin^4\theta \sin^2\phi \cos^2\phi = \frac{\pi}{315}, \tag{H 26}$$

$$\mathcal{B}_{532} = \mathcal{B}_{352} = \int_0^1 \mathrm{d}(\cos\theta) \int_{-\pi}^0 \mathrm{d}\phi \cos^3\theta \sin^7\theta \sin^5\phi \cos^2\phi = -\tfrac{32}{10395}, \tag{H 27}$$

$$\mathcal{B}_{152} = \mathcal{B}_{512} = \int_0^1 \mathrm{d}(\cos\theta) \int_{-\pi}^0 \mathrm{d}\phi \cos^5\theta \sin^3\theta \sin\phi \cos^2\phi = -\tfrac{16}{945}, \tag{H 28}$$

$$\mathcal{B}_{332} = \int_0^1 \mathrm{d}(\cos\theta) \int_{-\pi}^0 \mathrm{d}\phi \cos^3\theta \sin^5\theta \sin^3\phi \cos^2\phi = -\tfrac{8}{945}, \tag{H 29}$$

$$\mathcal{B}_{132} = \mathcal{B}_{312} = \int_0^1 \mathrm{d}(\cos\theta) \int_{-\pi}^0 \mathrm{d}\phi \cos^3\theta \sin^3\theta \sin\phi \cos^2\phi = -\tfrac{4}{105}, \tag{H 30}$$

$$\mathcal{B}_{222} = \int_0^1 \mathrm{d}(\cos\theta) \int_{-\pi}^0 \mathrm{d}\phi \cos^2\theta \sin^4\theta \cos^2\phi \sin^2\phi = \frac{\pi}{105}, \tag{H 31}$$

$$\mathcal{B}_{112} = \int_0^1 \mathrm{d}(\cos\theta) \int_{-\pi}^0 \mathrm{d}\phi \cos\theta \sin^3\theta \sin\phi \cos^2\phi = -\tfrac{2}{15}. \tag{H 32}$$

In the above calculation, we have utilized the following formulas:

$$\int_0^1 \mathrm{d}(\cos\theta) \cos^n\theta \sin^m\theta = \begin{cases} \displaystyle\int_0^1 \mathrm{d}x x^n (1-x^2)^{m/2} & (n, m : \text{even}) \\ \displaystyle\int_0^{\pi/2} \mathrm{d}\theta \cos^n\theta (1-\cos^2\theta)^{(m+1)/2} & (n, m : \text{odd}), \end{cases} \tag{H 33}$$

$$\int_{-\pi}^0 \mathrm{d}\phi \sin^n\phi = \begin{cases} \displaystyle 2 \cdot \frac{\pi}{2} \frac{(n-1)!!}{n!!} & (n : \text{even}) \\ \displaystyle -2 \cdot \frac{(n-1)!!}{n!!} & (n : \text{odd}). \end{cases} \tag{H 34}$$

From the above results for $\mathcal{B}_{pqr}$, we obtain $\mathcal{A}_{pqr;stu}$ via (H 10) as follows,

$$\mathcal{A}_{420;220} = \mathcal{A}_{240;220} = 2\frac{\pi}{35}\frac{\pi}{15} = \frac{2\pi^2}{525}, \tag{H 35}$$

$$\mathcal{A}_{420;130} = \mathcal{A}_{240;310} = 2\frac{\pi}{35}\left(-\frac{4}{15}\right) = -\frac{8\pi}{525}, \tag{H 36}$$

$$\mathcal{A}_{330;310} = \mathcal{A}_{330;130} = -2\tfrac{8}{105}(-\tfrac{4}{15}) = \tfrac{64}{1575}, \tag{H 37}$$

$$\mathcal{A}_{330;220} = -2\frac{8}{105}\frac{\pi}{15} = -\frac{16\pi}{1575}, \tag{H 38}$$

$$\mathcal{A}_{310;130} = \mathcal{A}_{130;130} = 2(-\tfrac{4}{15})^2 = \tfrac{32}{225}, \tag{H 39}$$

$$\mathcal{A}_{310;220} = \mathcal{A}_{130;220} = 2\left(-\frac{4}{15}\right)\frac{\pi}{15} = -\frac{8\pi}{225}, \tag{H 40}$$

$$\mathcal{A}_{310;112} = \mathcal{A}_{130;112} = 2(-\tfrac{4}{15})(-\tfrac{2}{15}) = \tfrac{16}{225}, \tag{H 41}$$

$$\mathcal{A}_{220;220} = 2\left(\frac{\pi}{15}\right)^2 = \frac{2\pi^2}{225}, \tag{H 42}$$

$$\mathcal{A}_{220;112} = 2\frac{\pi}{15}\left(-\frac{2}{15}\right) = -\frac{4\pi}{225}, \tag{H 43}$$

$$\mathcal{A}_{222;112} = 2\frac{\pi}{105}\left(-\frac{2}{15}\right) = -\frac{4\pi}{1575}, \tag{H 44}$$

$$\mathcal{A}_{040;310} = \mathcal{A}_{040;130} = 2\frac{\pi}{5}\left(-\frac{4}{15}\right) = -\frac{8\pi}{75}, \tag{H 45}$$

$$\mathcal{A}_{040;220} = 2\frac{\pi}{5}\frac{\pi}{15} = \frac{2\pi^2}{75}, \tag{H 46}$$

$$\mathcal{A}_{040;112} = 2\frac{\pi}{5}\left(-\frac{2}{15}\right) = -\frac{4\pi}{75}, \tag{H 47}$$

$$\mathcal{A}_{020;310} = \mathcal{A}_{020;130} = 2\frac{\pi}{3}\left(-\frac{4}{15}\right) = -\frac{8\pi}{45}, \tag{H 48}$$

$$\mathcal{A}_{020;220} = 2\frac{\pi}{3}\frac{\pi}{15} = \frac{2\pi^2}{45}, \tag{H 49}$$

$$\mathcal{A}_{020;112} = 2\frac{\pi}{3}\left(-\frac{2}{15}\right) = -\frac{4\pi}{45}, \tag{H 50}$$

$$\mathcal{A}_{510;220} = \mathcal{A}_{150;220} = -2\frac{16}{105}\frac{\pi}{15} = -\frac{32\pi}{1575}, \tag{H 51}$$

$$\mathcal{A}_{510;130} = \mathcal{A}_{150;130} = -2\tfrac{16}{105}(-\tfrac{4}{15}) = \tfrac{128}{1575}. \tag{H 52}$$

Appendix I. Four-point susceptibility

The simulation method for the four-point susceptibility is shown. The four-point density correlation function is given by

$$g^{(4)}(\boldsymbol{r}_1, \boldsymbol{r}_2, t) = \langle \rho(\boldsymbol{r}_1, 0)\rho(\boldsymbol{r}_1, t)\rho(\boldsymbol{r}_2, 0)\rho(\boldsymbol{r}_2, t)\rangle - \langle \rho(\boldsymbol{r}_1, 0)\rho(\boldsymbol{r}_1, t)\rangle\langle \rho(\boldsymbol{r}_2, 0)\rho(\boldsymbol{r}_2, t)\rangle, \tag{I 1}$$

where $\rho(\boldsymbol{r}, t) := \sum_{i=1}^{N} \delta(\boldsymbol{r} - \boldsymbol{r}_i(t))$ is the density. The four-point susceptibility is obtained by integrating the spatial degrees of freedom in $g^{(4)}(\boldsymbol{r}_1, \boldsymbol{r}_2, t)$,

$$\chi_4^0(t) = \frac{\beta V}{N^2} \int \mathrm{d}^3\boldsymbol{r}_1 \int \mathrm{d}^3\boldsymbol{r}_2\, g^{(4)}(\boldsymbol{r}_1, \boldsymbol{r}_2, t), \tag{I 2}$$

where β is the inverse temperature. This can be expressed by the order parameter

$$Q_0(t) := \int \mathrm{d}^3\boldsymbol{r}\rho(\boldsymbol{r}, 0)\rho(\boldsymbol{r}, t) = \sum_{i=1}^{N}\sum_{j=1}^{N} \delta(\boldsymbol{r}_i(0) - \boldsymbol{r}_j(t)) \tag{I 3}$$

as

$$\chi_4^0(t) = \frac{\beta V}{N^2}[\langle Q_0(t)^2\rangle - \langle Q_0(t)\rangle^2]. \tag{I 4}$$

There is a problem in evaluating $\chi_4^0(t)$ by a simulation, because $Q_0(t)$ is ill defined for a finite system. We follow the method of Glotzer, Novikov & Schröder (2000) and modify $Q_0(t)$ by an 'overlap' function $w(r)$ (Parisi 1997) that is unity inside a region of size a and zero otherwise, where a is chosen to be of the order of the particle diameter:

$$\begin{aligned} Q(t) &:= \int \mathrm{d}^3\boldsymbol{r}_1 \int \mathrm{d}^3\boldsymbol{r}_2 \rho(\boldsymbol{r}_1, 0)\rho(\boldsymbol{r}_2, t) w(|\boldsymbol{r}_1 - \boldsymbol{r}_2|) \\ &= \sum_{i=1}^{N}\sum_{j=1}^{N} \int \mathrm{d}^3\boldsymbol{r} w(|\boldsymbol{r}|)\delta(\boldsymbol{r} + \boldsymbol{r}_i(0) - \boldsymbol{r}_j(t)) = \sum_{i=1}^{N}\sum_{j=1}^{N} w(|\boldsymbol{r}_{ij} - \boldsymbol{\mu}_j|). \end{aligned} \tag{I 5}$$

Here $\boldsymbol{r}_{ij} := \boldsymbol{r}_i(0) - \boldsymbol{r}_j(0)$, $\boldsymbol{\mu}_i := \boldsymbol{r}_i(t) - \boldsymbol{r}_i(0)$ and a is chosen as $0.3\,d$. Replacing $Q_0(t)$ by $Q(t)$ yields

$$\chi_4(t) = \frac{\beta V}{N^2}[\langle Q(t)^2\rangle - \langle Q(t)\rangle^2], \tag{I 6}$$

which we have measured by MD simulation (cf. figure 9).

REFERENCES

ALDER, B. J. 1964 Triplet correlation in hard spheres. *Phys. Rev. Lett.* **12**, 317–319.

ANDREOTTI, B., BARRAT, J.-L. & HEUSSINGER, C. 2012 Shear flow of non-Brownian suspensions close to jamming. *Phys. Rev. Lett.* **109**, 105901.

BONNOIT, C., DARNIGE, T., LINDNER, E. & CLEMENTAND, A. 2010 Inclined plane rheometry of a dense granular suspension. *J. Rheol.* **54**, 65–79.

BOYER, F., GUAZZELLI, E. & POULIQUEN, O. 2011 Unifying suspension and granular rheology. *Phys. Rev. Lett.* **107**, 188301.

BRADY, J. F. 1993 The rheological behavior of concentrated colloidal dispersions. *J. Chem. Phys.* **99**, 567–581.

BRADY, J. F. & MORRIS, J. F. 1997 Microstructure of strongly sheared suspensions and its impact on rheology and diffusion. *J. Fluid Mech.* **348**, 103–139.

BREEDVELD, V., VAN DEN ENDE, D., BOSSCHER, M., JONGSCHAAP, R. J. J. & MELLEMA, J. 2002 Measurement of the full shear-induced self-diffusion tensor of noncolloidal suspensions. *J. Chem. Phys.* **116**, 10529–10535.

BREEDVELD, V., VAN DEN ENDE, D., TRIPATHI, A. & ACRIVOS, A. 1998 The measurement of the shear-induced particle and fluid tracer diffusivities in concentrated suspensions by a novel method. *J. Fluid Mech.* **375**, 297–318.

CHAMORRO, M. G., REYES, F. V. & GARZÓ, V. 2015 Non-Newtonian hydrodynamics for a dilute granular suspension under uniform shear flow. *Phys. Rev.* E **92**, 052205.

CHONG, J. S., CHRISTIANSEN, E. B. & BAER, A. D. 1971 Rheology of concentrated suspensions. *J. Appl. Polym. Sci.* **15**, 2007–2021.

CIAMARRA, M. P., CONIGLIO, A. & DE CANDIA, A. 2010 Disordered jammed packings of frictionless spheres. *Soft Matt.* **6**, 2975–2981.

COULAIS, C., SEGUIN, A. & DAUCHOT, O. 2014 Shear modulus and dilatancy softening in granular packings above jamming. *Phys. Rev. Lett.* **113**, 198001.

CWALINA, C. D. & WAGNER, N. J. 2014 Material properties of the shear-thickened state in concentrated near hard-sphere colloidal dispersions. *J. Rheol.* **58**, 949–967.

DAGOIS-BOHY, S., HORMOZI, S., GUAZZELLI, E. & POULIQUEN, O. 2015 Rheology of dense suspensions of non-colloidal spheres in yield-stress fluids. *J. Fluid Mech.* **776**, R2.

DEBOEUF, A., GAUTHIER, G., MARTIN, J., YURKOVETSKY, Y. & MORRIS, J. F. 2009 Particle pressure in a sheared suspensions: a bridge from osmosis to granular dilatancy. *Phys. Rev. Lett.* **102**, 108301.

DEGIULI, E., DÜRING, G., LERNER, E. & WYART, M. 2015 Unified theory of inertial granular flows and non-Brownian suspensions. *Phys. Rev.* E **91**, 062206.

DONEV, A., TORQUATO, S. & STILLINGER, F. H. 2005 Pair correlation function characteristics of nearly jammed disordered and ordered hard-sphere packings. *Phys. Rev.* E **71**, 011105.

DURIAN, D. J. & WEITZ, D. A. 1994 *'Foams' in Kirk–Othmer Encyclopedia of Chemical Technology*, 4th edn (ed. J. I. Kroschwitz), p. 783. Wiley.

EINSTEIN, A. 1905 Über die von der molekularkinetischen theorie der wärme geforderte bewegung von in ruhenden flüssigkeiten suspendierten teilchen. *Ann. Phys. (Berlin)* **322**, 549–560.

EISENMANN, C., KIM, C., MATTSSON, J. & WEITZ, D. A. 2010 Shear melting of a colloidal glass. *Phys. Rev. Lett.* **104**, 035502.

FOSS, D. R. & BRADY, J. F. 1999 Self-diffusion in sheared suspensions by dynamic simulation. *J. Fluid Mech.* **401**, 243–274.

FOSS, D. R. & BRADY, J. F. 2000 Structure, diffusion and rheology of Brownian suspensions by Stokesian dynamics simulation. *J. Fluid Mech.* **407**, 167–200.

GARZÓ, V. 2002 Tracer diffusion in granular shear flows. *Phys. Rev.* E **66**, 021308.

GARZÓ, V. 2013 Grad's moment method for a granular fluid at moderate densities: Navier–Stokes transport coefficients. *Phys. Fluids* **25**, 043301.

GDR MIDI 2004 On dense granular flows. *Eur. Phys. J.* E **14**, 341–365.

GLOTZER, S. C., NOVIKOV, V. N. & SCHRÖDER, T. B. 2000 Time-dependent, four-point density correlation function description of dynamical heterogeneity and decoupling in supercooled liquids. *J. Chem. Phys.* **112**, 509–512.

GRAD, H. 1949 On the kinetic theory of rarefied gases. *Commun. Pure Appl. Math.* **2**, 331–407.

GROUBA, V. D., ZORIN, A. V. & SEVASTIANOV, L. A. 2004 The superposition approximation: a critical review. *Intl J. Mod. Phys.* B **18**, 1–44.

HANSEN, J.-P. & MCDONALD, I. R. 2006 *Theory of Simple Liquids*, 3rd edn. Academic Press.

HAYAKAWA, H. & TAKADA, S. 2016 Kinetic theory of discontinuous shear thickening for a dilute gas–solid suspension. arXiv:1611.07295.

HAYAKAWA, H. & TAKADA, S. 2017 Kinetic theory of discontinuous shear thickening. *EPJ Web Conf.* **140**, 09003.

HAYAKAWA, H., TAKADA, S. & GARZÓ, V. 2017 Kinetic theory of shear thickening for a moderately dense gas–solid suspension: from discontinuous thickening to continuous thickening. *Phys. Rev.* E **96**, 042903.

HERDEGEN, N. & HESS, S. 1982 Nonlinear flow behavior of the Boltzmann gas. *Physica* A **115**, 281–299.

HEUSSINGER, C., BERTHIER, L. & BARRAT, J.-L. 2010 Superdiffusive, heterogeneous, and collective particle motion near the fluid-solid transition in athermal disordered materials. *Eur. Phys. Lett.* **90**, 20005.

IRANI, E., CHAUDHURI, P. & HEUSSINGER, C. 2014 Impact of attractive interactions on the rheology of dense athermal particles. *Phys. Rev. Lett.* **112**, 188303.

JEFFREY, D. J. & ONISHI, Y. 1984 Calculation of the resistance and mobility functions for two unequal rigid spheres in low-Reynolds-number flow. *J. Fluid Mech.* **139**, 261–290.

JENKINS, J. T. & MCTIGUE, D. F. 1990 Transport processes in concentrated suspensions: the role of particle fluctuations. In *The IMA Volumes in Mathematics and its Applications* (ed. D. D. Joseph & D. G. Schaeffer). Springer.

JENKINS, J. T. & RICHMAN, M. W. 1985*a* Grad's 13-moment system for a dense gas of inelastic spheres. *Arch. Rat. Mech. Anal.* **87**, 355–377.

JENKINS, J. T. & RICHMAN, M. W. 1985*b* Kinetic theory for plane flows of a dense gas of identical, rough, inelastic, circular disks. *Phys. Fluids* **28**, 3485–3494.

KAWASAKI, T., COSLOVICH, D., IKEDA, A. & BERTHIER, L. 2015 Diverging viscosity and soft granular rheology in non-Brownian suspensions. *Phys. Rev.* E **91**, 012203.

KIM, S. & KARRILA, S. J. 2005 *Microhydrodynamics*. Dover.

KIRKWOOD, J. G. 1935 Statistical mechanics of fluid mixtures. *J. Chem. Phys.* **3**, 300–313.

KREMER, G. M 2010 *An Introduction to the Boltzmann Equation and Transport Processes in Gases*. Springer.

KRIEGER, I. M. 1972 Rheology of monodisperse latices. *Adv. Colloid Interface Sci.* **3**, 111–136.

KUWANO, O. & HATANO, T. 2011 Flash weakening is limited by granular dynamics. *Geophys. Res. Lett.* **38**, L17305.

LAUN, H. M. 1994 Normal stresses in extremely shear thickening polymer dispersions. *J. Non-Newtonian Fluid Mech.* **54**, 87–108.

LEIGHTON, D. & ACRIVOS, A. 1987*a* Measurement of shear-induced self-diffusion in concentrated suspensions of spheres. *J. Fluid Mech.* **177**, 109–131.

LEIGHTON, D. & ACRIVOS, A. 1987*b* The shear-induced migration of particles in concentrated suspensions. *J. Fluid Mech.* **181**, 415–439.

LOOTENS, D., VAN DAMME, H., HEMAR, Y. & HEBRAUD, P. 2005 Dilatant flow of concentrated suspensions of rough particles. *Phys. Rev. Lett.* **95**, 268302.

MARI, R., SETO, R., MORRIS, J. F. & DENN, M. M. 2014 Shear thickening, frictionless and frictional rheologies in non-Brownian suspensions. *J. Rheol.* **58**, 1693–1724.

MEWIS, J. & WAGNER, N. J. 2012 *Colloidal Suspension Rheology*. Cambridge University Press.

MILLS, P. & SNABRE, P. 2009 Apparent viscosity and particle pressure of a concentrated suspension of non-Brownian hard spheres near the jamming transition. *Eur. Phys. J.* E **30**, 309–316.

MORRIS, J. F. & BOULAY, F. 1999 Curvilinear flows of noncolloidal suspensions: the role of normal stresses. *J. Rheol.* **43**, 1213–1237.

NOTT, P. R. & BRADY, J. F. 1994 Pressure-driven flow of suspensions: simulation and theory. *J. Fluid Mech.* **275**, 157–199.

O'HERN, C. S., LANGER, S. A., LIU, A. J. & NAGEL, S. R. 2002 Random packings of frictionless particles. *Phys. Rev. Lett.* **88**, 075507.

O'HERN, C. S., SILBERT, L. E., LIU, A. J. & NAGEL, S. R. 2003 Jamming at zero temperature and zero applied stress: the epitome of disorder. *Phys. Rev.* E **68**, 011306.

OLSSON, P. 2010 Diffusion and velocity autocorrelation at the jamming transition. *Phys. Rev.* E **81**, 040301(R).

ONO, I. K., O'HERN, C. S., DURIAN, D. J., LANGER, S. A., LIU, A. J. & NAGEL, S. R. 2002 Effective temperatures of a driven system near jamming. *Phys. Rev. Lett.* **89**, 095703.

OTSUKI, M. & HAYAKAWA, H. 2014 Avalanche contribution to shear modulus of granular materials. *Phys. Rev.* E **90**, 042202.

PARISI, G. 1997 Short-time aging in binary glasses. *J. Phys.* A **30**, L765.

PUSEY, P. N. 1991 *Liquids, Freezing and Glass Transition, Part II* (ed. J.-P. Hansen, D. Levesque & J. Zinn-Justin). Elsevier.

QUEMADA, D. 1977 Rheology of concentrated disperse systems and minimum energy dissipation principle. *Rheol. Acta* **16**, 82–94.

ROTNE, J. & PRAGER, S. 1969 Variational treatment of hydrodynamic interaction in polymers. *J. Chem. Phys.* **50**, 4831–4838.

SAITOH, K. & HAYAKAWA, H. 2019 (in preparation).

SANGANI, A. S., MO, G., TSAO, H.-K. & KOCH, D. L. 1996 Simple shear flows of dense gas–solid suspensions at finite Stokes numbers. *J. Fluid Mech.* **313**, 309–341.

SANTOS, A., GARZÓ, V. & DUFTY, J. W. 2004 Inherent rheology of a granular fluid in uniform shear flow. *Phys. Rev.* E **69**, 061303.

SCALA, A., VOIGTMANN, TH. & MICHELE, C. D. 2007 Event-driven Brownian dynamics for hard spheres. *J. Chem. Phys.* **126**, 134109.

SETO, R., MARI, R., MORRIS, J. F. & DENN, M. M. 2013 *Phys. Rev. Lett.* **111**, 218301.

SUZUKI, K. & HAYAKAWA, H. 2015 Divergence of viscosity in jammed granular materials: a theoretical approach. *Phys. Rev. Lett.* **115**, 098001.

TORQUATO, S. 1995 Nearest-neighbor statistics for packings of hard spheres and disks. *Phys. Rev.* E **51**, 3170–3182.

TSAO, H.-K. & KOCH, D. L. 1995 Simple shear flows of dilute gas–solid suspensions. *J. Fluid Mech.* **296**, 211–245.

ZARRAGA, I. E., HILL, D. A. & LEIGHTON, D. T. 2000 The characterization of the total stress of concentrated suspensions of noncolloidal spheres in newtonian fluids. *J. Rheol.* **44**, 185–220.